

**CRACK DETECTION ON ALUMINIUM  
CANTILEVER BEAMS THROUGH COMPUTER  
AIDED VIBRATION ANALYSIS AND DEEP  
LEARNING**

*Dissertation submitted  
in partial fulfillment of requirements  
for the award of degree of*

**Bachelor of Technology**

**in**

**Mechanical Engineering**

**By**

**S. Amarthya (Regd. No: 18131A0343)**

**R. Lalith Sai Madhav (Regd. No: 18131A03F1)**

**R.S.S. Naveen (Regd. No: 18131A03F4)**

**S. Vamsi Varma (Regd. No: 18131A03H4)**

**Under the guidance of**

**Dr. P. Krishna Kiran**

**Dr. L . Venkat**

**Assistant Professor**

**Department of Mechanical  
Engineering**

**Associate Professor**

**Department of Civil  
Engineering**



**COLLEGE OF ENGINEERING  
(AUTONOMOUS)**

**Department of Mechanical Engineering  
GAYATRI VIDYA PARISHAD COLLEGE OF ENGINEERING  
(AUTONOMOUS)  
(Affiliated to J.N.T. University, Kakinada)  
VISAKHAPATNAM – 530048  
May 2022**



COLLEGE OF ENGINEERING  
(AUTONOMOUS)

## CERTIFICATE

This is to certify that the project titled “**CRACK DETECTION ON ALUMINIUM CANTILEVER BEAMS THROUGH COMPUTER AIDED VIDRABTION ANALYSIS AND DEEP LEARNING**” is a bonafide work done by

**R. Lalith Sai Madhav (Regd. No: 18131A03F1)**

in partial fulfillment of the requirements for the award of the degree of **Bachelor of Technology in Mechanical Engineering** at Gayatri Vidya Parishad College of Engineering (Autonomous) affiliated to Jawaharlal Nehru Technological University Kakinada during the year 2021-2022.

<b>Supervisor</b> <b>(Dr. P. Krishna Kiran)</b> Assistant Professor <b>Department of Mechanical Engineering</b> <b>GVP College of Engineering (A)</b>	<b>Supervisor</b> <b>(Dr. L. Venkat)</b> Associate Professor <b>Department of Civil Engineering</b> <b>GVP College of Engineering (A)</b>
---	---

**Head of the department**  
**(Dr. B. Govinda Rao)**  
**Professor and Head of the Department**  
**Department of Mechanical Engineering**  
**GVP College of Engineering (A)**

**Project Viva-Voce held on:** \_\_\_\_\_

**External Examiner**

## **ABSTRACT**

A new approach to detect damage on cantilever structures based on modal parameters is presented in this study. The changing loading patterns, the ageing of structures with time, and the environment's influence may cause cracks in the structure especially in engineering structures with long service life. Thus, early detection of damage can prevent the catastrophic failure of structures by appropriately monitoring the system's response. Artificial Neural Network (ANN) techniques to monitor structural health are becoming increasingly popular. Therefore, we present a reverse engineering method for predicting the location and severity of cracks using a deep learning model which implements multilayer perceptrons.

Cantilever beams of different grades of Aluminium alloys viz. Al 6061, Al 6013, Al 5052 and Al 5024 are considered for analysis purposes with the crack position at intervals of 50mm from the fixed end at varying crack depths of 10%, 20%, 30%, 40%, 50% and 60% of the total beam depth. The frequencies of both damaged and undamaged beams are obtained by performing modal analysis in ANSYS, and the frequency ratios along with the corresponding crack position ratio and crack severity ratio are given as input parameters to the deep learning model for the purpose of training . The Artificial Neural Network tool in MATLAB is used to perform the prediction.

## **ACKNOWLEDGMENT**

It is with a sense of great respect and gratitude that we express our sincere thanks to **Dr. P. Krishna Kiran**, Assistant Professor, Department of Mechanical Engineering, and **Dr. L. Venkat**, Associate Professor, Department of Civil Engineering, Gayatri Vidya Parishad College of Engineering (Autonomous) for their inspiring guidance, supervision and encouragement towards the successful completion of our project work.

We take this opportunity to thank **Dr. B. Govinda Rao**, Professor and Head of the Department of Mechanical Engineering, Gayatri Vidya Parishad College of Engineering(A) for permitting us to pursue the project.

We express our sincere thanks to **Dr. A. Bala Koteswara Rao**, Principal of Gayatri Vidya Parishad College of Engineering (A) for granting permission for providing all the necessary resources for completing the project.

We wish to express our appreciation and heartfelt thanks to our parents who supported us towards our goal and we would like to thank our friends, who helped and inspired us in odd and even hours for successful completion of our project work.

We would like to convey special thanks to all those who helped either directly or indirectly for the completion of our project work.

**S. Amarthya (Regd. No: 18131A0343)**  
**R. Lalith Sai Madhav (Regd. No: 18131A03F1)**  
**R.S.S. Naveen (Regd. No: 18131A03F4)**  
**S. Vamsi Varma (Regd. No: 18131A03H4)**

# CONTENTS

<b>Chapter Contents</b>	<b>Page No.</b>
<i>Certificate</i>	I
<i>Abstract</i>	ii
<i>Acknowledgement</i>	iii
<i>Contents</i>	iv
<i>List of Tables</i>	vi
<i>List of Figures</i>	vii
<b>1. INTRODUCTION</b>	1
1.1 General	1
1.2 Motivation for damage identification	1
1.3 Aim of the project	2
1.4 Organization of the project	4
<b>2. LITERATURE REVIEW</b>	6
2.1 Introduction	6
2.2 Methodologies for fault detection	6
2.3 Analysis of different methodologies for crack detection	9
2.3.1 Crack detection using classical methods	10
2.3.2 Crack detection using finite element method	17
2.3.3 Crack detection using neural networks	20
<b>3. EVALUATION OF DYNAMIC CHARACTERISTICS OF BEAMSTRUCTURE WITH TRANSVERSE CRACKS</b>	23
3.1 Introduction	23
3.2 Vibration characteristics of a cracked cantilever beam	24
3.2.1 Vibration analysis of the cracked cantilever beam	24
3.2.2 Numerical analysis	24
3.2.3 Results for theoretical analysis	25
<b>4. ANALYSIS OF FINITE ELEMENT FOR CRACK DETECTION</b>	26
4.1 Introduction	26
4.2 Finite Element Analysis	27
4.2.1 Analysis of cracked beam using finite element analysis(FEA)	28
<b>5. ANALYSIS OF ARTIFICIAL NEURAL NETWORK</b>	30

## **FOR CRACK DETECTION**

5.1	Introduction	30
5.2	Neural network technique	33
5.2.1	Model of a neural network	33
5.2.2	Use of back propagation neural network	35
5.3	Analysis of neural network model used for crack detection	36
5.3.1	Neural model mechanism for crack detection	37
5.3.2	Neural model for finding out crack depth and crack location	38
<b>6.</b>	<b>METHODOLOGY</b>	<b>39</b>
6.1	General	39
6.2	Modal Analysis	40
6.3	Importing geometry	41
6.4	Assigning materials to the geometry	42
6.5	Meshing	42
6.6	Construction of path	43
6.7	Materials used	44
6.8	ANSYS results	44
6.9	Modal Assurance Criterion	45
<b>7.</b>	<b>RESULTS AND DISCUSSIONS</b>	<b>47</b>
7.1	Total Deformation and Directional Deformation	47
7.2	3-D Graphs	52
7.3	MATLAB Results	56
7.3.1	Without MAC	56
7.3.2	With MAC	58
<b>8.</b>	<b>CONCLUSIONS</b>	<b>62</b>
	<b>References</b>	<b>63</b>
	<b>Appendix A</b>	<b>75</b>
	<b>Appendix B</b>	<b>78</b>

## **LIST OF TABLES**

<b>Table No.</b>		<b>Page No.</b>
2.1.	Examples activation functions used in ANN	23
5.1.	Test patterns for NN model other than test data	39
6.1.	Material Properties	45

## LIST OF FIGURES

<b>Fig.</b>	<b>Contents</b>	<b>Page no.</b>
3.1.	Cantilever Beam Elemental model	26
5.1.	Neuron model	35
5.2.	Back Propagation Technique	37
5.3.	Neural Model	38
5.4.	Multi-layer feed forward back propagation neural model for damage detection	39
6.1.	Plane view of cantilever beam	42
6.2.	Catia sketch of the beam	43
6.3.	Opening of Design Modeller	43
6.4.	ANSYS view of the beam	44
6.5.	Mesh model of the beam	45
6.6.	Construction path	45
6.7.	Formula to evaluate MAC	47
7.1. (a)	Total Deformation, Mode 1	49
7.1. (b)	Total Deformation, Mode 2	49
7.1. (c)	Total Deformation, Mode 3	50
7.1. (d)	Total Deformation, Mode 4	50
7.1. (e)	Total Deformation, Mode 5	50
7.1. (f)	Total Deformation, Mode 6	51
7.1. (g)	Total Deformation, Mode 7	51
7.1. (h)	Total Deformation, Mode 8	51
7.1. (i)	Total Deformation, Mode 9	52
7.1. (j)	Total Deformation, Mode 10	52
7.1. (k)	Directional Deformation, Mode1	52
7.1. (l)	Directional Deformation, Mode 2	53
7.1. (m)	Directional Deformation, Mode 3	53
7.1. (n)	Directional Deformation, Mode 4	53

7.1. (o)	Directional Deformation, Mode 5	54
7.1. (p)	Directional Deformation, Mode 6	54
7.1. (q)	Directional Deformation, Mode 7	54
7.1. (r)	Directional Deformation, Mode 8	55
7.1. (s)	Directional Deformation, Mode 9	55
7.1. (t)	Directional Deformation, Mode 10	55
7.2. (a)	3-D Graph for Mode 1	56
7.2. (b)	3-D Graph for Mode 2	56
7.2. (c)	3-D Graph for Mode 3	57
7.2. (d)	3-D Graph for Mode 4	57
7.2. (e)	3-D Graph for Mode 5	58
7.2. (f)	3-D Graph for Mode 6	58
7.2. (g)	3-D Graph for Mode 7	59
7.2. (h)	3-D Graph for Mode 8	59
7.2. (i)	3-D Graph for Mode 9	60
7.2. (j)	3-D Graph for Mode 10	60
7.3.1. (a)	ANN Tool without MAC	61
7.3.1. (b)	Output of Regression Analysis without MAC	61
7.3.1. (c)	Overall Performance Curves without MAC	62
7.3.1. (d)	Regression Graphs without MAC	62
7.3.1. (e)	Training state curves without MAC	62
7.3.2. (a)	ANN Tool with MAC	63
7.3.2. (b)	Output of Regression Analysis with MAC	64
7.3.2. (c)	Overall Performance Curves with MAC	64
7.3.2. (d)	Regression Graphs with MAC	65
7.3.2. (e)	Training state curves with MAC	65

# **CHAPTER 1**

## **INTRODUCTION**

### **1.1. General**

The science and engineering community has paid close attention to crack diagnostics in vibrating structures in the last three decades. If cracks in a structure are undiscovered for an extended time, the system will fail, potentially resulting in losing lives and resources. One of the commonly established crack identification methods in many engineering systems is to use the member's dynamic response. The present chapter focuses on the various fault diagnosis approaches. The background and motivation in dynamically vibrating damaged structure analysis were presented in the first section. The research's goals and objectives are described in the second section of this chapter. The present chapter concludes with a brief overview of each thesis chapter relevant to the current study.

### **1.2. Motivation for damage identification**

Engineering structures are fundamental in today's society. They are usually made to have a longer lifespan. Failure or poor performance of engineering structures can cause transportation system disruptions and loss of life and property. It is critical to monitor the structural integrity of the members and take appropriate remedial action to assure safety and efficiency.

For fault diagnosis, many strategies have been used in the past. Some are obvious (the dye penetrant approach), while others rely on sensors to detect local flaws (e.g., acoustic emission, magnetic field, eddy current, radiographs and thermal fields). These procedures are time-consuming, and they cannot guarantee that a structure is fault-free without thoroughly evaluating it. Furthermore, if a break is hidden deep within the structure, these targeted methods may not be able to identify it. Researchers have developed Artificial Intelligence (AI) based algorithms for fault identification for a single crack scenario based on changes in the modal parameters. Artificial

intelligence algorithms have been developed to predict structural flaws more quickly and accurately. For the reasons stated above, this thesis proposes investigating the usage of AI techniques such as neural networks for early crack detection in engineering structures by recording vibration characteristics.

### **1.3. Aim of the project**

In aeronautical, civil, and mechanical engineering, the process of monitoring and finding problems is critical. Civil or mechanical engineering structures associated with aerospace must be free from cracks to ensure safe operation. Cracks in the machine or any engineering systems may lead to catastrophic failure of the machine and must be detected early.

Beams are utilized as structural components in various engineering systems (for example, steel structures and industrial machines) and are subjected to static and dynamic loads. They may crack due to loads and environmental effects, substantially reducing the structural system's life cycle. The presence of cracks in the system may be considered while developing an analytical model to investigate the effect of cracks on the system's modal response. Damage to the beam member introduces stiffness, which can be used to formulate the vibration characteristic equation and obtain the mode shape, natural frequency of vibration, and crack parameters such as relative crack severities and relative crack positions, along with the prevailing boundary conditions. The current study seeks to provide a multi-crack recognition method for intelligent structure condition monitoring based on changes in structural member modal characteristics caused by cracks.

For this purpose, a cantilever beam with a uniform cross-section has been considered, which acts as a structural member in various engineering applications. The dynamic responses of the cantilever beam have been measured in the undamaged state, which acts as a reference. Afterwards, a damage was induced, and sequential modal identification analysis was performed at each damaged stage, aiming to find adequate correspondence between the dynamic behaviour and the presence of cracks in the structure.

Comparison between different techniques based on the performance to identify the various cracks level have been carried out to find out the most suitable method to

identify cracks in damaged structures. The aim is to use the dynamic response parameters to develop AI methods for structural health monitoring in a crack scenario. A literature evaluation on fault diagnosis in engineering applications was conducted in the current study. According to the prior review, the researchers' findings have not been systematically applied to generate tools for real-world applications such as crack diagnosis. An attempt has been made to design and create a crack diagnosis tool based on the dynamic behaviour of cracked and complete cantilever beam constructions using theoretical analysis, finite element analysis, experimental analysis, and artificial intelligence approaches.

The different phases for the present study are listed below:

1. Theoretical analysis for the cantilever structure with two transverse cracks has been performed to evaluate the modal parameters.
2. Finite Element Analysis (FEA) has been carried out to measure the cracked and undamaged cantilever beam's vibration parameters with different crack configurations.
3. The modal parameters such as natural frequencies and mode shapes obtained from theoretical, finite elements, and experimental analysis have been used to design and train the artificial intelligence techniques. The developed AI-based methodologies utilize the first three relative natural frequencies and the first three average relative mode shape differences as the input parameters, and relative crack locations and relative crack depths are the outputs from the AI model.

The theoretical study has been developed for a cantilever beam with two transverse cracks to obtain the dynamic characteristics by utilizing the expressions of strain energy release rate and stress intensity factors. The presence of cracks produces local flexibility in the vicinity of the crack locations and reduces the structure's stiffness. With different boundary conditions, the stiffness matrix has been derived to find out the effect of relative crack depths on the dimensionless compliances of the structure. The derived vibration signatures from theoretical, finite elements and experimental analysis of the beam member have been used to design and train the AI model (neural networks). Finally, relative crack locations and relative crack depths are the outputs from the model.

The results obtained from the various methodologies such as theoretical, finite element, experimental, and neural networks devised in the present research have been compared, and a close agreement has been found. Concrete conclusions have been drawn from the results of the respective sections. Experimental analysis has been carried out to validate the different techniques cited above.

#### **1.4. Organization of the project**

The project material is structured as follows:

The latest research analyses for fault identification in damaged structures are described in the seven chapters.

The first chapter explains how fractures affect the functionality of various engineering applications and explore the approaches used by the scientific community to diagnose problems in various industrial applications. This chapter also explains why the research was conducted and the current investigation.

The literature review part of Chapter 2 represents state of the art in the subject of damage detection using vibration analysis and fault detection using artificial intelligence approaches.

This section also explains the rationale for the present research's direction and the classification of defect detection approaches.

The theoretical model for measuring vibration indicators (natural frequencies, mode shapes) using SIF, strain energy release rate, and varied boundary conditions is introduced in Chapter 3.

The break that occurred in the structure causes flexibility in its area, resulting in a decrease in natural frequencies and a change in mode shapes. This foundation was used in the numerical analysis to find cracks in the cantilever construction and assess their locations and severity.

The finite element analysis applied to the cracked beam element to assess the dynamic response of a cracked cantilever beams is described in Chapter 4 of the thesis. The measurements are then used to determine the presence of cracks and their characteristics. For validation, the results of the finite element approach are compared to those of the experimental method and numerical analysis.

In Chapter 5, an inverse analysis using an artificial neural network technique is used to assess fracture damage in a cracked cantilever structure with a transverse crack.

The input and output parameters of a multi-layer perceptron are shown and discussed. The artificial neural network results are provided and discussed to demonstrate the AI model's applicability.

In Chapter 6, the methodology adopted in the project is discussed in detail.

The findings from all of the approaches employed in the current study are summarised in Chapter 7.

Chapter 8 reviews the current research findings and makes recommendations in the same field.

## **CHAPTER 2**

### **LITERATURE REVIEW**

The structural damage identification using dynamic models is summarized in this chapter. The primary purpose is to look back on the advances made by researchers over the last few decades. The historical backdrop of damage methods applicability, general categorization methods, and a discussion of a chosen group of approaches are all discussed. Finally, past and present breakthroughs in artificial intelligence approaches for crack diagnosis are explored.

#### **2.1. Introduction**

The literature review section presents the analysis of the published work confined to structural health monitoring, damage detection algorithm, fault diagnostic methodologies and modal testing. The review begins with a description of different vibration analysis methods used for damage identification. Next, dynamics of cracked structures, fault identification methodologies for developing a crack diagnostic tool using Finite Element Analysis (FEA) and wavelet technique are discussed. Intelligent models for crack identification can be designed following artificial intelligence techniques (neural networks). The present investigation aims to propose an artificial intelligence technique capable of predicting the presence of a crack in vibrating structures. The examination of the literature referenced in this section might be used to determine possible research directions.

The published papers show that the concept of fault discovery in various systems varies greatly. Even though fault diagnostic methodology has evolved in various ways, the next section includes an overview of the literature on damage detection and fault diagnosis.

#### **2.2. Methodologies for fault detection**

Researchers to date have focused on many methodologies for the detection of a fault in various segments of engineering structures. Vibration-based methods are found to be

effectively used for health monitoring in faulty systems. The recent methods adapted for fault diagnosis are outlined below.

Moore et al. [1] have proposed a new method to identify a single crack's size, location, and orientation in a simply supported plate subjected to free vibration by employing the finite element method and Markov-chain Monte-Carlo implementation of Bayes' Rule.

They have claimed that their approach can effectively identify the crack present in the real engineering system. Lang et al. [2] have applied the concept of transmissibility to the non-linear case by introducing the transmissibility of Non-linear Output Frequency Response Functions.

They have developed a NOFRF transmissibility-based technique for detecting and locating both linear and non-linear damage in MDOF structural systems. Their proposed technique has been verified by the numerical simulation and experimental analysis on a three-storey building. Hein et al. [3] have presented a new method for identifying the delamination of homogeneous and composite beams.

They have used Haar wavelets and neural networks to establish the mapping relationship between frequencies, Haar series expansion of fundamental mode shapes of the vibrating beam and delamination status.

They have revealed that the simulations show that the proposed complex method can detect the location of delaminations and identify the delamination extent with high precision. Huh et al. [4] have proposed a new local damage detection method for damaged structures using the vibratory power estimated from accelerations measured on the beam structure.

A damage index is newly defined by them based on the proposed local damage detection method and is applied to identify structural damage. Numerical simulations and experiments are conducted for a uniform beam to confirm the validity of the proposed method. In the experiments, they considered the damage as an open crack such as a slit inflicted on the top surface of the beam. Salam et al. [5] have proposed a simplified formula for the stress correction factor in the crack depth to the beam height ratio.

They have used the proposed formula to examine the lateral vibration of a Euler-Bernoulli beam with a single edge open crack and compared the mode shapes for the cracked and

undamaged beam to identify the crack parameters. Douka et al. [6] have presented a method for crack identification based on the sudden change in the spatial variation of the transformed response of the beam structures using wavelet analysis.

They have established an intensity factor law for the accurate prediction of crack size, and the results from the proposed method have been validated experimentally. Nahvi et al. [7] have developed a technique for identifying cracks in cantilever beams using an analytical, finite element method based on measured natural frequencies and mode shapes of the beam structure.

The results from the proposed method have been authenticated using the results obtained from the experimental analysis. Tahaa et al. [8] have introduced a method to improve pattern recognition and damage detection by supplementing intelligent health monitoring with a fuzzy inference system.

The Bayesian methodology is used to demarcate the levels of damage for developing the fuzzy system and is examined to provide damage identification using data obtained from finite element analysis for a pre-stressed concrete bridge. Mahamad et al. [9] have proposed an artificial neural network (ANN) based methodology to predict accurate remaining useful life (RUL) for a bearing system.

The ANN model has been designed using measurements of hazard rates of root mean square and kurtosis from its present and previous state. Kong et al. [10] have proposed a fault diagnosis methodology using wavelet transformer fuzzy logic and neural network technique to identify the faults.

They have found a good agreement between analytical and experimental results. Liu et al. [11] have taken the help of a genetic algorithm (GA) for optimal sensor placement on a spatial lattice structure. They have taken the model strain energy (MSE) and modal assurance criterion (MAC) as the fitness function.

A computational simulation of the 12-bay plain truss model has been used as a modified GA, and the data were compared against the existing GA using the binary coding method and found better results through the modified GA. Sanza et al. [12] have presented a new technique for health monitoring of rotating machinery by integrating the capabilities of wavelet transform and auto associative neural network for analyzing the vibration

signature. The proposed technique's effectiveness has been evaluated using the numerical and experimental vibration data, and the developed technique has demonstrated accurate results.

Hoffman et al. [13] have employed a diagnostic technique based on a neural network. As described in the paper, it is impossible to determine the degree of imbalance in a bearing system using a single vibration feature and overcome this problem. They have used the neural network technique to process multiple features.

They have employed different neural network techniques for fault detection of different bearing conditions and compared their performances. They have found that the developed algorithm can be suitably used for identifying the presence of defects. Murgendrappa et al. [14] have proposed a technique based on the measurement of natural frequency change to detect cracks in long pipes containing fluid at different pressure. In their experimental analysis, they have used aluminium & mild steel Pipes with water as the fluid and used pressure gauges to obtain the change in natural frequency, which are subsequently used to locate the crack present on the pipes carrying fluids.

Darpe et al. [15] have studied the unbalanced response of a cracked rotor with a single centrally situated crack subjected to periodic axial impulses using an electrodynamics exciter for both rotating & non-rotating conditions. They have found that the spectral response of the crack rotor with and without axial excitation is found to be distinctly different.

They have concluded that the rotor response to axial impulse excitation can be a reliable diagnostic tool for rotor crack. Curry et al. [16] have proposed a closed-loop system with the help of sensors to formulate a fault detection and isolation methodology based on a fixed threshold. They have observed that the proposed technique can detect and isolate failures for each of the particular sensors.

The various techniques employed by the researchers in the domain of fault detection vary in their approach to identifying the faults present in a system. The following section depicts the different methods used for fault diagnosis in engineering systems.

### **2.3. Analysis of different methodologies for crack detection**

In this current investigation, the various methods applied for crack identification in

damaged dynamic structures have been described briefly. The different methods that various authors for damage identification have proposed are sectioned into four different categories such as:

1. Classical method
2. Finite Element Method
3. AI method
4. Miscellaneous

### **2.3.1. Crack detection using classical methods**

The current section discusses the spatial variation of the transferred response, modal response methods, energy-based methods, analytical methods, and algorithms based on Vibration used for locating the crack location and its intensity in dynamically vibrating damaged structures. The research papers connected to the above techniques are discussed below.

Muller et al. [17] have proposed a method for crack detection in dynamic systems. They have established a relation between shaft cracks in turbo rotors by applying a model-based method using the theory of Lyapunov exponents. Their research has studied chaotic motions and strange attractors in turbo rotors.

Owolabi et al. [18] have carried out experimental investigations of crack location and crack intensity for fixed beams and simply supported beams made of Aluminum. They have measured the changes in the first three natural frequencies and the corresponding amplitudes to forecast the crack in a structure.

Chinchalkar [19] has developed a generalized numerical method for fault finding using a finite element approach. His approach is based on the measurement of the first three natural frequencies of the cracked beam. The developed fault detection method accommodates different boundary conditions and has wide variations in crack depth.

Tada et al. [20] have established a platform to formulate a compliance matrix for damaged structural members to estimate the crack location and depth.

Loutridis et al. [21] have proposed a new technique for crack detection in beams based on the instantaneous frequency and empirical mode decomposition. The dynamic behaviours of the structure have been investigated both theoretically and experimentally.

They concluded that the variation of the instantaneous frequencies increases with an increase in crack depth, and this variation has been used to estimate the crack size.

Song et al. [22] have described an exact solution methodology based on the Laplace transform to analyze the bending free Vibration of a cantilever laminated composite beam having surface cracks. They have used Hamilton's variational principle in conjunction with the Timoshenko beam model to develop the technique for damage detection in crack structures.

Ravi et al. [23] have carried out the modal analysis of an aluminium sheet having microcracks. They have used compression loading to generate the micro-cracks on the sheet's surface and monitored the deformation using the acoustic emission technique. Using the line scans around the area of deformation, they have detected the effect of microcracks and the modal parameters of the aluminium sheet specimen.

Law et al. [24] have proposed a time-domain method for crack identification in the structural member using strain or displacement measurement. They have modelled the open crack using the Dirac delta function and evaluated the dynamic response based on modal superposition. They have validated the proposed identification algorithm by comparing the results from impact hammer tests on a beam with a single crack.

Dado [25] has formulated a mathematical model to predict the crack location and their severities for beams with various end conditions such as pinned-pinned, clamped free, clamped-pin and clamped-clamped. They have developed the mathematical model, assuming the beam to be a rectangular Euler-Bernoulli beam. They have concluded that, though the assumption of the beam does not meet the requirements for real-time application, the results obtained for the model developed can be used as an initial step to formulating crack identification methodology, which can be used in general practice.

Douka et al. [26] have studied the nonlinear dynamic behaviour of a cantilever beam both theoretically and experimentally. They have analyzed both the simulated and experimental response data by applying empirical mode decomposition and the Hilbert transform method. They have concluded that the developed methodology can accurately analyze the nonlinearities caused by the presence of a breathing crack.

Benfratello et al. [27] have presented numerical and experimental investigations to assess the capability of non-Gaussianity measures to detect crack presence and position. They

have used the skewness coefficient of the rotational degrees of freedom the identification purpose of the crack in a damaged structure.

Feldman [28] has introduced the application of the Hilbert transform to non-stationary and nonlinear vibration systems. He has demonstrated concepts of actual mechanical signals and utilizes the Hilbert transform for machine diagnostics and identification of mechanical systems.

Ruotolo et al. [29] have analyzed the vibrational response of cracked beams due to harmonic forcing to evaluate the nonlinear characteristics. They have used the frequency response function to identify the location and depth of the crack to set a basis for the development of an experimental structural damaged identification algorithm.

Behzad et al. [30] have devised a continuous model for flexural Vibration of beams containing edge cracks perpendicular to the neutral plane of the beam. They have taken the displacement field as a superposition of the Euler Bernoulli displacement and displacement due to the presence of a crack. They have taken the crack displacement as the product of time function and exponential space function. The results obtained are in good agreement with the results obtained from finite element analysis. They have used the beam with a horizontal and vertical edge crack.

Prasad et al. [31] have investigated the effect of crack location from the free end to the fixed end in a vibrating cantilever beam. They compared and analyzed crack growth rates at different frequencies using the experimental setup.

Rezaee et al. [32] have used the perturbation method to analyze the Vibration of a simply supported beam with a breathing crack. From the analysis, it is observed that for a given crack location on the beam structure with the increase in the relative crack depth, the stiffness of the beam decreases with time.

Dimarogonas et al. [33] have proposed a technique for crack identification in cracked rotating shafts using the system's dynamic response. They have stated that the change in the modal response is due to the local flexibility introduced due to the presence of crack and different moments of inertia. He has found that the system behaves non-linearly because of the crack present in the rotating shaft. The results obtained from the developed analytical method for the closing crack condition are based on the assumption of large static deflections commonly found in turbomachinery.

Faverjon et al. [34] have used the constitutive relation error updating method to develop a crack diagnosis tool in damaged beam structures.

Mazanoglu et al. [35] have carried out vibration analysis of non-uniform Euler – Bernoulli beams with cracks using the energy-based and Rayleigh-Ritz approximation methods. They have measured the change in strain in the cracked beam due to bending. They have also analyzed the beam using a finite element program, compared the obtained results with that of the analytical method, and found the results to be in good agreement.

Wang et al. [36] have studied a composite cantilever having a surface crack and found that the variation in the modal response depends on two parameters, i.e. crack location and material properties. They have concluded that the change in frequency can be effectively used to locate the crack position and measure its severities.

Al-said [37] has presented a crack diagnostic method using the change in natural frequencies for a stepped cantilever beam carrying concentrated masses. He has also applied finite element analysis to validate the results obtained from the proposed method. He successfully used the developed algorithm to identify cracks in overhead gantry and girder cranes.

Lee [38] has proposed a damage detection methodology in beam structures using the Newton-Rapson method and assuming the cracks present in the system as rotational springs.

Yumin et al. [39] have analyzed cracked pipes to measure the local flexibility matrix and stress intensity factor in developing an algorithm for damage identification. They have developed the method by dividing the cracked pipe into thin annuli. Experimentally, they have calculated the local flexibility matrix of the damaged pipes without calculating the Stress intensity factor.

A modified version of the local flexibility has been proposed by Zou et al. [40] has studied cracked rotors' vibrational behaviour to design a crack diagnostic model. They have described that their developed method is suitable for the theoretical model.

Cerri et al. [41] have investigated the vibrational characteristics of a circular arch both in the damaged and undamaged state obtained from the theoretical model and compared the results with the experimental analysis to present a crack identification method. They have used the natural frequencies and vibration modes to develop the crack identification methodology by assuming the arch as a torsion spring at the cracked section.

Nobile et al. [42] have presented a technique to determine the crack initiation and direction for circumferentially cracked pipes and cracked beams by adapting the strain energy density factor. The strain energy density theory can effectively analyze the different features of material damage in the mixed-mode crack propagation problem.

Humar et al. [43] have investigated different vibration-based crack identification techniques and found their drawbacks.

The modal response parameters, stiffness, and damping are directly affected by the presence of a crack in the structure. According to them, most vibration-based crack diagnosis techniques fail to perform when applied to real structures because of the inherent difficulties. They have presented computer simulation studies for some of the commonly used methodologies and suggested the conditions under which they may or may not perform. They have concluded that all the practical challenges present in a real system cannot be simulated through computer applications entirely, making the vibration-based crack estimation methods a challenging field.

Viola et al. [44] have studied the dynamic behaviour of multi-stepped and multi-damaged circular arches. They have analyzed the arches in damaged and undamaged conditions to find the numerical solutions using the Euler characteristics exponent procedure and generalized differential quadrature method.

Shin et al. [45] have analyzed the vibration characteristics of circular arches having variable cross-sections. They have presented the equation for deriving the system's natural frequencies at different boundary conditions with the help of the generalized differential quadrature method and differential transformation method. The results obtained from their proposed method have been compared with the previously published work.

Cerri et al. [46] have investigated a hinged plane circular arch to develop a structural damage detection technique by studying the changes in the natural frequencies of the system. They have discussed two different approaches for crack detection. One of the approaches is based on comparing the variation of natural frequencies obtained from the experimental and theoretical method, and the other is based on a search of an intersection joint of curves obtained by the modern equations.

Labuschagne et al. [47] have studied Euler – Bernoulli, Timo Shenko and two-dimensional elasticity theories for three models of cantilever beams. From the analysis of the vibration parameters, they have concluded that the Timo Shenko theory is close to the

two-dimensional theory for practical purposes and the application of Euler – Bernoulli theory is limited.

Babu et al. [48] have presented a technique, i.e. amplitude deviation curve, which modifies the operational deflection shape for crack identification in rotors. They have described that the parameters used to characterize the cracks for the damage diagnosis in rotors are very complicated.

Xia et al. [49] have proposed a technique for damage detection by selecting a subset of measurement points and corresponding modes. In their study, two factors have been used for detecting the cracks, the sensitivity of a residual vector to the structural damage and the sensitivity of the damage to the measured noise. They have claimed that the developed method is independent of damage status and is capable of detecting damage using the undamaged state of the structure.

Douka et al. [50] have derived the effect of cracks on the anti-resonances of a cracked cantilever beam using analytical and experimental methods. They have used the shift in the anti-resonances to locate cracks in the structure. The results obtained from their theoretical model have been validated using the results obtained from experimentation of Plexiglas beams for crack diagnosis.

Sinha [51] has analyzed the nonlinear dynamic behaviour in a mechanical system using higher-order spectra tools to identify the presence of harmonics in signals obtained from the system. They have found that misaligned rotating shafts and cracked shafts exhibit nonlinear behaviour due to higher harmonics present in the signal. According to them, the higher-order spectra tools can be effectively used for condition monitoring of mechanical systems.

Patil et al. [52] have derived an algorithm for damage assessment in slender Euler-Bernoulli beams using variation in natural frequencies and the transfer matrix method. They have assumed the cracks as rotational springs to develop the proposed technique for crack detection.

Kim et al. [53] have presented a methodology for crack diagnosis in structures using the dynamic response of a two-span continuous beam. During the technique development, they reviewed two algorithms and eliminated some of the assumptions and limitations in those methods. They have stated that their methodology shows an improved accuracy in crack detection.

Ebersbach et al. [54] have proposed a vibration-based expert system for health monitoring of plant machinery and laboratory equipment to perform routine analysis. They have concluded that their system can be used for high accuracy fault detection using the system's dynamic response.

Gounaris et al. [55] have presented a crack identification method in beam structures, assuming the crack to be open and using eigenmodes of the structure. They found the relationship between the crack parameters and modal response during the investigation. Finally, they have checked the authenticity of their method by comparing the eigenmodes for the damaged and undamaged beams in pre-plotted graphs.

Shen et al. [56] have proposed a crack diagnostic procedure by measuring the natural frequencies and mode shapes. They have checked the robustness of their proposed method from the simulation results of a simply supported Bernoulli-Euler beam with a one-side or symmetric crack.

Ebrahimi et al. [57] have presented a new continuous model for bending analysis of a beam with a vertical edge crack which can be used for load-deflection and stress-strain assessment of the crack beam subject to pure bending. Their proposed model assumes that the displacement field is a superposition of the classical Euler–Bernoulli beam's displacement and a displacement due to the crack. The cracked beam's developed bending differential equation has been calculated using static equilibrium equations. They have found a good agreement between the analytical results and the finite element method.

Jasinski et al. [58] have developed a method for analyzing higher-order spectra to forecast and identify the degree of degradation of a sample's dynamic properties. They have proposed residual bi-spectrum as a basis to determine the initiation of a beam's fatigue-related crack. They have developed an experimental setup for checking the robustness of their proposed technique for fatigue crack identification present in a system.

Hasheminejad et al. [59] have studied the free vibration of cracked nanowires considers the effects of surface elasticity and residual surface stress. The Euler–Bernoulli beam theory has been used by them, and the crack is modelled by a rotational spring representing the discontinuity in the slope and proportional to the crack severity. They have demonstrated examples to evaluate the influence of beam length and crack position, and severity on the calculated values of natural frequencies of an anodic alumina nanowire in the presence of surface effects. They have stated that their proposed study

may be of interest for the design, performance improvement, and health monitoring of nanowire-based components.

Rubio et al. [60] have presented a flexibility expression for cracked shafts having elliptical cracks based on the polynomial fitting of the stress intensity factors, taking into account the size and shape of the elliptical cracks. They have calculated the static displacements in bending of the shaft for different boundary conditions. From the analysis of the results obtained from experimental setup and finite element analysis, they have concluded that their methodology can be suitably used to analyze the cracked shaft's behaviour.

Argatov et al. [61] have considered the problem of detecting localized large-scale internal damage in structures with imperfect bolted joints. Their analysis utilized the structural damping and an equivalent linearization of the bolted lap joint response to separate the combined boundary damage from localized large-scale internal damage. Their approach illustrated the longitudinal vibrations in a slender elastic bar with both ends clamped by bolted lap joints with different levels of damage. They have concluded that their proposed strategy can be utilized to estimate internal damage severity in structures.

Farshidi et al. [62] have investigated the non-contact EMA for evaluating the structural dynamics of a beam structure by exciting a cantilever beam using a collimated air impulse controlled by a solenoid valve. They measured the reflected airwave from the beam surface by a microphone array. They have stated that the experimental tests demonstrate their proposed methodology's effectiveness in accurately and cost-effectively measuring structural dynamics in translational and rotational degrees using a non-contact excitation and sensor mechanism.

Casini et al. [63] have investigated the nonlinear modal properties of a vibrating 2-degree freedom system. They have found that its nonlinear frequencies are independent of the energy level and uniquely depend on the damage parameter. They have analyzed the nonlinear normal modes for a wide range of damage parameters by employing numerical procedures and Poincare maps. The influence of damage on the nonlinear frequencies has been investigated, and modes in internal resonance, with a significantly different shape than modes on a fundamental branch, have been proposed.

Carr et al. [64] have studied the influence of a surface fatigue crack on the vibration behaviour of tee-welded plates, and results are compared to the influence of machined

through-thickness cuts on the dynamic response of cantilever beams. They have analyzed the influence of naturally grown fatigue cracks on the oscillation frequencies and compared two and three-dimensional numerical modelling results. The results obtained from their analysis showed the ability of the experimental technique to detect fatigue cracks relatively earlier than the other method studied.

Ribeiro and Fontul [65] have studied the dynamic response of structure excited at a given set of coordinates using the transmissibility concept to identify fault present in the structure. The finite element methods and wavelet analysis have been used to locate cracks size and severity, and those are being discussed in the next section.

### **2.3.2. Crack detection using finite element method**

Other than the classical methods, the finite element methods are also applied by various researchers for crack detection in damaged structures, and those have been described in this section.

Saavedra et al. [66] have presented a theoretical and experimental vibration analysis of a multi-beam structure containing a transverse crack. They have derived a new cracked finite element stiffness matrix from analyzing the vibrational behaviour of crack systems with different boundary conditions.

Qian et al. [67] have developed a finite element model for crack detection in a damaged beam using stress intensity factors. They have also validated their model with the experimental results obtained for a cantilever beam. According to them, their method is also applicable to complex structures with cracks.

Andreausa et al. [68] have investigated the features of the non-linear response of a crack beam using a two-dimensional finite element model (FEM). They have considered the behaviour of the breathing crack as a frictionless contact problem. They have compared the linear dynamic response with the non-linear dynamic response of the cantilever beam and presented a non-linear technique for crack identification.

Viola et al. [69] have developed a finite element model for a cracked Timoshenko beam for crack identification based on the changes in the structure's dynamic behaviour. They derived the stiffness matrix and consistent mass matrix from developing the crack identification technique.

Chondros et al. [70] have studied the torsional vibrational behaviour of a circumferentially cracked cylindrical shaft using analytical and numerical finite element analysis; they have used HU-WASHIZU-BARR variational formulation to develop the analytical method for the cracked shaft.

Ariaei et al. [71] have presented an analytical approach for determining the dynamic response of the undamped Euler-Bernoulli beams with breathing crack and subjected to the moving mass using the discrete element technique and finite element method. They have observed that the presence of cracks alters the beam response patterns.

Potirniche et al. [72] have developed a two-dimensional finite element method to study the influence of local flexibility on the dynamic response of a structure. Narkis [73] has detected the crack by using the inverse technique, that is, by measuring the frequency of the first two natural frequencies of a simply supported uniform beam. He has validated the developed method by comparing the results from numerical finite element calculations.

Ostachowicz et al. [74] have analyzed the forced vibrations of the beam and found out the impact of crack parameters such as crack position and its severity on the vibrational characteristics and discussed a basis for crack diagnosis. They have modelled the beam with triangular disk finite elements and assumed the crack to be a breathing crack.

Zheng et al. [75] have analyzed a cracked and undamaged beam's natural frequencies and mode shapes by developing an overall additional flexibility matrix using the finite element method. They have also developed a shape function to compute the vibrational characteristics of the cracked beam. The gauss quadrature and least square method compute the overall additional flexibility matrix. The authors have constructed the shape function, which can very well satisfy the local flexibility conditions of the crack locations. Kisa et al. [76] have used finite element and component mode synthesis methods to analyze the free vibration of uniform and stepped cracked beams of the circular cross-section. They have used stress intensity factor and strain energy release rate functions to calculate the flexibility matrix and inverse of the compliance matrix, taking into account inertia forces. According to them, crack depth and crack location considerably affect the natural frequencies and mode shapes of the cracked beam with non-propagating open cracks.

Karthikeyan et al. [77] have proposed a technique for estimating crack location and size in beam structure from the free and forced response of the beam. They have used the finite element method to analyze the modal response for the beam structure with transverse open crack. This work has included the effect of proportionate damping and used an external unit to excite the beam harmonically. They have used an iterative algorithm and regularization technique for locating the crack positions and size on the cracked beam, and the results are in good agreement with other methods, even in the presence of error and noise.

Hearndon et al. [78] have formulated a methodology using Euler-Bernoulli and Timoshenko theories to analyze the effect of crack on the dynamic properties of a cantilever beam subjected to bending. A finite element model has been proposed to evaluate the influence of crack location and size on the structural stiffness and calculation of transfer function. According to them, the reduction in global component stiffness due to the crack is used to determine its dynamic response by a modal analysis computational model. This work revealed that the natural frequencies decrease with increasing crack length.

Al-Said [79] has proposed an algorithm based on a mathematical model to identify crack location and depth in a Euler-Bernoulli beam carrying a rigid disk. He has applied Lagrange's equation to develop the mathematical model for analyzing the lateral vibration of the beam model. The proposed method utilizes mode shapes of two uniform beams connected by a massless torsional spring to establish the trial function. The presented method utilizes the first three natural frequencies to estimate the crack parameters. Results from the presented technique have been authenticated using finite element software.

Shekhar et al.[80] has derived a method to calculate the vibration characteristics using a model based on finite element analysis.

Panigrahi [81] have performed a three-dimensional non-linear finite element analysis to evaluate the normal and shear stress along the overlap zone in a fibre reinforced composite material. Excepting the classical wavelet analysis and finite element methods, Artificial Intelligence Techniques are also being adapted by authors for damage identification.

### **2.3.3. Crack detection using neural networks**

In this section, different neural network methods applied for crack identification are described. Artificial Neural Networks (ANN) have been used as a promising technique in an inverse problem for fault identification.

Schlechtingen et al. [82] have compared results among the regression-based model and two artificial neural network-based approaches, which are a full signal reconstruction and an autoregressive normal behaviour model used for condition monitoring of condition bearings in a wind turbine. The comparison of results revealed that all three models were capable of detecting incipient faults. They have concluded that the neural network model provides the best result with a faster computational time than the regression-based model. Ghate et al. [83] have proposed a multi-layer perceptron neural network-based classifier for fault detection in induction motors which is inexpensive and reliable by employing more readily available information such as stator current. They have used simple statistical parameters as input feature space, and principal component analysis has been used to reduce input dimensionality. They have also verified their methodology to noise and found the performance of the proposed technique encouraging.

Eski et al. [84] have presented a fault detection based on a neural network for an experimental industrial welding robot. They have considered joint accelerations of the robot as evaluation criteria. For this purpose, an experimental setup has been used to collect the corresponding values, and the accelerations of the welding robot, which has six degrees of freedom, are analyzed. The results obtained show that the proposed RBNN has robust stability to analyze the accelerations of the manipulator's joints during a prescribed trajectory.

Fan et al. [85] have presented a fault detection and diagnosis (FDD) strategy for the local system of air handling units. Their strategy consists of two stages: the fault detection stage and the fault diagnosis stage, respectively. In the first stage, the neural network fault detection model was used by them to generate estimates of sensor values, and they were compared to actual values to produce residuals. The proposed neural network fault detection model has been trained using an abundance of characteristic information from the historical data in the HVAC system. They have claimed that the trained neural model can detect abnormal conditions in the system.

Paviglianiti et al. [86] have devised a scheme for detecting and isolating sensor faults in industrial robot manipulators. They have adopted a procedure for decoupling the disturbance effect from the effect of the fault generated in the system. The dynamics of the proposed scheme have been improved by using radial basis functions neural network. Wang et al. [87] have proposed a new fault diagnosis method by using the difference of AR coefficients with a backpropagation neural network. The diagnosis results are compared with the three methods, which include the difference of AR coefficients with BPNN, the AR coefficients with BPNN and the distance of AR coefficients method for various samples. They have found that the difference between AR coefficients with BPNN was superior to AR coefficients with BPNN and distance of AR coefficients methods.

Suresh et al. [88] have presented a method considering the flexural vibration in a cantilever beam having a transverse crack. They have computed modal frequency parameters analytically for various crack locations and depths, and these parameters are used to train the neural network to identify the damage location and size. In this paper, they have made a comparative study of the performance of two widely used neural networks, i.e., multi-layer perception (MLP) network and radial basis function (RBF) network and shown the variation of actual output with the network output. Finally, they have concluded that the radial basis function network performance is better than the multi-layer perception network.

Little et al. [89] have solved exactly a linearized version of the model and explicitly show that the memory capacity is related to the number of synapses rather than the number of neurons. In addition, the research has shown that to utilize this large capacity, the network must store a significant part of the information in memory to generate patterns that evolve with time.

Mehrjoo et al. [90] have presented a fault detection inverse algorithm to estimate the damage intensities of joints in truss bridge structures using the backpropagation neural network method. Agosto et al. [91] have applied a neural network method with vibration and thermal damage detection signatures to develop a damage detection tool. They have applied the developed technique on sandwich composite for crack detection.

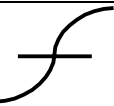
Saravanan et al. [92] have dealt with the robustness of an artificial neural network, wavelet and proximal support vector machine based on fault diagnostic methodology for

a gearbox. They have used the proposed methodology for fault diagnosis in the bevel gearbox. Oberholster et al. [93] have presented a methodology for online structure health monitoring of axially flowing blades using a neural network. The developed neural network has been trained with the extracted vibration features from the experimental test structures. They used frequency response function and finite element models to design the neural network-based technique. The proposed technique can handle the online damage classification using sensors for the test structures.

Wu et al. [94] have described condition monitoring and fault identification techniques for rotating types of machinery using wavelet transform and neural network method. The sound emission from the gear set has been used along with the continuous wavelet transform technique and feature selection of energy spectrum to design the neural network-based fault diagnostic tool. The experimental results from their methodology pointed out that the sound emission from the system can be used for effective fault diagnosis for condition monitoring.

Wu et al. [98] have investigated a fault diagnosis technique for internal combustion engines using discrete wavelet transform (DWT) and neural networks. The DWT technique has been combined with feature selection of energy spectrum to develop the proposed fault detection algorithm. Some of the activation functions researchers use in designing artificial neural networks are presented in Table 2.1 below.

Table 2.1 Examples of Activation Functions used in ANN

Name	Input/output Relation		Symbol
Hard Limit	$a=0$	$n < 0$	
	$a=1$	$n \geq 0$	
Symmetrical Hard Limit	$a= -1$	$n < 0$	
	$a= +1$	$n \geq 0$	
Hyperbolic tangentsigmoid	$e^n - e^{-n} a = e^n + e^{-n}$		

# **CHAPTER 3**

## **EVALUATION OF DYNAMIC CHARACTERISTICS OF BEAMSTRUCTURE WITH TRANSVERSE CRACKS**

It has been observed that the presence of cracks in structures or machine members leads to operational problems and premature failure. Many researchers worldwide are working on structural dynamics, particularly on structures with cracks' dynamic characteristics. The dynamic characteristic comprises natural frequencies, vibration amplitude responses, and mode shapes. Due to the presence of crack, the dynamic characteristics of the structure change, and there is a reduction in natural frequencies and an increase in modal damping.

### **3.1. Introduction**

Different scholars have recently successfully examined the dynamic behaviours of the broken structure. The existence of a fracture in the structure causes the modal parameters to vary, and the intensity of the variation is a function of the crack intensity and location. Engineers and scientists have focused on how cracks affect the inherent frequencies and mode forms of dynamically vibrating structures, which can be used to build crack detection algorithms. This chapter focuses on using a systematic method to develop a theoretical model for analysing the influence of many cracks on the modal response of a cantilever beam structure. The dimensionless compliance matrices and, consequently, the local stiffness matrices were calculated using the stress intensity factor and strain energy release rate from linear fracture mechanics theory. The stiffness matrix was used to determine the differences in dynamic response between the many cracked beams and the intact beam. The natural frequencies and mode shapes for the cantilever beam structure with varied fracture depths and crack locations have been computed using different boundary conditions in the theoretical analysis. By comparing the results with the experimental analysis, the modal responses derived from the theoretical analysis have been verified.

### 3.2. Vibration characteristics of a cracked cantilever beam

This section describes the method used to develop a theoretical model for measuring the modal characteristics of a cracked beam with a transverse crack, such as natural frequencies and mode shapes, for various relative crack depths and relative crack positions, as well as the undamaged beam structure. During the study of the theoretical results, it was discovered that near crack locations, a noticeable change in the first three mode forms had occurred.

#### 3.2.1. Vibration analysis of the cracked cantilever beam

A cantilever beam (Fig. 3.1) with a crack of length ' $L'$ ', width 'b', and depth 'h' has been investigated in this section, with a crack at a distance ' $L_c$ ' and with a crack depth of ' $h_c$ ' from the fixed end.

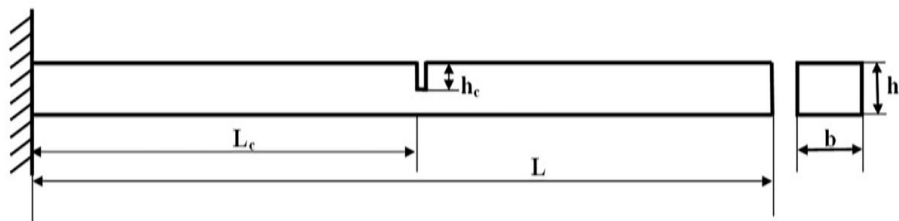


Fig. 3.1. Cantilever beam elemental model

#### 3.2.2. Numerical analysis

For numerical analysis, the cantilever beam with many cracks and undamaged circumstances was used to calculate the relative natural frequencies and vibration amplitude for various crack positions and severity. The cantilever beam model utilized for the vibration analysis in this study has the following dimensions.

Length of the beam = 1500mm

Width of the beam = 25mm

Depth of the beam = 10mm

Relative crack depth( $h_c/h$ ) = Varies from 0.1 to 0.6

Relative crack location( $L_c/L$ ) = Varies from 0.034 to 0.967

#### 3.2.3. Results for theoretical analysis

The theoretical analysis has been carried out to obtain the frequencies and mode shapes for the first ten modes of the cracked aluminum cantilever beam model with different crack locations and crack severities using the ANSYS modal module. The figures show the three-dimensional graphs with relative crack location on the x-axis, relative crack depth on the y-axis and relative frequencies on the z-axis.

# **CHAPTER 4**

## **ANALYSIS OF FINITE ELEMENT FOR CRACK DETECTION**

One form of damage that can lead to catastrophic failure of the beam structures is transverse cracks if undetected in their primary stages. However, it is challenging to locate a crack using visual inspection, and it may be detected usually by non-destructive techniques such as x-ray or ultrasonic tests. However, these techniques are unsuitable for various engineering systems as they require periodic inspection. In the past couple of decades, several models have been developed to predict the damage characteristics using the vibrational behaviour of the damaged beam structures. Vibration-based methods for the detection of cracks offer some advantages over conventional methods. This methodology can help determine the cracks' location and size from the vibration data collected from the cracked beam structure. The crack developed in the structure generates flexibility in the vicinity of the crack, giving rise to a reduction in natural frequencies and the change in the mode shapes. Hence, it may be possible to estimate the location and size of the cracks by measuring changes in the vibration parameters. Scientists have studied single crack detection in the beam by adopting an analytical structure model. This chapter introduces finite element analysis to identify cracks present in structural systems.

### **4.1. Introduction**

Automation of fault identification in various engineering systems can be termed as the implementation of a systematic approach to detect and quantify the presence of faults present in the system. Faulty beam has been a significant concern for failure analysts of structural systems for overall safety and performance. The modal responses of the damaged members can be potentially used for estimating the damage parameters present in the beam members. In due course of the development of different crack detection techniques, researchers have used energy-based methods, wavelet analysis, numerical techniques such as the finite element method, and artificial intelligent methods. In the last few decades, scientists have addressed the problem of detecting a single crack present in

a beam model using finite element analysis, and it is cited that the performance of FEA is better than the theoretical model developed for crack diagnosis. So, this technique can be used to detect the presence of single crack with its crack features, such as crack depth and crack location in systems using the vibration response of the system.

In this present investigation for fault identification in a cracked beam containing a single transverse crack, finite element analysis has been carried out to identify crack depths and positions. It has been established that a crack in a beam has an essential effect on its dynamic behaviour. Theoretical and experimental analyses have been done to validate the results obtained from the finite element analysis of the multi cracked cantilever beam structure. In the theoretical analysis, the strain energy density function is used to evaluate the additional flexibility produced due to the presence of a crack. Based on the flexibility, a new stiffness matrix is deduced, and subsequently, that is used to calculate the cracked beam's natural frequencies and mode shapes. The results from the finite element and experimental methods are compared with the results from the numerical analysis for validation. The results are found to be in good agreement.

## 4.2. Finite Element Analysis

The finite element analysis is a useful numerical technique that utilizes variational and interpolation methods for modelling and solving boundary value problems such as the one described in this current chapter. The finite element analysis is very systematic and can be helpful for the model with complex shapes. So, the finite element model can be suitably employed for solving vibration-based problems with different boundary conditions. Commercial finite element packages are available to address the practical problems. During finite element analysis, the structure is approximated in two ways. The first step is employed by dividing the structure into many small parts. The small parts are known as finite elements, and the procedure adopted to divide the structure is called discretization. Each element in the structure is usually associated with the equation of motion, which can be easily approximated. Each element on the finite element model has endpoints known as nodes. The nodes are used for connecting one element to another element. The finite element and nodes are collectively called finite element mesh or finite element grid. In the second approximation level, the vibration equation for each finite element is determined and solved. The solution for each finite element is brought together to generate the global mass and stiffness matrices describing the vibrational response of

the whole structure. The displacement associated with the solution represents the motion of the nodes of the finite element mesh. These global mass and stiffness matrices represent the lumped parameter approximation of the structure and can be analysed to obtain natural frequencies and mode shapes of damaged vibrating structures.

#### 4.2.1. Analysis of cracked beam using finite element analysis (FEA)

In the following section FEA is analyzed for vibration analysis of a cantilever cracked beam (Fig. 4.1). The relationship between the displacement and the forces can be expressed as;

$$\begin{Bmatrix} u_j - u_i \\ \theta_j - \theta_i \end{Bmatrix} = C_{ovl} \begin{Bmatrix} u_j \\ \phi_j \end{Bmatrix} \quad (4.1)$$

Where overall flexibility matrix  $C_{ovl}$  can be expressed as;

$$C_{ovl} = \begin{pmatrix} R_{11} & -R_{12} \\ -R_{21} & R_{22} \end{pmatrix}$$

The displacement vector in equation (4.1) is due to the crack.

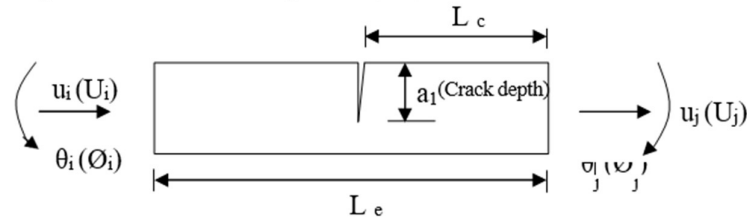


Figure 4.1 View of a crack beam element subjected to axial and bending forces.

Where,

$R_{11}$ : Deflection in direction 1 due to load in direction 1

$R_{12} = R_{21}$ : Deflection in direction 1 due to load in direction 2

$R_{22}$ : Deflection in direction 2 due to load in direction 2.

Under this system, the flexibility matrix  $C_{intact}$  of the intact beam element can be expressed as;

$$\begin{Bmatrix} u_j - u_i \\ \theta_j - \theta_i \end{Bmatrix} = C_{intact} \begin{Bmatrix} u_j \\ \phi_j \end{Bmatrix} \quad (4.2)$$

Where,

$$C_{\text{intact}} = \begin{pmatrix} Le/EA & 0 \\ 0 & Le/EI \end{pmatrix}$$

The displacement vector in equation (4.2) is for the intact beam.

The total flexibility matrix  $C_{\text{tot}}$  of the damaged beam element can now be obtained by

$$C_{\text{tot}} = C_{\text{intact}} + C_{\text{ovl}} = \begin{pmatrix} Le/EA + R_{11} & -R_{12} \\ -R_{21} & Le/EI + R_{22} \end{pmatrix} \quad (4.3)$$

Through the equilibrium conditions, the stiffness matrix  $K_c$  of a damaged beam element can be obtained as [80]

$$K_c = DC_{\text{tot}}^{-1} D^T \quad (4.4)$$

Where  $D$  is the transformation matrix and expressed as;

$$D = \begin{pmatrix} -1 & 0 \\ 0 & -1 \\ 1 & 0 \\ 0 & 1 \end{pmatrix}$$

# **CHAPTER 5**

## **ANALYSIS OF ARTIFICIAL NEURAL NETWORK FOR CRACK DETECTION**

The presence of damage in general in a structure undermines the structure's viability, leads to a shorter lifetime period, and opens the way for the system's complete failure. Hence, developing an automated method to identify cracks accurately in an engineering application is desirable. As it is known, the cracks present in a mechanical element increase the flexibility, decrease the vibration frequencies and modify the amplitude of vibration. Those changes can potentially be used to locate the crack positions and depths. So, it is of interest to design and develop an AI-based technique for online crack diagnosis to avoid catastrophic failure of the structural system. In the current chapter, an intelligent model has been designed using an artificial neural network to detect the presence of a crack in structural members. The proposed neural model is modelled with a feed-forward network trained with the backpropagation technique. Finally, the results from the model have been compared with the experimental results to establish the robustness of the proposed neural method.

### **5.1. Introduction**

This section of the thesis introduces basic neural network architectures and learning rules. The complex biological neural network in a human body has a highly interconnected set of neurons that facilitate various kinds of output such as thinking, breathing, driving etc. Generally, the neurons are believed to store the biological neural functions and memory, and learning of the neural system facilitates the establishment of new connections between the neurons. The most interesting feature of this artificial neural network (ANN) is the novel structure of the information processing system. It is composed of a large number of highly interconnected processing elements (neurons) working in parallel to solve specific applications, such as pattern recognition or data classification, through a learning process. Learning in biological systems involves adjustments to the synaptic weights between the neurons. With their remarkable ability to derive meaning from complicated or imprecise

data, neural networks can be used to recognize patterns and detect trends that are too complex to be noticed by either humans or other computer techniques. McCulloch and Pitts [96] have developed models of neural networks with several assumptions about how neurons work. The proposed networks were considered to be binary devices with fixed thresholds based on simple neurons. Rosenblatt [97] has designed and developed the Perceptron. The developed Perceptron has three layers, with the middle layer known as the association layer. This system could learn to connect or associate a given input to a random output unit. According to [95], a neural network is a significant parallel distributed processor made up of simple processing units, called neurons, which have a natural tendency to store experimental knowledge and make it available for use. Some of the advantages of the ANN are depicted below.

**Adaptive learning:** The ability of the neural system lies in the capacity to adapt to the changing environment by adjusting the synaptic weights and performing according to the situation. This feature makes the neural network a methodology to address industrial applications in a dynamic environment.

**Self-Organization:** An artificial neural network can produce results for inputs that are not used during training by creating its own representation of the information it receives during learning time. This capability helps in solving the problem of higher complexities.

**Real-Time Operation:** The neural network is composed of many interconnected neurons working in parallel to solve a specific problem. Neural networks learn by example. For this, special hardware devices are being designed and manufactured which take advantage of this capability.

**Fault Tolerance:** In case of failure of a neuron in a neural network system, there will be a partial destruction of a network, leading to the only deterioration of quality of output rather than collapsing the system as a whole.

In the last few decades, research has been carried out to develop a system for online condition monitoring of structural systems. As the presence of cracks reduces the service life of the structures and is also responsible for economic loss and, in some cases, maybe loss of human life, developing a fault diagnostic methodology is of paramount importance for the science community. Although different non-destructive techniques (e.g., acoustic emission, sensor) are available to identify cracks present in a system, the response of the

techniques is feeble in terms of accuracy and computational time for a complex system. Moreover, developing a mathematical model for a complex system with changing environment becomes impossible. In this scenario, the use of ANN, with its parallel computing and pattern recognition capabilities, is suitable for designing an intelligent system for damage assessment in cracked structures with higher accuracy and faster computational time. In recent times, scientists have made much effort to develop crack diagnostic tools using ANN. Schlechtingen et al. [82] have compared results among the regression-based model and two artificial neural network-based approaches, which are a full signal reconstruction and an autoregressive typical behaviour model used for condition monitoring of condition bearings in a wind turbine. The comparison of results revealed that all three models were capable of detecting incipient faults. They have concluded that the neural network model provides the best result with a faster computational time than the regression-based model. Ghate et al. [83] have proposed a multi-layer perceptron neural network-based classifier for fault detection in induction motors which is inexpensive and reliable by employing more readily available information such as stator current. They have used simple statistical parameters as input feature space, and principal component analysis has been used to reduce input dimensionality. They have also verified their methodology to noise and found the performance of the proposed technique encouraging.

This section introduces a feed-forward multi-layer neural network trained with a backpropagation technique for online damage detection in beam members. The proposed neural network system has been designed with six input parameters (first three relative natural frequencies, first three relative mode shape differences) and four output parameters (relative first crack location, relative first crack depth, relative second crack location and relative second crack depth). A comparison of results obtained from fuzzy, numerical, FEA, neural and experimental analysis has been carried out, and it is observed that the developed neural network provides more accurate results than other mentioned methods. The robustness of the neural system has been validated using the experimental set-up.

The present chapter has been arranged into five different sections. The first section, i.e., introduction (Section 5.1), gives a brief introduction to neural network algorithms. Section 5.2 provides an in-depth view of the feed-forward neural network trained with the backpropagation technique. The analysis of the neural network model used for crack diagnosis is presented in section 5.3.

## 5.2. Neural network technique

Given this neural network description, it has been successfully implemented in many industrial applications such as industrial process control, sales forecasting, electronic noses, modelling, diagnosing the Cardiovascular System, etc. The parallel computing capability and the ability to perform under changing environments make the neural network a potential tool to address applications which are hard to solve using analytical or numerical methods.

### 5.2.1. Model of a neural network

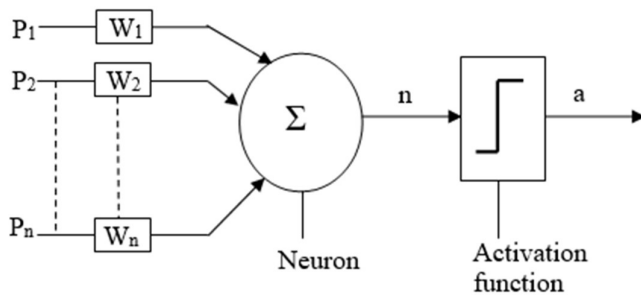


Fig 5.1 Neuron model

A neuron which can be used in a dynamic environment is shown in Fig. 5.1. An artificial neuron is a device with many inputs and one output. The neuron has two modes of operation; the training mode and the using mode. The neuron can be trained to fire (or not) for particular input patterns in the training mode. When a taught input pattern is detected at the input, its associated output becomes the current output in the user mode. If the input pattern does not belong in the taught list of input patterns, the firing rule is used to determine whether to fire or not.

The main features of the neural model are as follows,

1. The neurons inputs are assigned with synaptic weights, which affects the neural network's decision-making ability. The inputs to the neuron are called weighted inputs.
2. These weighted inputs are then summed together in an adder, and if they exceed a pre-set threshold value, the neuron fires. In any other case, the neuron does not fire.

3. An activation function for limiting the amplitude of the output of a neuron. Generally, the normalized amplitude range of the output of a neuron is given as the closed unit interval [0,1] or [-1,1].

### **Learning process of ANN:**

The learning for a neural network means following a methodology for modifying the weights to make the network adaptive in nature to changing environments. The learning rules may be broadly divided into three categories,

1. *Supervised learning*: The supervised learning rule is provided with a set of training data for proper network behaviour. When the inputs are applied to the network, the outputs from the network are compared with the targets. Through the learning process, the network will adjust the weights of the network in order to bring the outputs closer to the targets.
2. *Unsupervised learning*: In this type of learning, the network modifies the weights in response to the inputs to the network. This category is suitable for applications requiring vector quantization.
3. *Reinforcement learning*: In reinforcement learning, instead of providing the correct output, the algorithm is only given a score for each network input. The score is the measure of network performance over some sequence of inputs.

In mathematical terms, we can describe a neuron k by writing the following pair of equations:

$$u_k = \sum_{j=1}^p w_{kj} x_j \quad (5.1)$$

$$y_k = f(u_k) \quad (5.2)$$

Where  $x_1, x_2, \dots, x_p$  are the input signals,  $w_{k1}, w_{k2}, \dots, w_{kp}$  are the synaptic weights of neuron k,  $u_k$  is the linear combined output,  $f(\cdot)$  is the activation function, and  $y_k$  is the output signal of neuron.

#### **5.2.2. Use of back propagation neural network**

The backpropagation technique (Fig. 5.2) can be used to train the multilayer networks. This technique is an approximate steepest gradient algorithm in which the network's

performance is based on mean square error. In order to train the neural network, the weights for each input to the neural system should be so adjusted that the error between the actual output and desired output is minimum. The multilayer neural system would calculate the change in error due to an increase or decrease in the weights. The algorithm first computes each error weight by computing the rate of the error changes with the change in synaptic weights. The error in each hidden layer just before the output layer in a direction opposite to the way activities propagate through the network must be computed and fed to the network by a backpropagation algorithm to minimize the error in the actual output and desired outcome output by adjusting the parameters of the network.

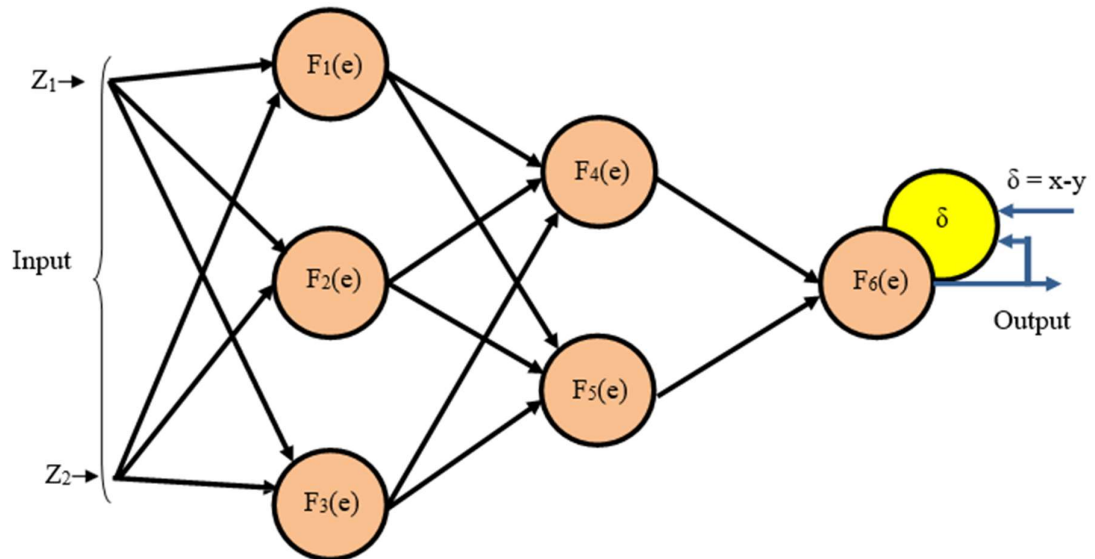


Fig. 5.2 Back propagation technique

### 5.3. Analysis of neural network model used for crack detection

A backpropagation neural model has been proposed to identify a cantilever beam structure's crack (i.e., relative crack locations, relative crack depths) (Fig. 5.3). The neural model has been designed with ten input parameters and two output parameters.

The inputs to the neural network model are the ratios of first ten natural frequencies of the damaged beam to those of the undamaged beam obtained from modal analysis in ANSYS and the output parameters consists of the relative crack location and relative crack depth.

The backpropagation neural network has been made with one input layer, one output layer and eight hidden layers. The input layer contains ten neurons, whereas the output layer contains two neurons. The number of neurons in each hidden layer is different in order to give the neural network a diamond shape and for better convergence of results (Fig. 5.4). The neurons associated with the network's input layer represent the first ten relative natural frequencies. The relative crack location and relative crack depth are represented by the two neurons of the output layer of the neural network.

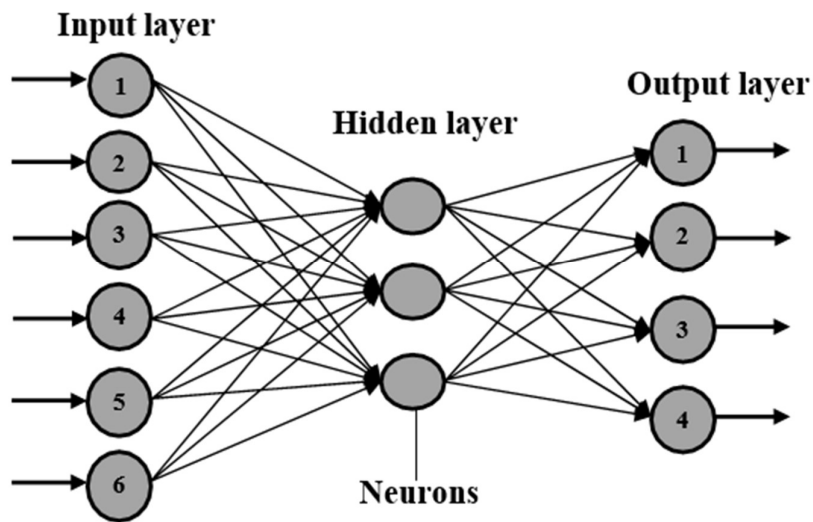


Fig. 5.3. Neural model

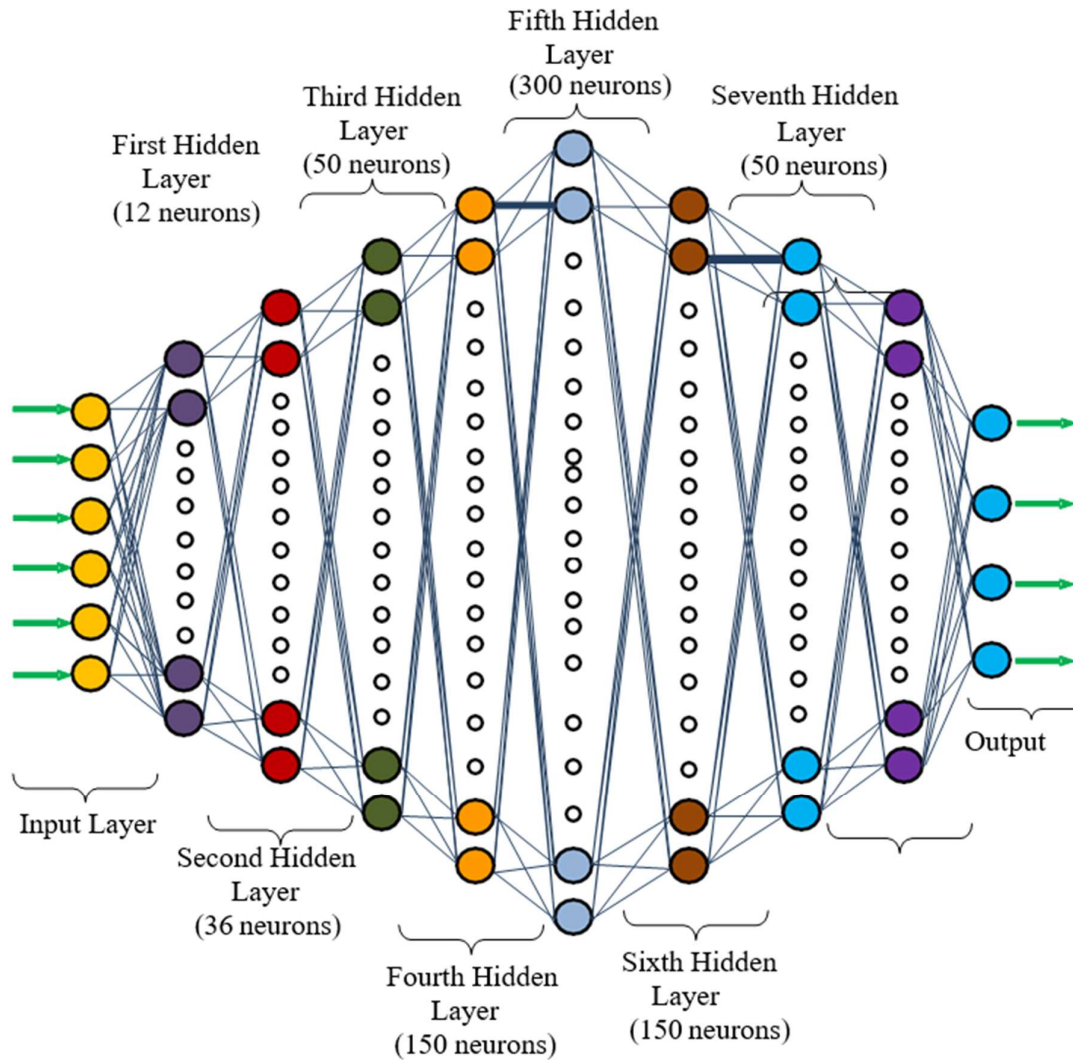


Fig. 5.4. Multi-layer feed forward back propagation neural model for damage detection

### 5.3.1. Neural model mechanism for crack detection

The neural network used in the current investigation is a ten-layer feed-forward neural network model trained with the backpropagation technique [95]. The chosen number of layers was found empirically to facilitate training. The first ten relative natural frequencies are the neurons representing the network's input layer, and relative crack location and relative crack depth are represented by the two neurons of the output layer. The hidden layers, i.e., 2nd, 3rd, 4th, 5th, 6th, 7th and 8th layer, comprise 12 neurons, 36 neurons, 50 neurons, 150 neurons, 300 neurons, 150 neurons, 50 neurons, and 8 neurons, respectively. The number of neurons in each hidden layer has been decided using the

empirical relation. Figure 5.4 depicts the neural network with its input and output signals.

### 5.3.2. Neural model for finding out crack depth and crack location

The feed-forward network has been trained with 696 different patterns of parameters to obtain the objective. Some of the test patterns are depicted in Table 5.1. The intelligent neural system has ten input parameters in the input layer, i.e., first ten relative natural frequencies. The output layer has two outputs: relative crack location and relative crack depth.

Table 5.1. Test patterns for NN model other than test data

Relative first natural frequency	Relative second natural frequency	Relative third natural frequency	Relative fourth natural frequency	Relative fifth natural frequency	Relative sixth natural frequency	Relative seventh natural frequency	Relative eighth natural frequency	Relative ninth natural frequency	Relative tenth natural frequency	Relative crack location	Relative crack depth
0.9984	0.9994	0.9987	0.9995	0.9990	0.9992	0.9996	0.9995	0.9996	0.9997	0.032	0.163
0.9946	0.9979	0.9958	0.9983	0.9968	0.9976	0.9987	0.9983	0.9989	0.9990	0.028	0.22
0.9881	0.9953	0.9908	0.9964	0.9930	0.9949	0.9972	0.9965	0.9977	0.9980	0.035	0.33
0.9769	0.9915	0.9827	0.9935	0.9870	0.9906	0.9950	0.9935	0.9958	0.9964	0.031	0.414
0.9625	0.9874	0.9799	0.9930	0.9903	0.9967	0.9965	0.9997	0.9997	0.9988	0.029	0.534
0.9588	0.9861	0.97	0.9895	0.9779	0.9843	0.9920	0.9894	0.9932	0.9942	0.033	0.592

# CHAPTER 6

## METHODOLOGY

### 6.1. General

Modal testing is an effective tool for structural health monitoring using vibration analysis and diagnosis. The principal objective of modal testing is to decide the resonant frequencies, damping parameters, and mode shapes. If the operating frequency of the beam and the natural frequency of the test beam match, then a resonance condition exists. Therefore, it is compulsory to recognize the resonant frequencies of the structure to be monitored before experimentation.

To develop the governing equation of motion, consider a beam structure of length = L, depth = h, and width = b, as shown in Fig. 6.1. Let P (x) is distributed load/length, M = bending moment and Q = shear force. Consider a Small part of length as dx at a distance of x from clamped support. By applying the equilibrium equation of the elemental part,  $P(x) = \partial Q / \partial x$ .

$P(x)$  is the ratio of change of shear force and length of the beam.

Shear force  $Q = \partial M / \partial x$

The ratio of the difference in bending moment and length of the beam is termed a shear force. The deflection equation of the beam is given by

$$EI \frac{\partial^2 y}{\partial x^2} = M$$

Where E is Young's Modulus and I' is the moment of inertia becomes

$$\frac{\partial^2}{\partial x^2} [ EI \frac{\partial^2 y}{\partial x^2} ] = P(x)$$

If beam density is  $\rho$  and cross-sectional area is A, then inertia force =  $ma$

$$P(x) = - \rho A \frac{d^2 y}{dt^2}$$

$$\frac{\partial^2}{\partial x^2} [ EI \frac{\partial^2 y}{\partial x^2} ] = - \rho A \frac{\partial^2 y}{\partial t^2}$$

$$\frac{\partial^4 y}{\partial x^4} + \rho A EI \frac{\partial^2 y}{\partial t^2} = 0$$

where 'y' is beam displacement in the vertical direction at 'x' from the clamped support.

The cantilever beam-free end is deflected from one region to another with maximum amplitude, but amplitude is zero at the fixed end and some other points.

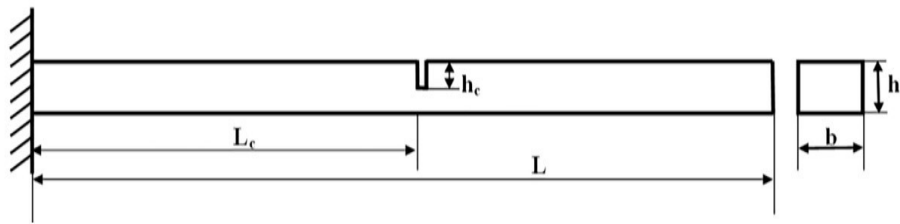


Fig. 6.1. Plane view of cantilever beam

## 6.2. Modal Analysis

Modal analysis is the study of the dynamic properties of structures under vibrational excitation. Modal analysis measures and analyses the dynamic response of structures or fluids during excitation. The modal analysis aims to find the shapes & frequencies at which the structure will amplify the effect of load. Modes are inherent properties of the structure and are determined by the structure's material properties and boundary conditions. Each mode is defined by natural frequencies, modal damping, and a mode shape.

A beam is considered, as shown in Fig. 6.1. The geometry is created using CATIA v5 R21 software and is shown in Fig. 6.2. Cracks at different positions of different depths are considered on the cantilever beam, starting from the fixed end up until the free end. ANSYS modal module is selected, and the geometry of the beam with different crack lengths and severities is imported into ANSYS Design Modeller. This beam consideration can comprehend for similar slender beams, irrespective of the cross-section and length, as we have considered the relative values of the severities and positions of the crack, i.e., the depth and length ratios, respectively. Four different Aluminium grade alloy materials viz Al 6061, Al 6013, Al 5052, and Al 5024 are used in this work, thus increasing the scope for collecting a number of data samples, for further analysis.

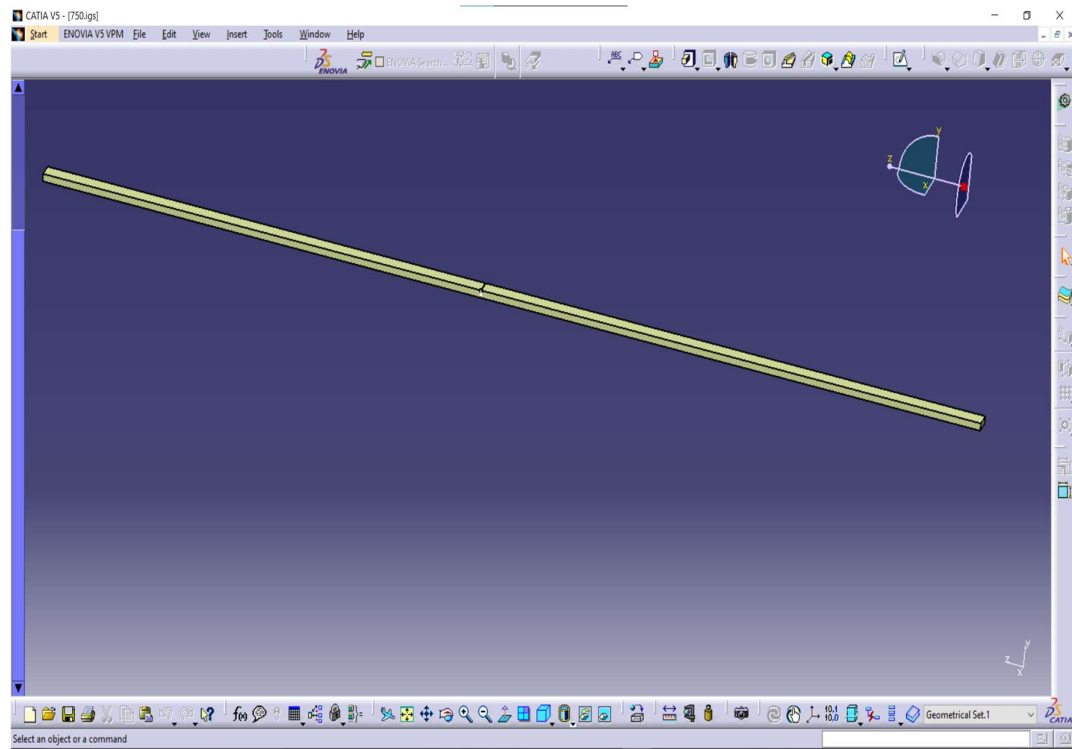


Fig. 6.2. Catia sketch of the beam

### 6.3. Importing geometry

The beam modelled in Catia VR 5 is converted into IGES(.igs) format and this IGES file is imported in the Design Modeller of Modal solver in ANSYS.

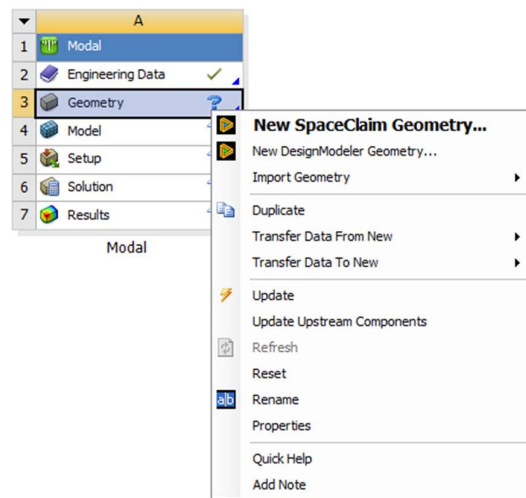


Fig. 6.3. Opening of Design Modeller

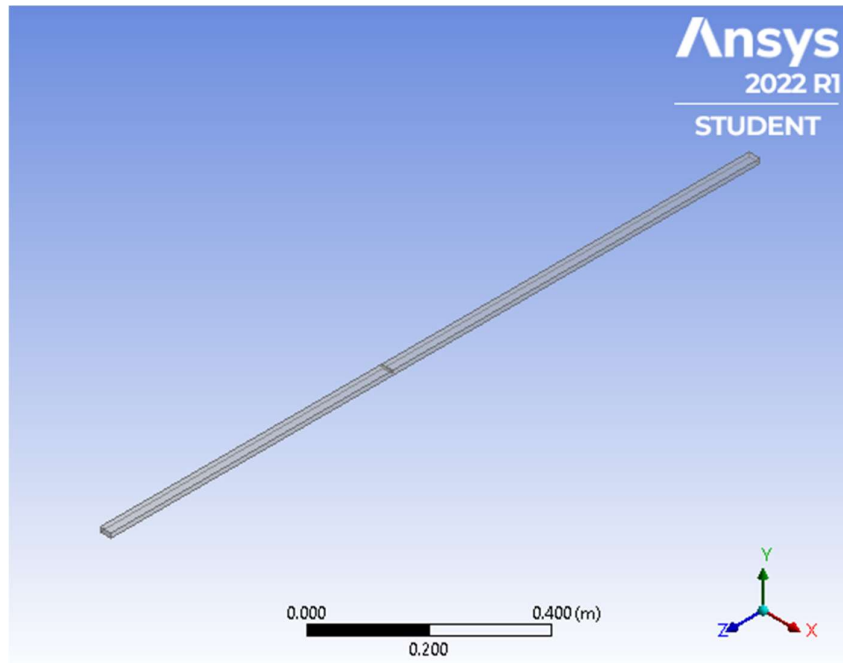


Fig. 6.4. ANSYS view of the beam

#### 6.4. Assigning materials to the geometry

After importing the geometry into Design Modeller, open Model and then in the geometry branch of the tree, assign the material whose properties are to be considered for the purpose of analysis.

#### 6.5. Meshing

After assigning the materials to the geometry, meshing is done. Meshing is an important process of analysis and it should be performed on the entire beam including the crack. Meshing is the process of dividing the created model in number of divisions or elements which consists of nodes. By applying meshing process, we can determine the efficiency and effectiveness of any analysis. Under mesh sizing, mesh was set to fine mesh and under mesh methods, elements are set to Quadrilateral to achieve accurate and precise results. A mesh element of size 3mm is used for fine meshing.

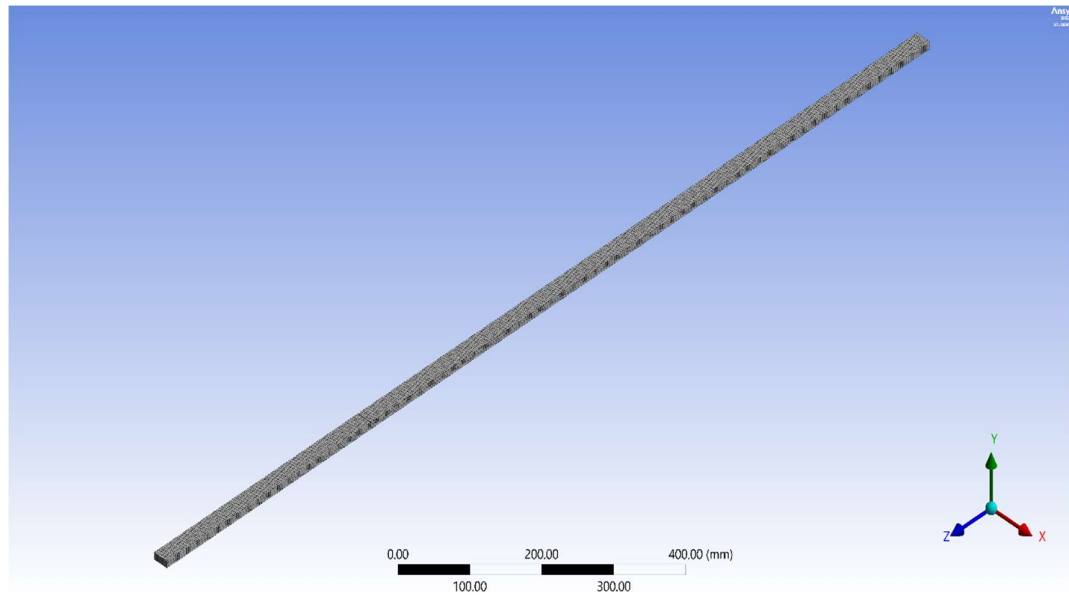


Fig. 6.5. Mesh model of the beam

## 6.6. Construction of path

In ANSYS Modal module, open model section, click on construction geometry and select path option. Further, specify the starting and ending points for the generation of path as (0,0,0) and (0,0,1500) respectively.

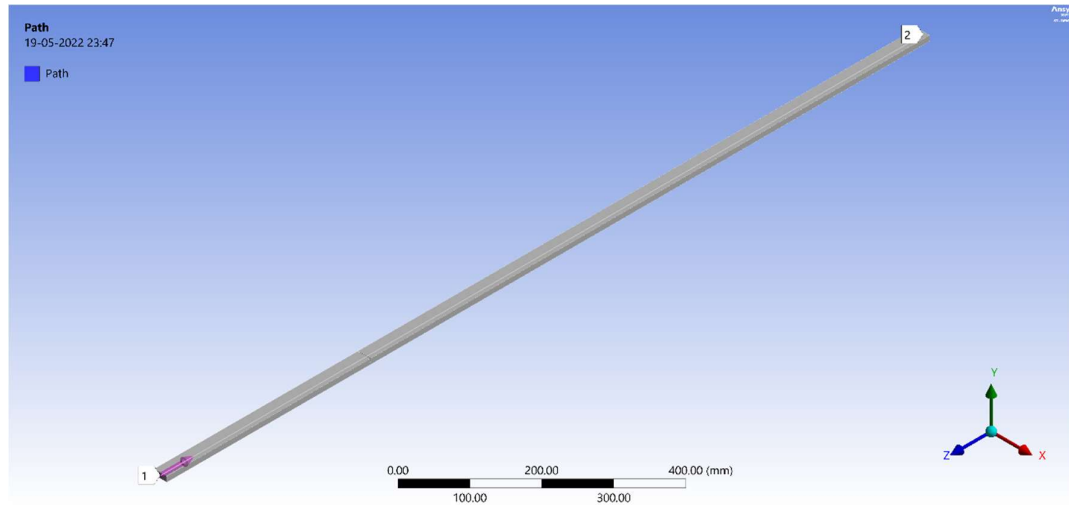


Fig. 6.6. Construction Path

## 6.7. Materials used

Four different grades of Aluminium alloy are used viz. Al 6061, Al 6013, Al 5052 and Al 5024, whose properties are shown in table 6.1.

Table 6.1. Material Properties

Material	Young's Modulus (GPa)	Density (g/cm <sup>3</sup> )	Poisson's ratio
Al 6061	68.9	2.7	0.3
Al 6013	69	2.8	0.33
Al 5052	69.3	2.68	0.33
Al 5024	72	2.65	0.33

## 6.8. ANSYS results

Modal Analysis is performed in ANSYS software, and the natural frequencies, mode shapes, directional deformations, and total deformations for the beam are calculated. The obtained results are tabulated which are shown in the further chapters. Apart from the tabulated results, 3-directional graphs are plotted, using MATLAB and Sigma Plot. These act as a helpful reference for further analysis.

Further, the obtained directional deformations serve as the basis for generating MAC (Modal Assurance Criterion) values. These MAC values are generated in order to fortify the accuracy of the results while performing functions like “training”, “testing”, and “validation” in MATLAB.

The obtained MAC values are tabulated for all modes, ranging from 1 to 10. The subsequent objective of the project is to deliver a data set (to be referred in Appendix B) consisting of the aforementioned relative frequencies, relative severities, relative positions, and MAC values.

The data obtained is fed to the Artificial Neural Network tool in MATLAB software to perform the “Training” operation for 80% of the total data set obtained, while the rest 20% of it is fed to the tool for “Testing” (to be referred in Appendix B).

The final objective is to predict the location and severity of the crack as a consequence of performing reverse-engineering using MATLAB's Neural Network tool. In other words, if the frequency obtained through practical apparatus is fed to the program, we would have trained the tool to predict the relative position and severity of the crack on the beam. "Validation" is performed by giving such frequency values of such cracks to get their severity and position on the beam.

## 6.9 Modal Assurance Criterion

The Modal Assurance Criterion is a statistical indicator that is most sensitive to large differences and relatively insensitive to small differences in the modes. Mode shapes that are used in the comparison can originate from a Finite Element Analysis or from experimental modal analysis.

Alongside the evaluation of the natural frequencies, the use of the Modal Assurance Criterion (MAC) to quantify a mode-to-mode correlation between 6 Journal Pre-proof Journal Pre-proof damaged and undamaged structures. It is calculated as the normalized scalar product of two modal vectors.

The MAC value between two modes is essentially the normalized dot product of the complex modal vector at each common node (i.e., points), as shown in Fig.6.7.

$$MAC_{ij} = \frac{|\{\phi_{A_i}\}^T \{\phi_{B_j}\}|^2}{\{\phi_{A_i}\}^T \{\phi_{A_i}\} \{\phi_{B_j}\} \{\phi_{B_j}\}^T}$$

Fig.6.7. Formula to evaluate MAC

where  $\{\phi_A\}$  and  $\{\phi_B\}$  are the damaged and undamaged modal vector for the  $i^{th}$  and  $j^{th}$  modes, respectively. This indicator can take values from 0 (no consistent correspondence) to 1 (consistent correspondence).

If a linear relationship exists (i.e., the vectors move the same way) between the two complex vectors, the MAC value will be near to one. If they are linearly independent, the MAC value will be small (near zero).

A complex vector simply includes both amplitude and phase, whereas a real vector is a real part only. In the above figure, it is also clear that the MAC is not sensitive to scaling, so if all mode shape components are multiplied with the same factor, the MAC will not be affected.

# CHAPTER 7

## RESULTS AND DISCUSSIONS

### 7.1. Total Deformations and Directional Deformations

In addition, Frequency responses, total deformation responses and directional deformation responses of the beam are calculated and tabulated for all the 10 modes corresponding to all the four materials considered, and the Modal Assurance Criterion values are also calculated.

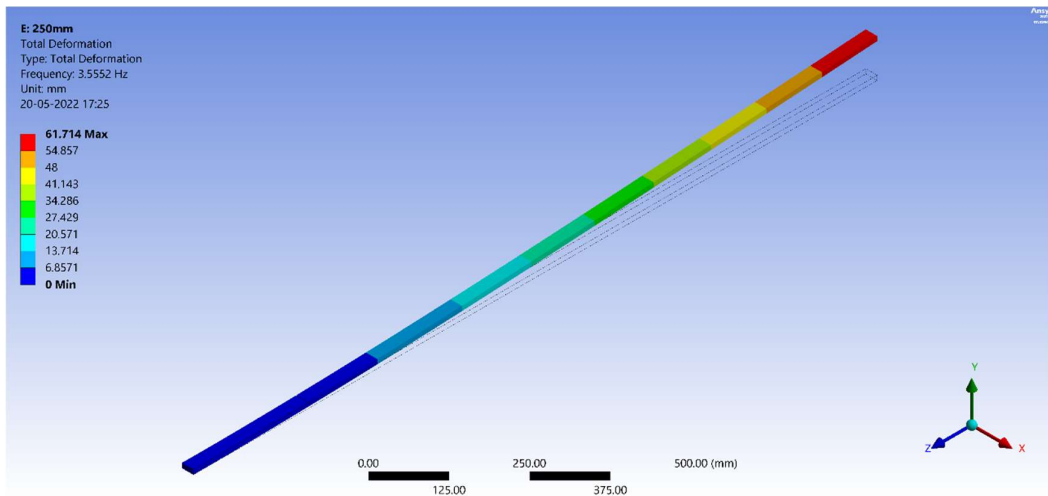


Fig. 7.1. (a) Total Deformation, Mode 1

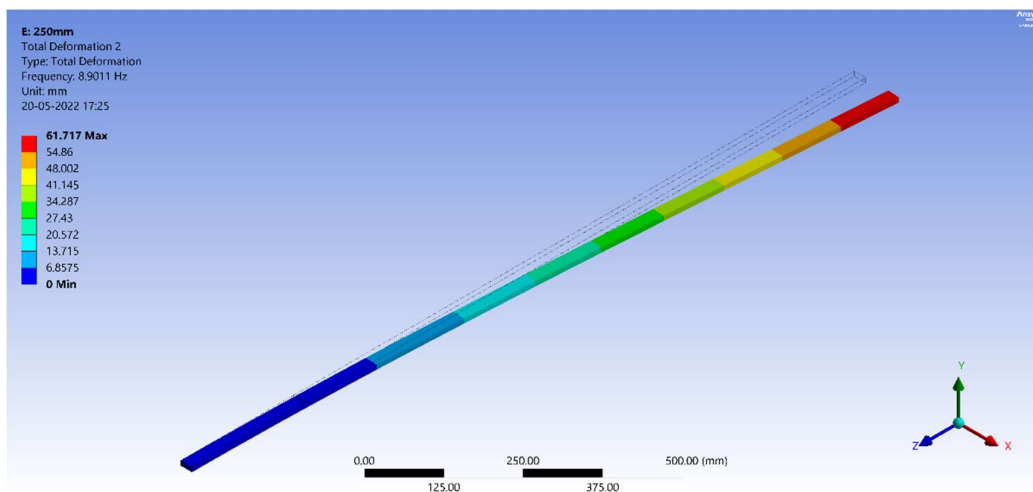


Fig. 7.1. (b) Total Deformation, Mode 2

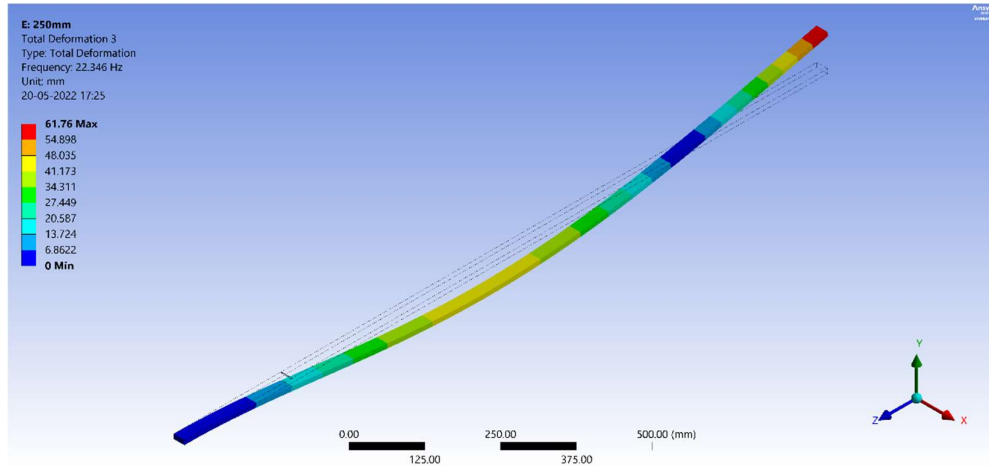


Fig. 7.1. (c) Total Deformation, Mode 3

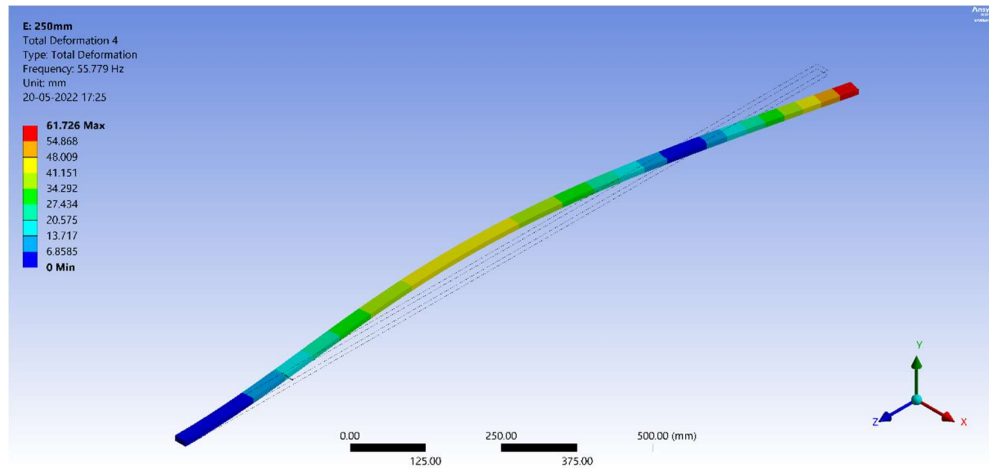


Fig. 7.1. (d) Total Deformation, Mode 4

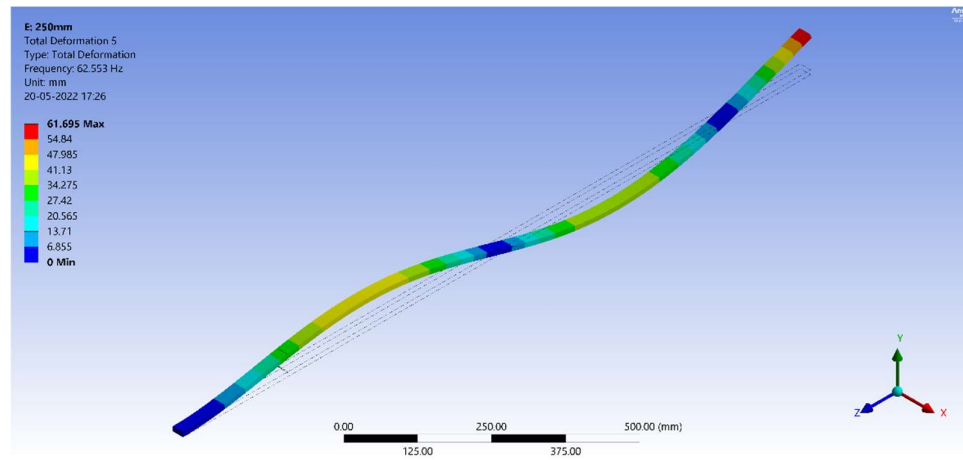


Fig. 7.1. (e) Total Deformation, Mode 5

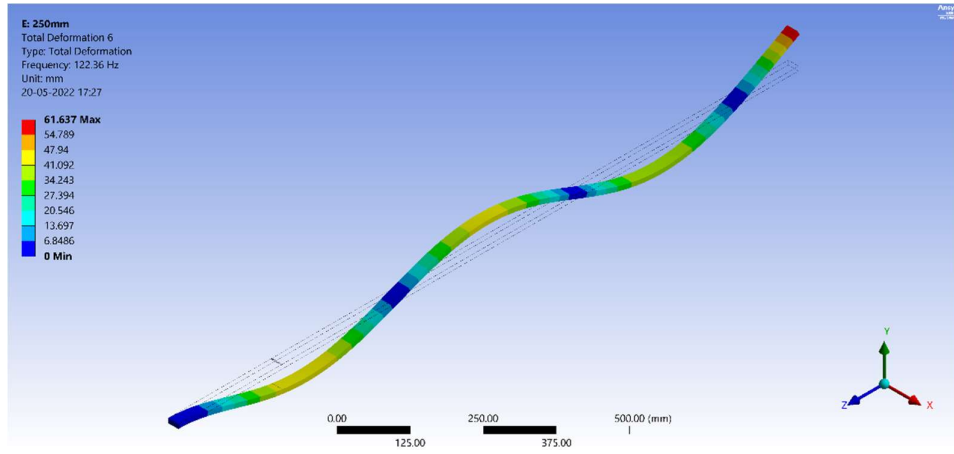


Fig. 7.1. (f) Total Deformation, Mode 6

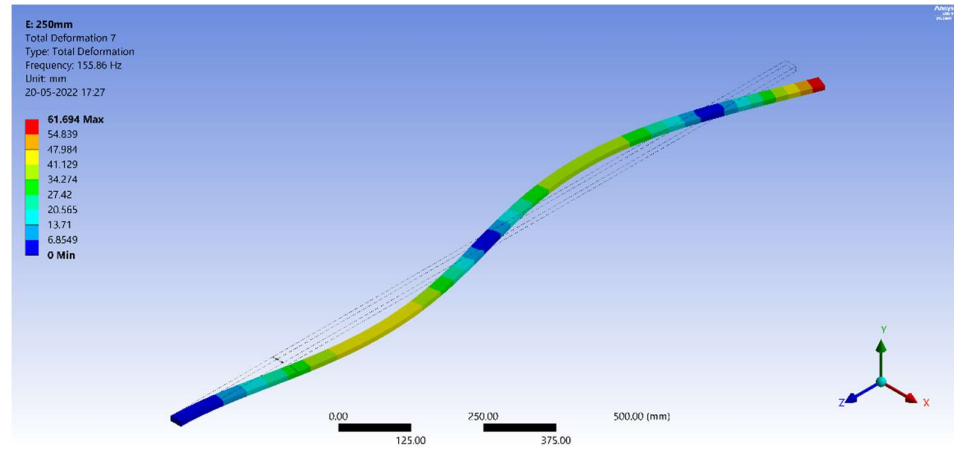


Fig. 7.1. (g) Total Deformation, Mode 7

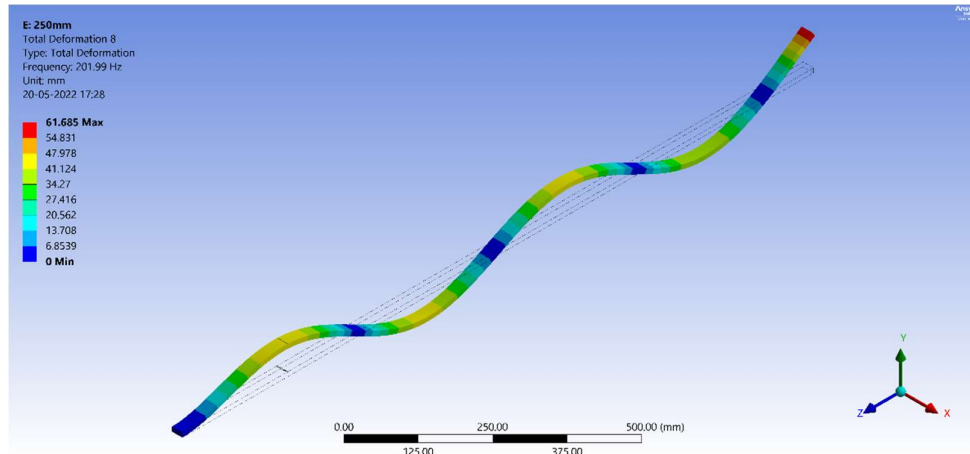


Fig. 7.1. (h) Total Deformation, Mode 8

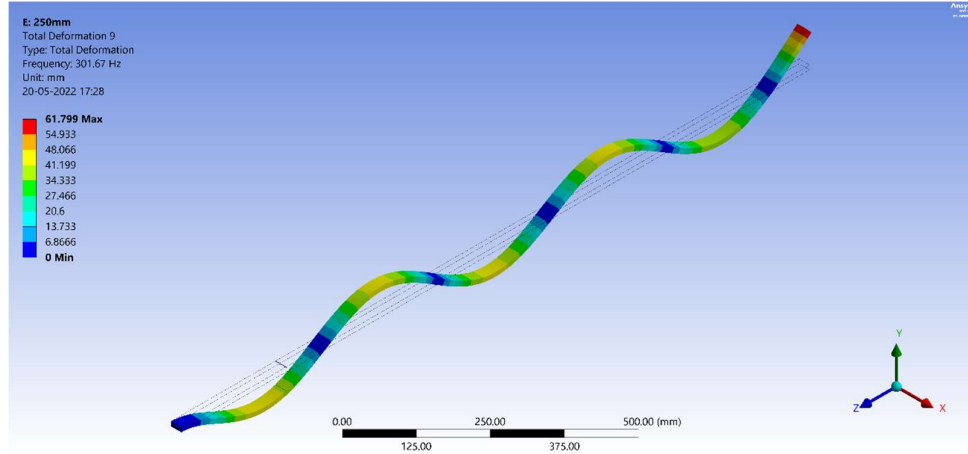


Fig. 7.1. (i) Total Deformation, Mode 9

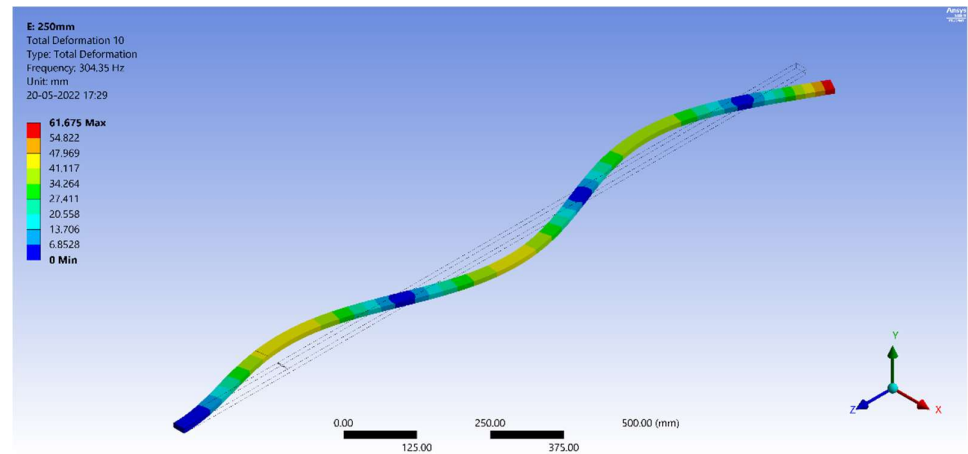


Fig. 7.1. (j) Total Deformation, Mode 10

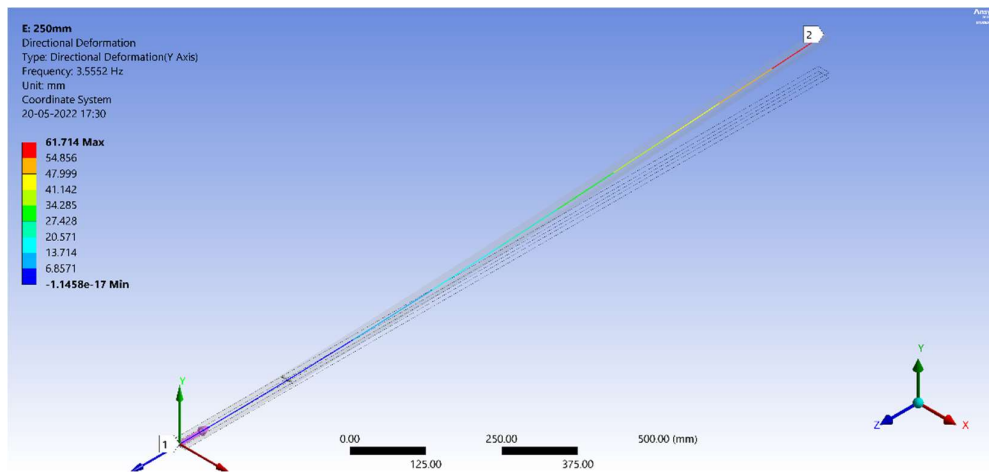


Fig. 7.1. (k) Directional Deformation, Mode 1

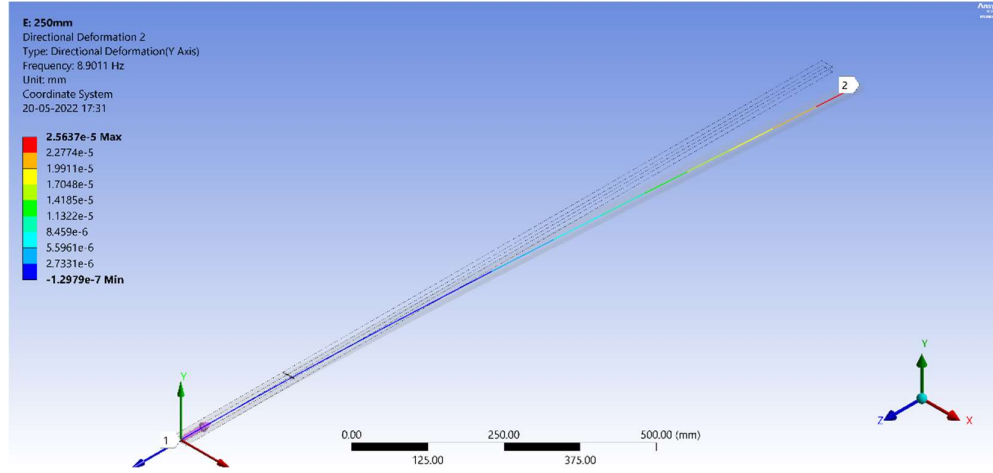


Fig. 7.1. (l) Directional Deformation, Mode 2

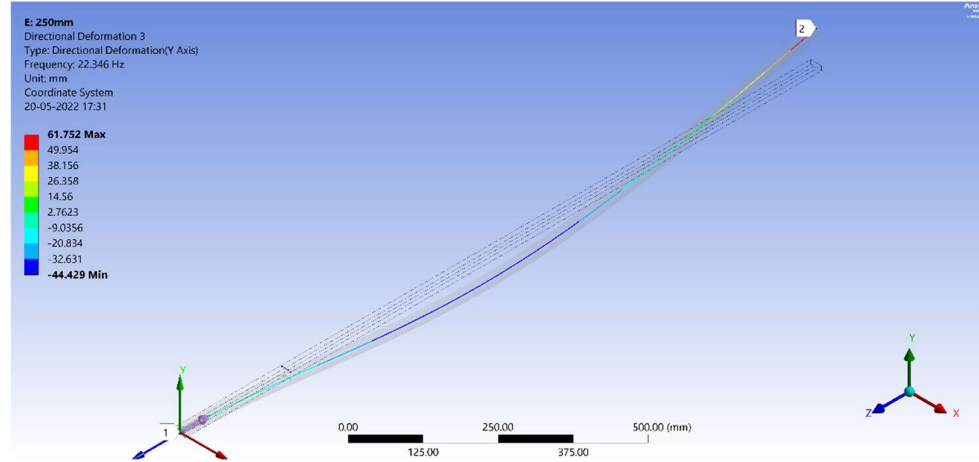


Fig. 7.1. (m) Directional Deformation, Mode 3

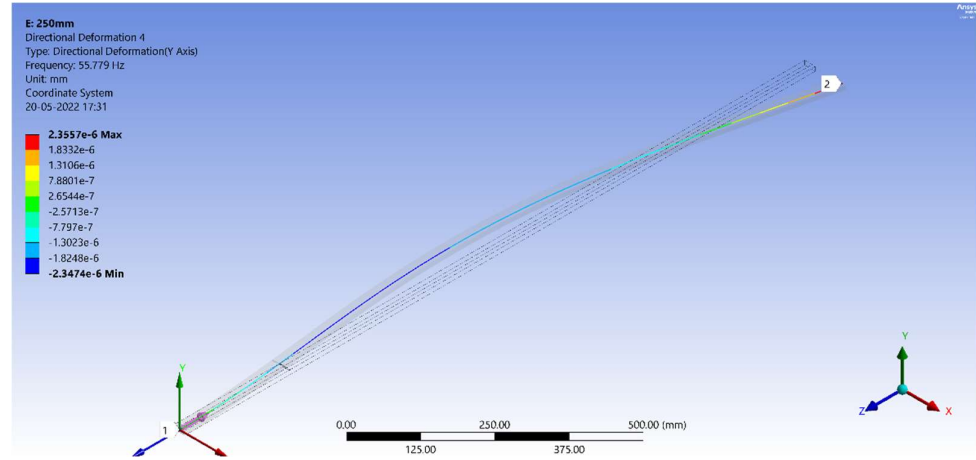


Fig. 7.1. (n) Directional Deformation, Mode 4

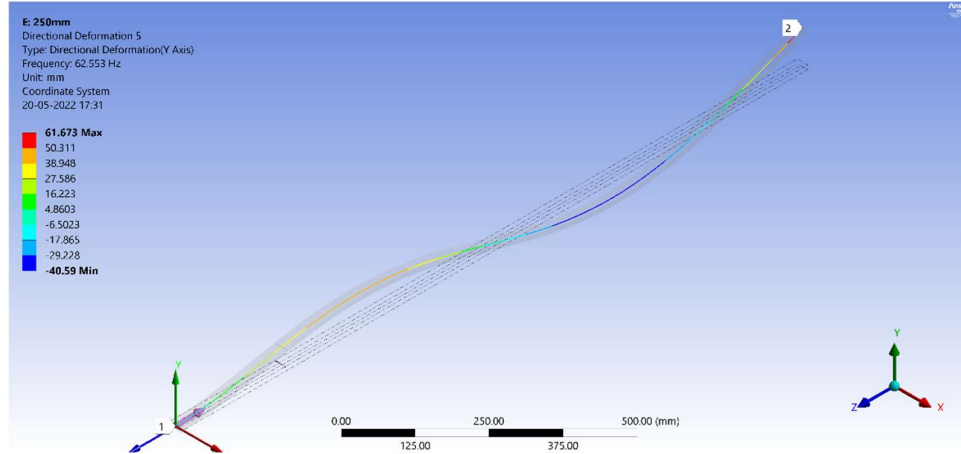


Fig. 7.1. (o) Directional Deformation, Mode 5

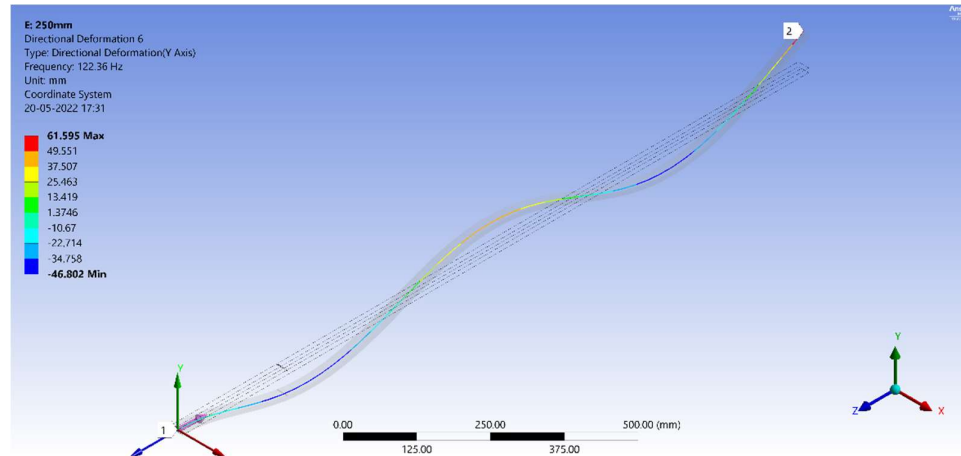


Fig. 7.1. (p) Directional Deformation, Mode 6

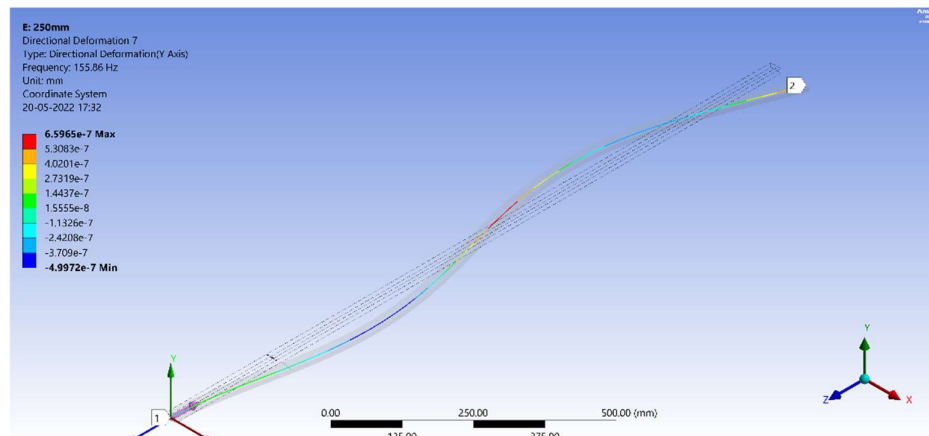


Fig. 7.1. (q) Directional Deformation, Mode 7

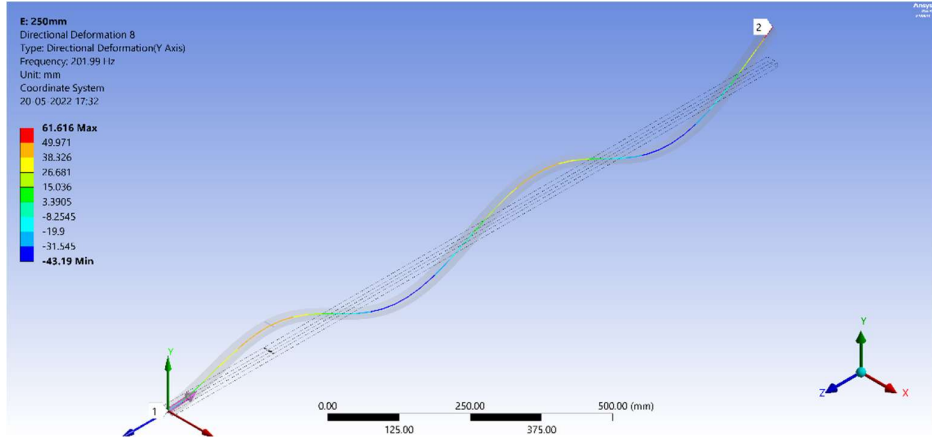


Fig. 7.1. (r) Directional Deformation, Mode 8

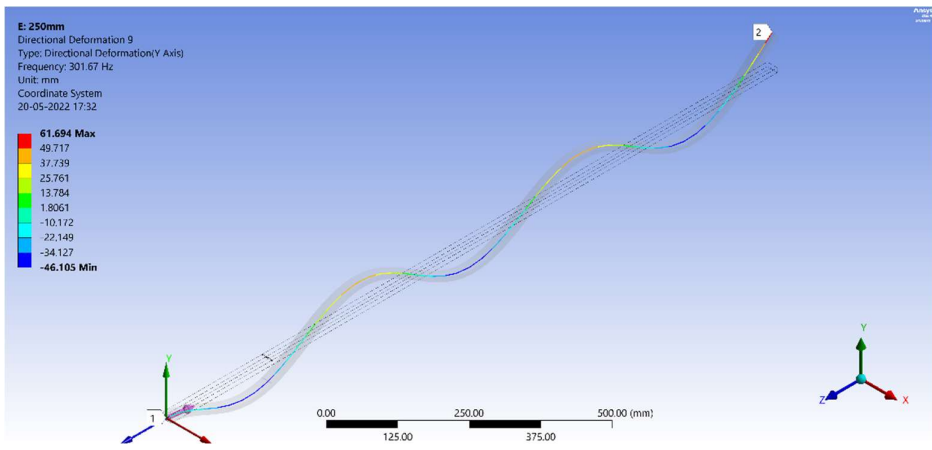


Fig. 7.1. (s) Directional Deformation, Mode 9

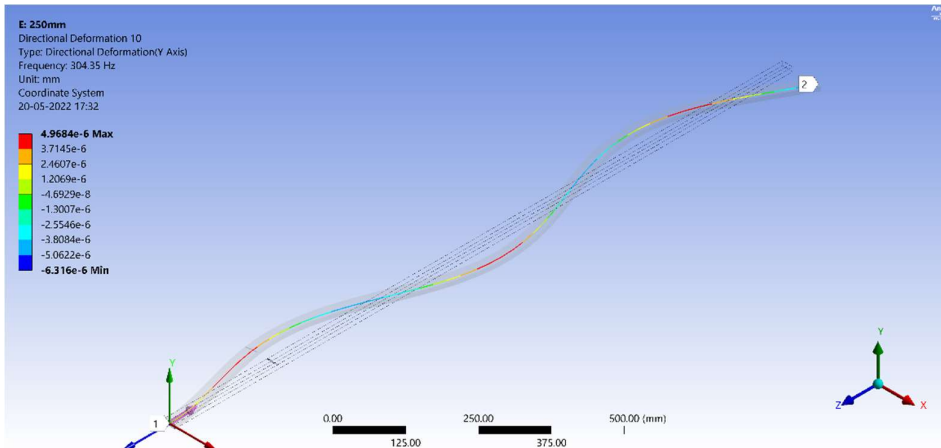


Fig. 7.1. (t) Directional Deformation, Mode 10

## 7.2. 3-D graphs

3-D graphs with the relative position on the X-axis, relative severity on the Y-axis, and frequencies on the Z-axis, respectively, are plotted for all the 10 modes for the four materials we have considered.

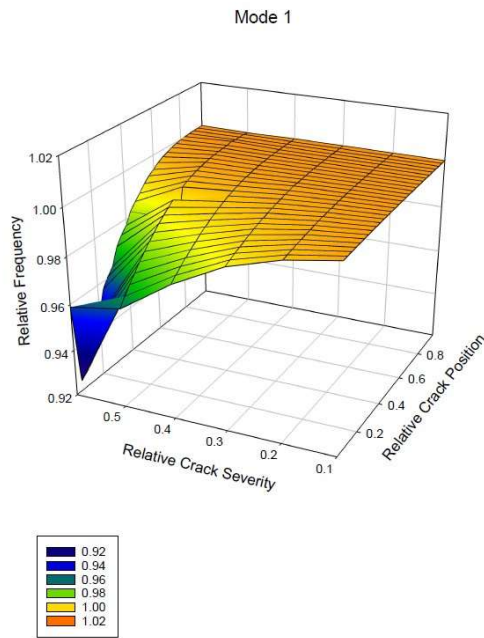


Fig. 7.2. (a). 3-D Graph for Mode 1

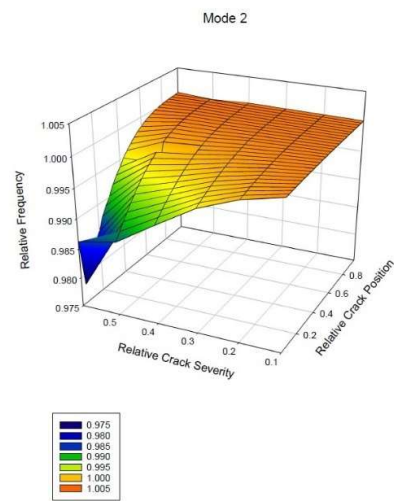


Fig. 7.2. (b). 3-D Graph for Mode 2

Mode 3

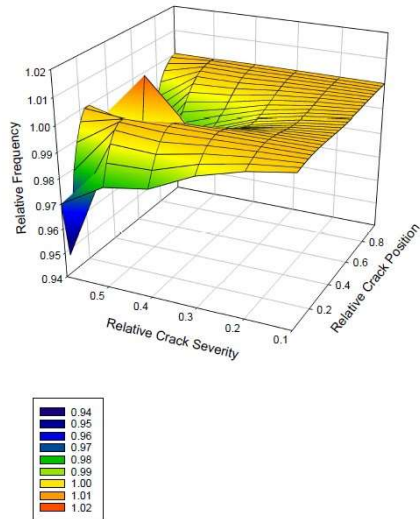


Fig. 7.2. (c). 3-D Graph for Mode 3

Mode 4

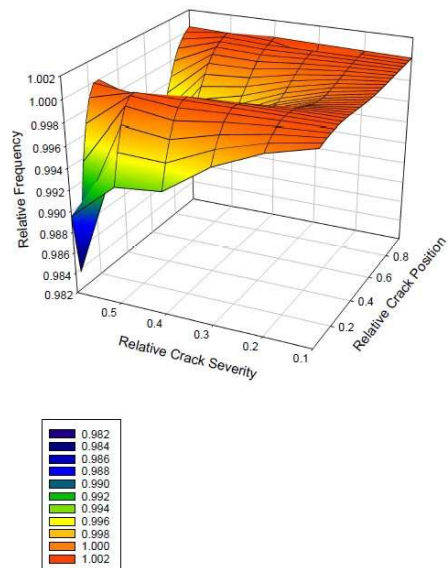


Fig. 7.2. (d). 3-D Graph for Mode 4

Mode 5

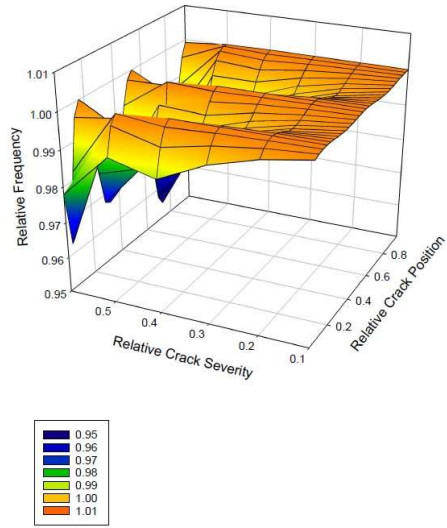


Fig. 7.2. (e). 3-D Graph for Mode 5

Mode 6

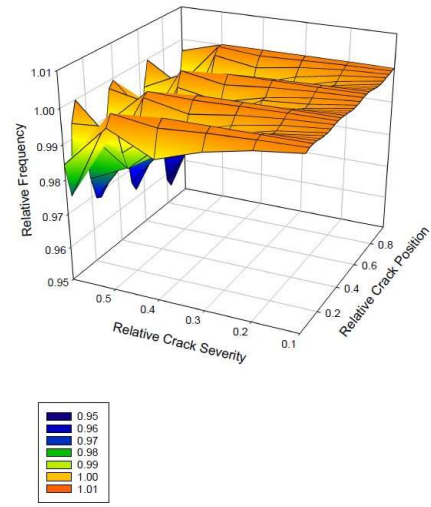


Fig. 7.2. (f). 3-D Graph for Mode 6

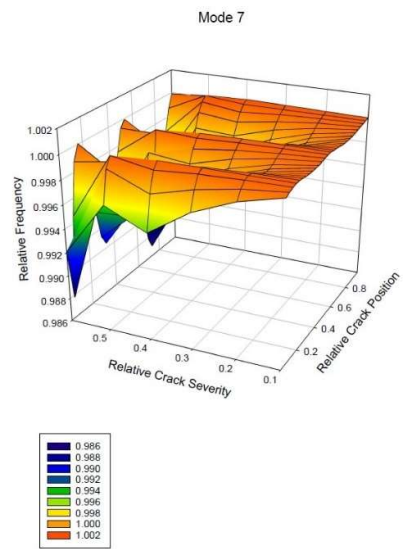


Fig. 7.2. (g). 3-D Graph for Mode 7

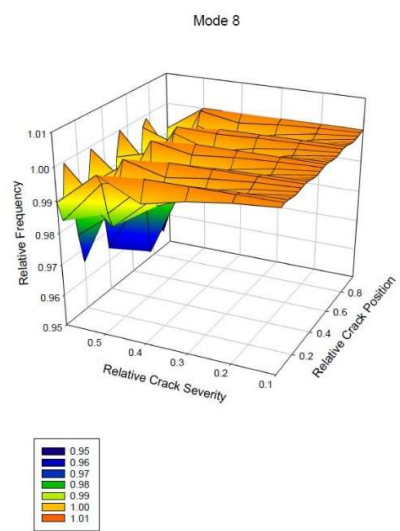


Fig. 7.2. (h). 3-D Graph for Mode 8

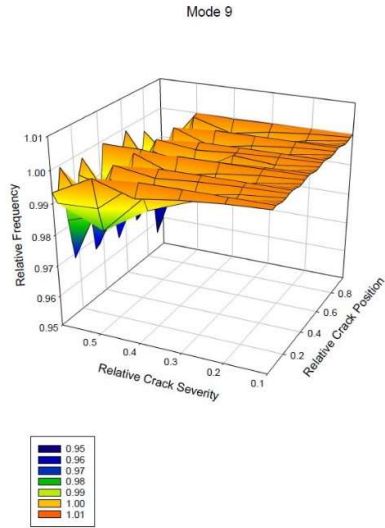


Fig. 7.2. (i). 3-D Graph for Mode 9

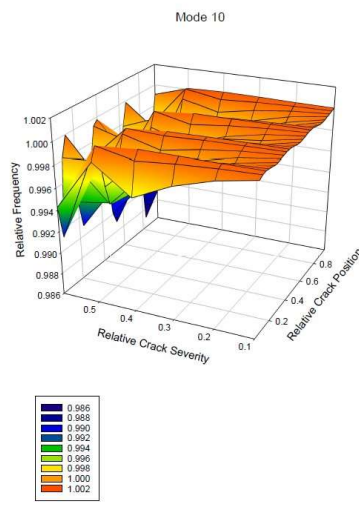


Fig. 7.2. (j). 3-D Graph for Mode 10

### 7.3. MATLAB results

#### 7.3.1. Without MAC

The final data set is imported to MATLAB for training using the ANN tool, followed by the “testing” phase. The following quantities are considered as the deciding outcomes for the trained data values to be validated accurately:

- NMSE (Normalized Mean Square Error):
  - i. NMSE-testing = 0.209093413531037
  - ii. NMSE-validation = 0.172048027898558

- $R^2$  coefficient:
  - $R^2$ -testing = 0.789555853510844
  - $R^2$ -validation = 0.827459070019925
- RMSE (Root Mean Square Error):
  - RMSE-testing = 0.078683018706796
  - RMSE-validation = 0.071179634285413

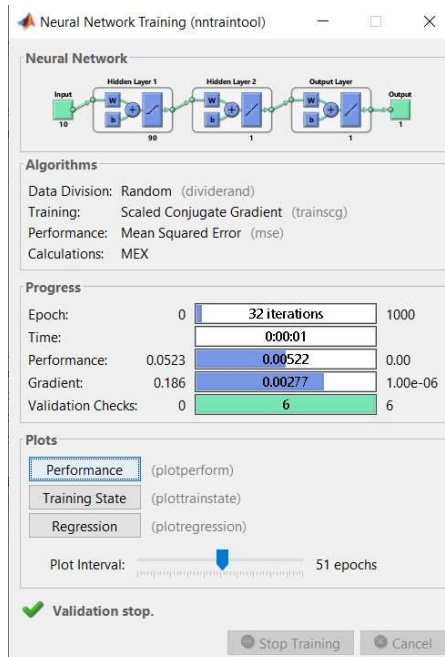


Fig. 7.3.1(a). ANN Tool without MAC

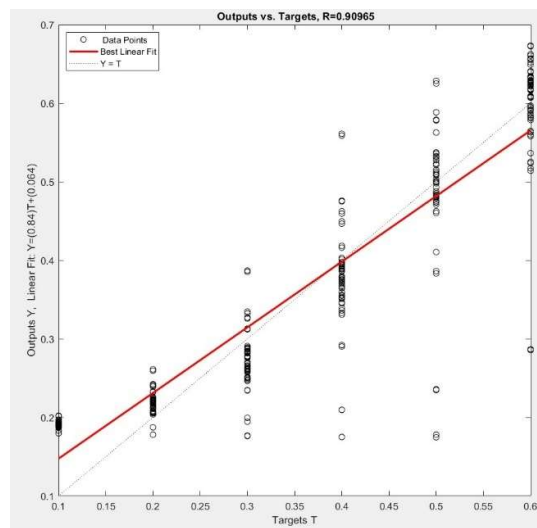


Fig. 7.3.1(b). Output of Regression Analysis without MAC

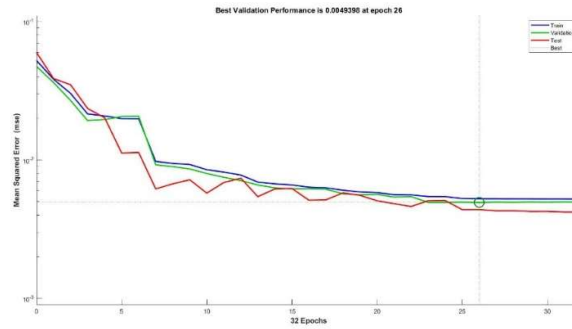


Fig. 7.3.1(c). Overall Performance Curves without MAC

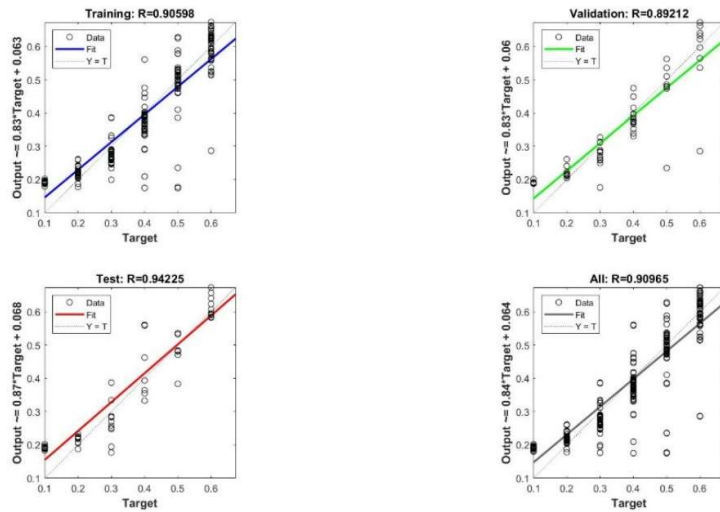


Fig. 7.3.1(d). Regression Graphs without MAC

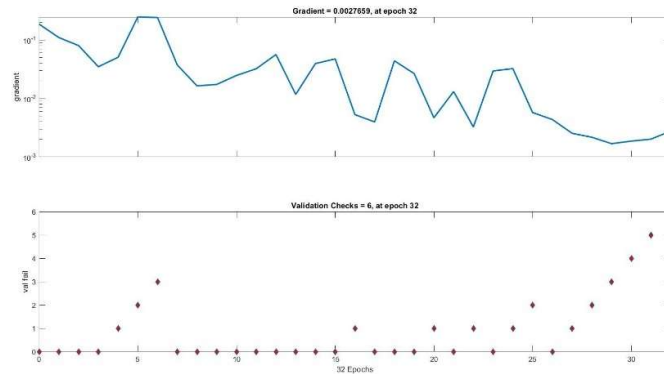


Fig. 7.3.1(e). Training State Curves without MAC

### 7.3.2. With MAC

The results obtained after the incorporation of MAC values into the frequency dataset are as follows,

- NMSE (Normalized Mean Square Error):
  - i. NMSE-testing = 0.178123760078
  - ii. NMSE-validation = 0.158367095642
- R<sup>2</sup> coefficient:
  - i. R<sup>2</sup>-testing = 0.788126700983
  - ii. R<sup>2</sup>-validation = 0.8269654281001
- RMSE (Root Mean Square Error):
  - i. RMSE-testing = 0.07329012765
  - ii. RMSE-validation = 0.0700543729981



Fig. 7.3.2(a). ANN Tool with MAC

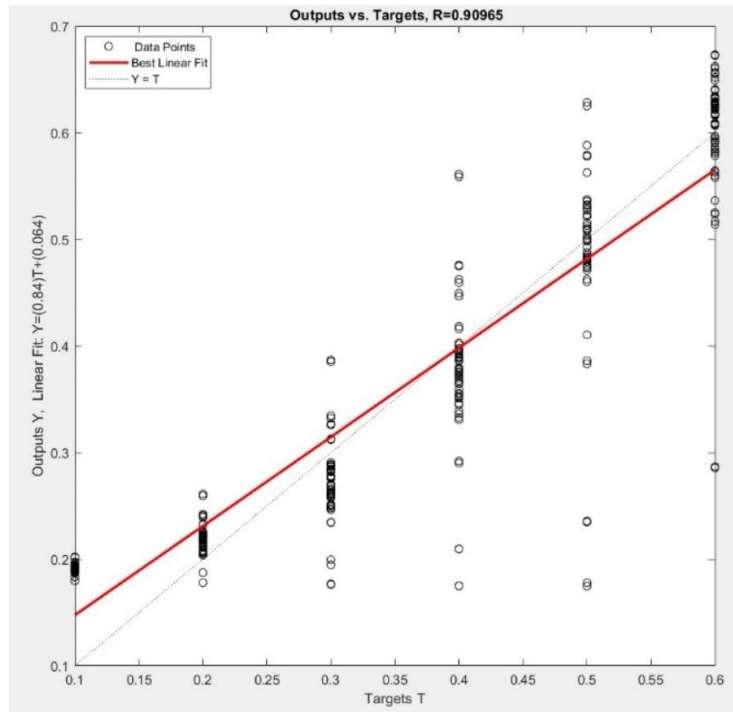


Fig. 7.3.2(b). Output of Regression Analysis with MAC

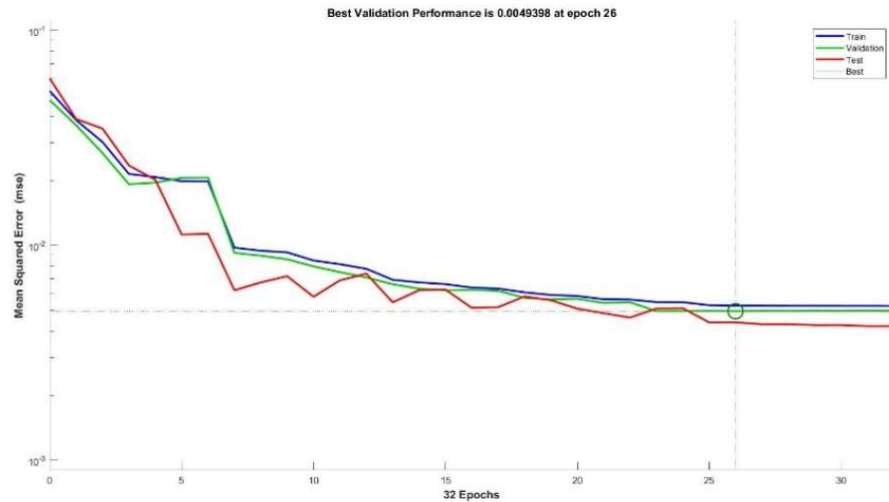


Fig. 7.3.2(c). Overall Performance Curves with MAC

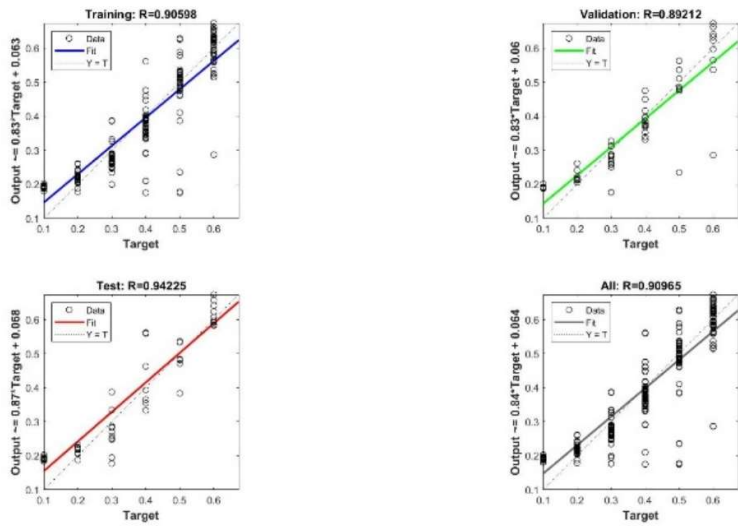


Fig. 7.3.2(d). Regression Graphs with MAC

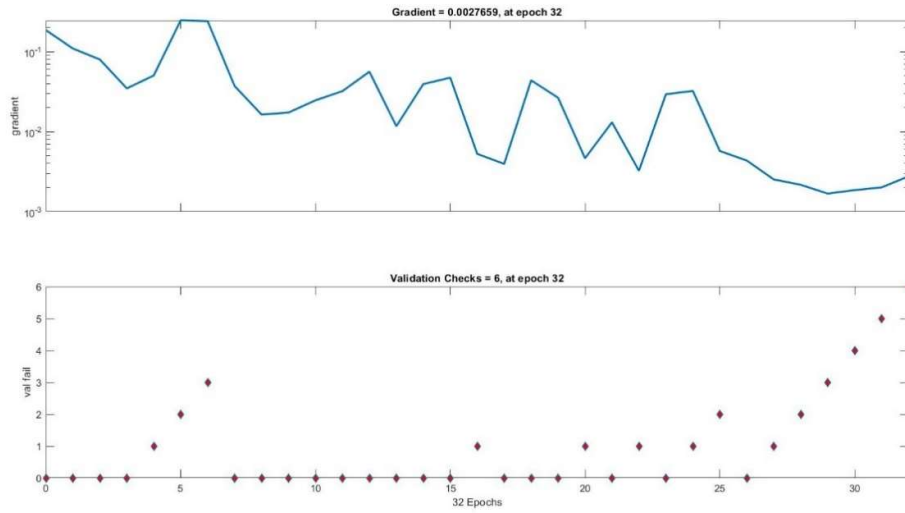


Fig. 7.3.2(e). Training State Curves with MAC

## **CHAPTER 8**

## **CONCLUSIONS**

The present study shows that ANN could accurately predict the responses of the relative crack position (RCL) and the relative crack depth (RCD), which are used in the health monitoring of the cantilever beam structures, as errors between the actual and the predicted responses is minor than 4.12%. It is seen that the prediction accuracy of the relative crack length is higher than that of the relative crack depth of the cantilever beam. The developed ANN model was found to predict the desired outputs convincingly. Thus, it shows that ANN modelling can be successfully used in the health monitoring of structures to predict their failure, reducing the enormous efforts being imparted and the tedious calculations involved in the monitoring process.

It has been observed that the natural frequency values of the beam decrease with an increase in severity of the crack, i.e. depth of the crack.

Modal Assurance Criterion (MAC) is used to quantify a mode-to-mode correlation between damaged and undamaged structures to find a clear correlation between a change in natural frequencies and the presence of damage. The MAC values can range between 0(no consistent correspondence) and 1(consistent correspondence). It is also observed that there has been an approximate 6% increase in regression accuracy after including MAC values to train the neural network tool.

## REFERENCES

- [1] E. Z. Moore, K.D. Murphy , J. M. Nichols , Crack identification in a freely vibrating plate using Bayesian parameter estimation, *Mechanical Systems and Signal Processing* (2011), 25(6),pp.2125-2134,2011.
- [2] Z.Q. Lang, G. Park, C.R. Farrar, M.D. Todd, Z. Mao, L. Zhao, K. Worden, Transmissibility of non-linear output frequency response functions with application in detection and location of damage in MDOF structural systems, *Int. J. Non-Linear Mech.* (2011), 46(6),pp.841-853,2011
- [3] H. Hein, L. Feklistova, Computationally efficient delamination detection in composite beams using Haar wavelets, *Mechanical Systems and Signal Processing*, 25(6), pp.2257- 2270, 2011.
- [4] Y. C. Huh, T.Y. Chung, S. J. Moon, H. G. Kil, J. K. Kim, Damage detection in beams using vibratory power estimated from the measured accelerations, *Journal of Sound and Vibration* ,330(15),pp.3645-3665,2011.
- [5] A. Salam, Y. Alsabbagh, O.M. Abuzeid , Mohammad H. Dado, Simplified stress correction factor to study the dynamic behavior of a cracked beam”, *Applied Mathematical Modelling*, 33, pp. 127–139,2009.
- [6] E. Douka, S. Loutridis, A. Trochidis, Crack identification in beams using wavelet analysis, *International Journal of Solids and Structures*, 40, pp. 3557–3569, 2003.
- [7] H. Nahvi and M. Jabbari, Crack detection in beams using experimental modal data and finite element mode, *International Journal of Mechanical Sciences*, 47, pp. 1477-1497, 2005.
- [8] M.M. R. Tahaa and J. Lucero, Damage identification for structural health monitoring usingfuzzy pattern recognition, *Engineering Structures*, 27, pp.1774–1783, 2005.
- [9] A.K. Mahamad, S. Saon and T. Hiyama, Predicting remaining useful life of rotating machinery based artificial neural network, *Computers and Mathematics with Applications*,60, pp.1078-1087, 2010.
- [10] F.Kong and R.Chen, A combined method for triplex pump fault diagnosis based on wavelet transform, fuzzy logic and neuro-networks, *Mechanical Systems and Signal Processing*, 18, pp.161–168, 2004.

- [11] W. Liu, W. Gao, Y. Sun, and M. Xu, Optimal sensor placement for spatial lattice structure based on genetic algorithms, *Journal of Sound and Vibration*, 317, pp. 175–189, 2008
- [12] J. Sanza, R. Pererab ,C. Huertab, Fault diagnosis of rotating machinery based on auto- associative neural networks and wavelet transforms, *Journal of Sound and Vibration*, 302, pp.981–999, 2007
- [13] A.J. Hoffman and N.T. van der Merwe, The application of neural networks to vibrational diagnostics for multiple fault conditions, *Computer Standards & Interfaces*, 24, pp.139–149, 2002.
- [14] S.M. Murigendrappa, S.K. Maiti and H.R. Srirangarajan, Experimental and theoretical study on crack detection in pipes filled with fluid, *Journal of Sound and Vibration*, 270, pp.1013–1032, 2004.
- [15] A.K. Darpe, K. Gupta and A. Chawla, Experimental investigations of the response of a cracked rotor to periodic axial excitation, *Journal of Sound and Vibration*, 260, pp. 265–286,2003.
- [16] T.Curry and E.G. Collins, Robust Fault Detection and Isolation Using Robust  $\ell_1$  Estimation, *Proceeding of the 2004 American Control Conference Boston*, Massachusetts, June 30 - July 2, 2004.
- [17] P. C. Muller, J. Bajkowski and D. Söfftker, Chaotic motions and fault detection in a cracked rotor, *Nonlinear Dynamics*, 5, pp.233-254, 1994.
- [18] G. M. Owolabi, A. S. J. Swamidas and R. Seshadri, Crack detection in beams using changes in frequencies and amplitudes of frequency response functions, *Journal of Soundand Vibration*, 265, pp.1-22, 2003.
- [19] S. Chinchalkar, Determination of crack location in beams using natural frequencies, *Journal of Sound and Vibration*, 247, pp. 417-429, 2001
- [20] H. Tada, P.C. Paris and G.R. Irwin, *The stress analysis of cracks hand book*. Del Research Corp. Hellertown, Pennsylvania, 1973.
- [21] S. Loutridis, E. Douka and L.J. Hadjileontiadis, Forced vibration behaviour and crack detection of cracked beams using instantaneous frequency”, *NDT&E International*, 38, pp. 411–419, 2005.
- [22] O. Song, T.W. Ha and L. Librescu, Dynamics of anisotropic composite cantilevers weakened by multiple transverse open cracks, *Engineering Fracture Mechanics*, 70, pp. 105–123, 2003.

- [23] D. Ravi and K.M. Liew, A study of the effect of micro crack on the vibration modeshape, *Engineering Structures*, 22, pp. 1097–1102, 2000.
- [24] S.S. Law and Z.R. Lu, Crack identification in beam from dynamic responses, *Journal of Sound and Vibration*, 285, pp. 967–987, 2005.
- [25] M. H. Dado, A Comprehensive Crack Identification Algorithm for Beams Under Different End Conditions, *Applied Acoustics*, 51, pp. 381-398, 1997.
- [26] E. Douka and L.J. Hadjileontiadis, Time–frequency analysis of the free vibration response of a beam with a breathing crack, *NDT&E International*, 38, pp. 3–10, 2005.
- [27] S. Benfratello, P. Cacciola, N. Impollonia, A. Masnata and G. Muscolino, Numerical and experimental verification of a technique for locating a fatigue crack on beams vibrating under Gaussian excitation, *Engineering Fracture Mechanics*, 74, pp. 2992–3001, 2007.
- [28] M.Fledman, Hilbert transform in vibration analysis, Mechanical systems and signalprocessing, Vol. 25(3), pp.735–802, 2011.
- [29] R. Ruotolo, C. Surace, P. Crespu and D. Storer, Harmonic analysis of the vibrations of a cantilevered beam with a closing crack, *Computers & Structures*, 61(6), pp. 1057-1074,1996.
- [30] M. Behzad, A. Ebrahimi and A. Meghdari, A Continuous Vibration Theory for Beams with a Vertical Edge Crack, *Scientia Iranica*, 17, pp. 194-204, 2010.
- [31] R.S. Prasad, SC Roy and KP Tyagi, Effect of Crack Position along Vibrating Cantilever Beam on Crack Growth Rate, *International Journal of Engineering Science and Technology*, 2, pp.837-839, 2010.
- [32] M. Rezaee and R.Hassannejad, free vibration analysis of simply supported beam with breathing crack using perturbation method”, *Acta Mechanica Solida Sinica*, 23, pp.459-470, 2010.
- [33] A.D. Dimarogonas and C.A. Papadopoulos, Vibration of cracked shafts in bending, *Journal of Sound and Vibration*, 91, pp- 583-593,1983.
- [34] B. Faverjon and J.J. Sinou, Identification of open crack in a beam using an a posteriori error estimator of the frequency response functions with noisy measurements, *European Journal of Mechanics*,28, pp.75-85, 2009.
- [35] K. Mazanoglu, I. Yesilyurt and M. Sabuncu, Vibration analysis of multiple cracked non- uniform beams, *Journal of sound and vibration*, 320, pp.977-989,

2009.

- [36] K.Wang, J.D.Inman and R.F.Charles, Modeling and analysis of a cracked composite cantilever beam vibrating in coupled bending and torsion, *Journal of sound and vibration*, 284, pp.23-49, 2004.
- [37] S. M. Al-said , Crack detection in stepped beam carrying slowly moving mass, *Journal of sound and vibration*, 14, pp.1903-1920,2008.
- [38] J. H. Lee, Identification of multiple cracks in a beam using natural frequencies, *Journal of sound and vibration*, 320, pp.482-490, 2009.
- [39] H.Yumin, Y. Junjie, C. Xuefeng and H. Zhengjia ,Discussion on calculation of local flexibility due to crack in a pipe, *Mechanical systems and signal processing*, 23, pp.804- 810,2009.
- [40] J. Zou, J. Chen, J.C. Niu, and Z.M. Geng ,Discussion on the local flexibility due to the crack in a cracked rotor system, *Journal of sound and vibration*, 262, pp.365-369,2003
- [41] M.N. Cerri, M. Dilena, and G.C. Ruta, Vibration and damage detection in undamaged and cracked circular arches: Experimental and Analytical results', *Journal of sound and vibration*, 314, pp.83-94,2008.
- [42] L. Nobile, C. Carloni, and M. Nobile ,Strain energy density prediction of crack initiation and direction in cracked T beams and pipes, *Theoretical and Applied fracture mechanics*, 41, pp.137-145,2004.
- [43] J. Humar, A. Bagchi, and H. Xu , Performance of vibration-based techniques for the identification of structural damage, *Structural health monitoring*, 5, pp.215-241,2006.
- [44] E. Voila, M. Dilena and F. Tornabene, Analytical and Numerical Results for Vibration Analysis of multi-stepped and multi-damaged circular arches, *Journal of Sound and vibration*, 299, pp.143-163,2007.
- [45] Y.J. Shin , K.M. Kwon, and J.H. Yun, Vibration analysis of a circular arch with variable cross section using differential transformation and generalized differential quadrature, *Journal of Sound and Vibration* ,309, pp.9-19,2008.
- [46] M.N. Cerri, and G.C. Ruta, Detection of localized damage in plane circular arches by frequency data, *Journal of Sound and vibration* , 270, pp.39-59,2004.
- [47] A. Labuschagne, N.F.J. Van Rensburg and A.J.V. Merwe, Comparison of linear beam theories, *Mathematical and Computer Modeling*, 79, pp.20-30, 2009.

- [48] T.R. Babu, and A.S. Sekhar, Detection of two cracks in a rotor-bearing system using amplitude deviation curve, *Journal of Sound and Vibration*, 314, pp.457-464, 2008.
- [49] Y. Xia and H. Hao, Measurement Selection for vibration based Structural damageidentification, *Journal of Sound and Vibration*, 236, pp. 89-104, 2009.
- [50] E. Douka, G. Bamnios and A. Trochidis, A method for determining the location and depth of cracks in double cracked beams, *Applied Acoustics*, 65, pp.997-1008, 2009.
- [51] J.K. Sinha, Higher order spectra for crack and misalignment identification in the shaft of rotating machine, *Structural health Monitoring*, 6 , pp-325-334,2007.
- [52] D.P. Patil and S.K. Maiti, Detection cracks using frequency measurements, *Engineering Fracture Mechanics*, 70, pp.1553-1572, 2003.
- [53] J.T. Kim and M. Stubbs ,Improved Damage Identification Method based on modal information, *Journal of Sound and Vibration*, 252, pp. 223-238,2002.
- [54] S. Ebersbach and Z. Peng, Expert system development for vibration analysis in machine condition monitoring, *Expert systems with Applications*, 34, pp-291-299, 2008.
- [55] G.D. Gounaris and C.A. PapadoPoulos ,Analytical and experimental crack identification of beam structures in air or in fluid, *Computers and Structures*, 65, pp.633-639,1997.
- [56] M. H. H. Shen and Y.C. Chu, Vibrations of beams with a fatigue crack, *Computers & Structures*, 45, pp. 79-93, 1992.
- [57] A. Ebrahimi, M.Behzad and A.Meghdari, A bending theory for beams with vertical edge crack, *International Journal of Mechanical Sciences*, 52, pp.904–913, 2010.
- [58] M.Jasinski, S.Radkowski, Use of the higher spectra in the low-amplitude fatigue testing, *Mechanical Systems and Signal Processing*, 25, pp.704–716, 2011.
- [59] M. H.Seyyed, G. Behnam, M.Yaser and A.Saeed, Free transverse vibrations of cracked nano beams with surface effects, *Thin Solid Films*, 519 pp.2477–2482, 2011.
- [60] L. Rubio, B.M. Abella, G.Loaiza, Static behavior of a shaft with an elliptical crack, *Mechanical Systems and Signal Processing* ,25 ,pp.1674–1686,2011.
- [61] I. Argatov and E.Butcher, On the separation of internal and boundary damage in

- slender bars using longitudinal vibration frequencies and equivalent linearization of damaged bolted joint response, *Journal of Sound and Vibration*, 330, 3245–3256, 2011.
- [62] R. Farshidi, D. Trieu, S.S. Park and T. Freiheit, Non-contact experimental modal analysis using air excitation and a microphone array, *Measurement*, 43, 755–765, 2010.
- [63] P. Casini and F. Vestroni, Characterization of bifurcatingn on linear normal modes in piecewise linear mechanical systems, *International Journal of Non-Linear Mechanics*, 46, 142–150, 2011.
- [64] G.E. Carr, M.D. Chapetti , On the detection threshold for fatigue cracks in welded steel beams using vibration analysis, *International Journal of Fatigue*, 33, 642–648, 2011.
- [65] M. Fontul, A.M.R. Ribeiro, and J.M.M. Silva, Transmissibility matrix in harmonic and random processes, *Journal Shock and Vibration*, 11, pp. 563-571, 2004.
- [66] P.N. Saavedra and L.A. Cuitino, Crack detection and Vibration behavior of Cracked beams ,*Computers and Structures*, 79, pp.1451-1459, 2001.
- [67] G. L. Qian, S. N. Gu and J. S. Jiang, The dynamic behaviour and crack detection of a beam with a crack , *Journal of Sound and Vibration*, 138, pp. 233-243, 1990.
- [68] U. Andreadusa, P. Casini, and F. Vestroni, Non-linear dynamics of a cracked cantilever beam under harmonic excitation, *International Journal of Non-Linear Mechanics*, 42, pp.566-575, 2007.
- [69] E. Viola, L. Federici, and L. Nobile, Detection of crack location using cracked beam element method for structural analysis, *Theoretical and Applied Fracture Mechanics*, 36, pp.23-35, 2001.
- [70] T.G. Chondros and G.N. Labeas, Torsional vibration of a cracked rod by vibrational formulation and numerical analysis, *Journal of Sound and Vibration*, 301, pp. 994–1006, 2007.
- [71] A. Ariaei, S. Ziaei-Rad and M. Ghayour, Vibration analysis of beams with open and breathing cracks subjected to moving masses, *Journal of Sound and Vibration*, 326, pp.709– 724, 2009.
- [72] G.P. Potirniche, J. Hearndon, S.R. Daniewicz, D. Parker, P. Cuevas, P.T. Wang

- and M.F. Horstemeyer, A two-dimensional damaged finite element for fracture applications, *Engineering Fracture Mechanics*, 75, pp.3895–3908,2008.
- [73] Y. Narkis, Identification of crack location in vibrating simply supported beams, *Journal of sound and vibration*, 172, pp. 549-558, 1994.
- [74] W. M. Ostachowicz, and M. Krawczuk, Vibration analysis of a cracked beam, *Computers& Structures*, 36, pp. 245-250, 1990.
- [75] D.Y. Zheng and N.J. Kessissoglou, Free vibration analysis of a cracked beam by finite element method, *Journal of Sound and Vibration*, 273, pp. 457–475, 2004.
- [76] M. Kisa, and M. G.Arif ,Free vibration analysis of uniform and stepped cracked beams with circular cross sections, *International journal of engineering science*, 45, pp.364- 380,2007.
- [77] M. Karthikeyan, R. Tiwari, and S. Talukdar, Crack localization and sizing in a beam based on free and forced response measurements , *Journal of mechanical systems and signal processing*, 21, pp-1362-1385,2007.
- [78] J.L. Hearndon, , G.P. Potirniche, D. Parker, P.M. Wevas, H. Rinehart, P.T. Wang and, M.F.H. Meyer ,Monitoring structural damage of components using an effective modulus approach, *Theoretical and applied fracture mechanics*, 50, pp.23-29,2008.
- [79] S. M. Al-Said , Crack Identification in a stepped beam carrying a rigid disk, *Journal of Sound and Vibration*, 300, pp. 863-876,2007.
- [80] A.S. Shekhar and B.S. Prabhu, Crack detection and vibration characteristics of cracked shafts, *Journal of sound and vibration*, 157, pp. 375-381, 1992.
- [81] S. K Panigrahi, Damage analyses of adhesively bonded single lap joints due to delaminated FRP composite adherends, *Applied Composite Materials*, 4, pp. 211-223, 2009.
- [82] M. Schlechtingen and I. F. Santos, Comparative analysis of neural network and regression-based condition monitoring approaches for wind turbine fault detection, *Mechanical Systems and Signal Processing*, 25, pp.1849–1875, 2011.
- [83] V. N. Ghate, S.V. Dudul, Optimal MLP neural network classifier for fault detection of three phase induction motor, *Expert Systems with Applications*, 37, pp.3468–3481, 2010.
- [84] I. Eski,S. Erkaya,S. Savas, S. Yildirim, Fault detection on robot manipulators

using artificial neural networks, *Robotics and Computer-Integrated Manufacturing*, 27 ,pp. 115– 123,2011.

- [85] B. Fan, Z. Du, X. Jin, X. Yang, Y. Guo, A hybrid FDD strategy for local system of AHU based on artificial neural network and wavelet analysis, *Building and Environment* ,45, pp.2698-2708.
- [86] G. Paviglianiti, F. Pierri, F. Caccavale and M. Mattei, Robust fault detection and isolation for proprioceptive sensors of robot manipulators, *Mechatronics*, 20, 162– 170, 2010.
- [87] C.C.Wang, Y. Kang, P.C. Shen, Y.P. Chang and Y.L.Chung, Applications of fault diagnosis in rotating machinery by using time series analysis with neural network, *Expert Systems with Applications*, 37, 1696–1702, 2010.
- [88] S. Suresh,S.N. Omkar, R. Ganguli and V. Mani, Identification of crack location and depth in a cantilever Beam Using a Modular Neural Network Approach, *Smart Materials and Structures*, 13, pp. 907-916,2004.
- [89] W. A. Little and G. L. Shaw, Analytic study of the memory storage capacity of a neural network, *Mathematical Biosciences*, 39(3-4), pp. 281-290, 1978.
- [90] M. Mehrjoo, N. Khaji, H. Moharrami and A. Bahreininejad, Damage detection of truss bridge joints using Artificial Neural Networks, *Expert Systems with Applications*, 35, pp. 1122–1131, 2008.
- [91] F.J.Agosto, D. Serrano, B. Shafiq and A. Cecchini, Neural network based nondestructive evaluation of sandwich composites, *Composites: Part B*, 39, pp. 217–225, 2008.
- [92] N. Saravanan , V.N.S. Kumar Siddabattuni and K.I. Ramachandran, Fault diagnosis of spur bevel gear box using artificial neural network (ANN), and proximal support vector machine (PSVM), *Applied Soft Computing*, 10, pp. 344– 360, 2010.
- [93] A.J. Oberholster and P.S. Heyns , On-line fan blade damage detection using neural networks, *Mechanical Systems and Signal Processing*, 20, pp. 78–93, 2006.
- [94] J.D. Wu and J.J .Chan, Faulted gear identification of a rotating machinery based on wavelet transform and artificial neural network, *Expert Systems with Applications*, 36, pp. 8862–8875, 2009.

- [95] S. Haykin, Neural Networks, A comprehensive foundation. *Pearson Education*, 2006.
- [96] W. McCulloch and W. Pitts, A logical calculus of the ideas immanent in nervous activity, *Bulletin of Mathematical Biophysics*, 5, pp. 115-133, 1943.
- [97] F. Rosenblatt, the perceptron: A probabilistic model for information storage and organization in the brain, *Psychological Review*, 65, pp.386-408, 1958.
- [98] J.D. Wu and C.H.Liu, Investigation of engine fault diagnosis using discrete wavelet transform and neural network, *Expert Systems with Applications*, 35, pp.1200–1213, 2008.

## APPENDIX A

### 1. MATLAB CODE:

```
clc
clear all
fid11=fopen('resultsan','w');
load 'crackdetection_modell.mat';
FR=data(:,1:20);
h=length(data(:,1));
y=data(:,21);
train_x=FR(1:418,:);
train_y=y(1:418);
test_x1=train_x;
test_y1=train_y;
test_x2=FR(419:end,:);
test_y2=y(419:end,:);
net1=newff(train_x',train_y',[90 1],{'tansig'
'purelin'},'trainscg');
net1.trainParam.epochs = 1000;
net2=train(net1,train_x',train_y');
predict_label1= sim(net2,test_x1');
predict_label2= sim(net2,test_x2');

R11=corr(predict_label1',test_y1);
R22=corr(predict_label2',test_y2);

R2v=(R11*R11);
R2t=(R22*R22);

figure(1)
plot(predict_label1','b');
hold
plot(test_y1,'r');
hold off
figure(2)
plot(test_y1,'r');
hold off
figure(3)
[m11,b11,r11]=postreg(predict_label1,test_y1');

figure(4)
plot(predict_label2','b');
```

```

hold
plot(test_y2, 'r');
hold off
figure(5)
plot(test_y2, 'r');
hold off
figure(6)
[m2,b2,r2]=postreg(predict_label2,test_y2');

data1=[test_y1,predict_label1'];
data2=[test_y2,predict_label2'];
data1=abs(data1);
data2=abs(data2);
avg1=mean(data1(:,1));
avg2=mean(data2(:,1));
clc

len1=length(data1);
len2=length(data2);
for j=1:len1
x0v(j)=(data1(j,1)-data1(j,2))^2;
y0v(j)=(data1(j,1)-avg1)^2;
end
for j=1:len2
x0t(j)=(data2(j,1)-data2(j,2))^2;
y0t(j)=(data2(j,1)-avg2)^2;
end
x10v=sum(x0v)/85;
y10v=sum(y0v)/84;
x10t=sum(x0t)/85;
y10t=sum(y0t)/84;
NMSEv=x10v/y10v;
NMSET=x10t/y10t;

sumx1=0;
sumx2=0;
for j=1:len1
x1=(data1(j,1)-data1(j,2))^2;
sumx1=sumx1+x1;
end
for j=1:len2
x2=(data2(j,1)-data2(j,2))^2;
sumx2=sumx2+x2;
end
rmsev=sqrt(sumx1/len1);

```

```

rmset=sqrt(sumx2/len2);
sum1=0;
sum2=0;
for j = 1:len1
    sum1 = sum1 + abs((data1(j,2)-
data1(j,1))/(data1(j,1)));
end
for j = 1:len2
    sum2 = sum2 + abs((data2(j,2)-
data2(j,1))/(data2(j,1)));
end
mv= (sum1/len1);
mt= (sum2/len2);

mov=sum(data1(:,1))/len1;
mot=sum(data2(:,1))/len2;

sumx1=0;
sumy1=0;
sumx2=0;
sumy2=0;
for j=1:len1
    x1=(data1(j,1)-data1(j,2))^2;
    yel=(data1(j,1)-mov)^2;
    sumx1=sumx1+x1;
    sumy1=(sumy1+yel);
end
ev=(1-((sumx1)/(sumy1)));
for j=1:len2
    x2=(data2(j,1)-data2(j,2))^2;
    ye2=(data2(j,1)-mot)^2;
    sumx2=sumx2+x2;
    sumy2=(sumy2+ye2);
end
et=(1-((sumx2)/(sumy2)));

fprintf(fid11,'%6.4f\t%6.4f\t%6.4f\t%6.4f\t%6.4f\t//%
6.4f\t%6.4f\t%6.4f\t%6.4f\t%6.4f\t',NMSEv,R2v,rmsev,m
v,ev,NMSEt,R2t,rmset,mt,et);
fclose all

```

0.99962	0.99942	0.99877	0.99956	0.99906	0.99928	0.9962	0.99956	0.99967	0.99974	1	0.992	1	0.479	1	1	0.6349	1	1	0.5879	0.1	50
0.99466	0.99792	0.99587	0.9984	0.99683	0.99767	0.99874	0.9984	0.99896	0.9991	1	0.9946	1	0.5756	1	1	0.5778	1	1	0.5882	0.2	50
0.9881	0.99539	0.9909	0.99646	0.99309	0.99495	0.99729	0.99655	0.99776	0.99803	1	0.9986	0.073	0.5837	0.9999	0.9999	0.1062	0.9999	0.9999	0.6089	0.3	50
0.97694	0.99152	0.98272	0.99352	0.98702	0.99062	0.99502	0.99359	0.99587	0.99642	1	0.9984	0.0761	0.9414	0.9996	0.9995	0.0431	0.9996	0.9997	0.6254	0.4	50
0.96253	0.98746	0.97991	0.99308	0.99032	0.99679	0.9966	0.99976	0.99971	0.99887	0.9999	0.9974	0.0177	0.976	0.9998	0.9999	0.0513	1	1	0.3093	0.5	50
0.95889	0.9862	0.97001	0.98954	0.97794	0.98436	0.99206	0.98942	0.99324	0.99426	0.9999	0.9963	0.0184	0.9032	0.9988	0.9986	0.3984	0.9988	0.9992	0.6045	0.6	50
0.99859	0.99947	0.99921	0.9997	0.99961	0.99984	0.99981	1	1	0.99997	1	0.9997	0.0156	0.6515	1	1	0.7606	1	1	0.5617	0.1	100
0.99515	0.99811	0.99727	0.99894	0.99866	0.99952	0.99943	1	0.99997	0.99984	1	0.9969	0.0158	0.5335	1	1	0.7357	1	1	0.5518	0.2	100
0.9892	0.99581	0.99398	0.99767	0.99705	0.99904	0.9988	0.99995	0.99993	0.99965	1	0.9873	0.0162	0.4783	1	1	0.6721	1	1	0.5537	0.3	100
0.97903	0.9923	0.98848	0.99574	0.99441	0.99816	0.99786	0.9999	0.99984	0.99932	1	0.9986	0.0168	0.6573	0.9999	1	0.7523	1	1	0.5834	0.4	100
0.96614	0.9887	0.98795	0.9959	0.99775	0.99992	0.99924	0.99636	0.98982	1	1	0.989	0.0172	0.1439	0.9999	1	0.2361	0.9996	0.9978	0.58	0.5	100
0.92445	0.97827	0.94759	0.98372	0.96282	0.97434	0.98777	0.98291	0.98917	0.99122	0.9995	0.1162	0.0208	0.4399	0.9966	0.9962	0.0417	0.9969	0.9979	0.5088	0.6	100
0.99873	0.99953	0.99952	0.99982	0.99991	1	0.99994	0.9999	0.99964	1.00003	1	0.9469	0.0156	0.5907	1	1	0.0266	1	1	0.6025	0.1	150
0.99562	0.9983	0.99837	0.99938	0.9997	1	0.99987	0.99961	0.99873	1.00003	1	0.9064	0.0158	0.6236	1	1	0.2038	1	1	0.595	0.2	150
0.99025	0.99623	0.99644	0.99863	0.99934	1	0.99975	0.99903	0.99714	1.00003	1	0.5017	0.016	0.7003	1	1	0.7426	1	0.9998	0.589	0.3	150
0.98107	0.99306	0.99314	0.99748	0.99873	1	0.9995	0.99801	0.99434	1.00003	1	0.9932	0.0165	0.2735	1	1	0.0923	0.9999	0.9993	0.6134	0.4	150
0.96945	0.98984	0.99393	0.99797	1.00008	0.99527	1.00006	0.98655	0.98195	0.99852	1	0.9977	0.0166	0.7397	1	0.9996	0.7575	0.998	0.9957	0.612	0.5	150
0.92647	0.97981	0.96232	0.98895	0.98233	0.99423	0.99458	0.99956	0.99938	0.99819	0.9997	0.9999	0.0199	0.9295	0.9993	0.9997	0.0811	1	0.9999	0.5655	0.6	150
0.99887	0.99957	0.99978	0.99993	1.00002	0.99984	1	0.99956	0.99932	0.99997	1	0.9951	0.0156	0.5628	1	1	0.5719	1	1	0.5837	0.1	200
0.99609	0.99848	0.99921	0.9997	1.00003	0.99944	1	0.99835	0.99763	0.99984	1	0.995	0.0157	0.5791	1	1	0.7073	1	0.9999	0.5828	0.2	200
0.99124	0.99661	0.99824	0.99933	1.00005	0.99864	1	0.99621	0.9947	0.99958	1	0.9994	0.0159	0.6528	1	1	0.2212	0.9998	0.9996	0.6045	0.3	200
0.98297	0.99377	0.99657	0.99877	1.00006	0.99735	1	0.99252	0.98972	0.99913	1	0.9965	0.0162	0.9108	1	0.9999	0.00072	0.9994	0.9986	0.3044	0.4	200
0.97261	0.99093	0.99789	0.99933	0.99799	0.98741	0.99937	0.98155	0.98631	0.99603	1	9941	0.0162	0.1368	0.9999	0.9989	0.202	0.9974	0.9976	0.0078	0.5	200
0.94013	0.9825	0.97929	0.99369	0.99615	0.99992	0.9988	0.99349	0.98198	0.99997	0.9999	0.9916	0.0184	0.3379	0.9999	1	0.2241	0.9988	0.9932	0.1131	0.6	200
0.99898	0.99963	0.99991	0.99998	0.99994	0.99952	1	0.99937	0.99948	0.9999	1	0.9947	0.0156	0.0044	1	1	0.1971	1	1	0.5617	0.1	250
0.9965	0.99864	0.99974	0.99991	0.99978	0.9984	0.99994	0.99762	0.99815	0.99948	1	0.9828	0.0156	0.5728	1	1	0.3143	1	1	0.5682	0.2	250
0.99218	0.99698	0.99938	0.99979	0.99947	0.99647	0.99981	0.99461	0.99584	0.99877	1	9977	0.0157	0.3183	1	0.9999	0.3174	0.9998	0.9998	0.5589	0.3	250
0.98476	0.99444	0.99881	0.99959	0.99892	0.99302	0.99962	0.98956	0.99207	0.99761	1	0.9947	0.0159	0.1161	1	0.9996	0.0175	0.9992	0.9992	0.5208	0.4	250
0.9757	0.99197	0.99982	0.99998	0.99309	0.98196	0.99786	0.98514	0.99623	0.99422	1	0.9995	0.0157	0.7314	0.9997	0.9987	0.3606	0.9984	0.9994	0.5997	0.5	250
0.94402	0.98406	0.98914	0.99683	1.00009	0.99126	1.00006	0.97558	0.96849	0.99761	0.9999	9225	0.0176	0.4254	1	0.9988	0.0044	0.9934	9871	0.3791	0.6	250
0.99909	0.99967	1	1.00002	0.99978	0.99936	0.99994	0.99947	0.99984	0.99981	1	0.9894	0.0156	0.7359	1	1	0.0023	1	1	0.1798	0.1	300

0.99691	0.9988	1	1.00002	0.99917	0.99767	0.99975	0.99806	0.99948	0.99923	1	0.9958	0.0156	0.8379	1	1	0.0243	1	1	0.0375	0.2	300
0.99308	0.99733	0.99996	1.00002	0.9981	0.99479	0.99931	0.99558	0.99886	0.99816	1	0.9995	0.0156	0.588	1	0.9999	0.0118	0.9999	0.9999	0.5048	0.3	300
0.9865	0.99508	0.99991	1	0.99621	0.98989	0.99874	0.9915	0.99782	0.99651	1	0.9904	0.0157	0.307	0.9999	0.9996	0.2188	0.9995	0.9998	0.5665	0.4	300
0.97854	0.99293	0.99987	1.00002	0.98743	0.98171	0.99603	0.99349	0.99967	0.99406	1	0.9974	0.0154	0.9827	0.9995	0.999	0.4786	0.9993	0.9999	0.5827	0.5	300
0.94669	0.98546	0.99595	0.99891	0.99603	0.97562	0.99899	0.96578	0.97571	0.99351	1	0.9955	0.0167	0.6398	0.9997	0.996	0.9467	0.9913	0.9822	0.1289	0.6	300
0.9992	0.9997	1	1.00002	0.99958	0.99928	0.99987	0.99976	0.99997	0.99981	1	0.9909	0.0155	0.4979	1	1	0.5063	1	1	0.6037	0.1	350
0.99727	0.99894	1	1.00004	0.99846	0.99759	0.9995	0.99917	0.99997	0.99919	1	0.9933	0.0155	0.4922	1	1	0.0935	1	1	0.7139	0.2	350
0.99391	0.99765	1	1.00004	0.99648	0.99463	0.99874	0.99806	0.9999	0.9981	1	0.9997	0.0155	.6774	1	0.9999	0.2415	0.9999	1	0.5986	0.3	350
0.9881	0.99568	0.99996	1.00004	0.99306	0.98965	0.9976	0.99626	0.9998	0.99639	1	0.9971	0.0154	0.8852	0.9998	0.9997	0.0326	0.9988	1	0.4413	0.4	350
0.98118	0.99383	0.99829	0.99952	0.98296	0.98629	0.99451	0.99961	0.99093	0.99555	1	9988	0.015	0.0615	0.9995	0.9993	0.2731	0.9999	0.9978	0.2114	0.5	350
0.9568	0.98756	0.99969	0.99995	0.98767	0.96872	0.9966	0.97519	0.99372	0.99096	1	0.8006	0.0159	0.7504	0.9991	0.9961	0.0081	0.9955	0.9983	0.3676	0.6	350
0.99931	0.99975	0.99996	1.00002	0.9994	0.99944	0.99981	1	0.99967	0.99987	1	0.9864	0.0155	0.6608	1	1	0.2287	1	1	0.7812	0.1	400
0.99763	0.99908	0.99982	0.99996	0.99788	0.99824	0.99924	0.99995	0.99886	0.99939	1	0.9847	0.0155	0.8431	1	1	0.004	1	1	0.6062	0.2	400
0.99468	0.99795	0.99956	0.99988	0.99519	0.99599	0.99823	0.9999	0.9974	0.99858	1	0.9928	0.0154	0.3297	1	0.9999	0.0305	1	0.9998	0.5906	0.3	400
0.98959	0.99623	0.99908	0.99974	0.99054	0.99222	0.99672	0.99981	0.99496	0.99729	1	0.8461	0.0153	0.8099	0.9998	0.9998	0.2224	1	0.9993	0.619	0.4	400
0.98369	0.99466	0.99551	0.99864	0.98099	0.99318	0.99388	0.99772	0.98039	0.99781	1	0.9962	0.0148	0.9288	0.9996	0.9995	0.6916	0.9996	0.9969	0.5492	0.5	400
0.96074	0.98893	0.99974	1	0.97714	0.968	0.9937	0.98879	0.99831	0.9918	1	0.0659	0.0152	0.4201	0.9984	0.9968	0.5726	0.9979	0.9997	0.579	0.6	400
0.99942	0.99978	0.99987	0.99998	0.99932	0.99976	0.99981	0.99995	0.99925	0.99994	1	0.1785	0.0155	0.5816	1	1	0.2528	1	1	0.5706	0.1	450
0.99796	0.99921	0.99947	0.99984	0.99761	0.99912	0.99918	0.99971	0.99743	0.99971	1	0.9378	0.0155	0.3496	1	1	0.0804	1	0.9999	0.5471	0.2	450
0.9954	0.99824	0.99877	0.99959	0.99458	0.998	0.99805	0.99937	0.99428	0.99929	1	0.7185	0.0159	0.3896	1	1	0.2307	1	0.9997	0.529	0.3	450
0.99099	0.99674	0.99754	0.99921	0.9894	0.99615	0.99628	0.99874	0.98891	0.99868	1	0.9999	0.0151	0.5367	0.9999	0.9999	0.1541	0.9999	0.999	0.5722	0.4	450
0.98598	0.99542	0.99195	0.9975	0.98184	0.99872	0.99414	0.98874	0.98065	0.99958	1	0.9981	0.0146	8.3E-05	0.9997	0.9999	0.3788	0.9983	0.9974	0.3367	0.5	450
0.96366	0.99014	0.99666	0.99919	0.96773	0.97506	0.99124	0.99927	0.98293	0.99287	1	0.9394	0.0146	0.3904	0.9982	0.9976	0.0127	0.9998	0.9926	0.1698	0.6	450
0.9995	0.99981	0.99974	0.99993	0.99936	0.99992	0.99981	0.99961	0.99925	1	1	0.9718	0.0155	0.3886	1	1	0.0717	1	1	0.5615	0.1	500
0.99826	0.99933	0.99903	0.99968	0.99771	0.99984	0.99918	0.99859	0.9974	0.99994	1	0.9472	0.0154	0.4178	1	1	0.0262	1	1	0.4764	0.2	500
0.99606	0.99849	0.99776	0.99924	0.9948	0.9996	0.99811	0.9968	0.99421	0.99987	1	0.9861	0.0153	0.3107	1	1	0.0251	0.9999	0.9998	0.5256	0.3	500

0.99229	0.99721	0.9956	0.99852	0.98984	0.99928	0.99641	0.99369	0.98888	0.99974	1	0.9998	0.015	0.0391	0.9999	1	0.1798	0.9995	0.9992	0.5403	0.4	500
0.98807	0.99613	0.98808	0.99625	0.98519	0.99968	0.99521	0.98024	0.99073	0.99987	1	0.9953	0.0145	98276	0.9997	1	0.4334	0.9983	0.9981	0.5441	0.5	500
0.9708	0.99172	0.99195	0.99783	0.96682	0.98837	0.99042	0.99602	0.9665	0.99658	1	9696	0.0142	0.3671	0.9988	0.9986	0.2006	0.9988	0.9913	0.4573	0.6	500
0.99959	0.99985	0.9996	0.99989	0.99947	0.99992	0.99981	0.99927	0.99964	1	1	0.9905	0.0155	0.1997	1	1	0.453	1	1	0.5093	0.1	550
0.99851	0.99944	0.99855	0.99951	0.99813	0.99992	0.99931	0.99748	0.99876	1	1	0.9967	0.0154	0.9192	1	1	0.8736	1	1	0.5431	0.2	550
0.99667	0.99873	0.99666	0.99882	0.99576	0.99992	0.99842	0.99427	0.99724	0.99997	1	0.9938	0.0152	0.0201	1	1	0.8408	1	0.9998	0.5247	0.3	550
0.99344	0.99764	0.99345	0.99774	0.99172	0.99976	0.9971	0.98888	0.9947	0.9999	1	0.9857	0.0149	0.6901	0.9999	1	0.8316	0.9999	0.9994	0.5023	0.4	550
0.99	0.99677	1.01069	0.99501	0.9901	0.99519	0.99678	0.97922	0.99948	0.99842	1	0.9884	0.0144	0.4432	0.9997	0.9995	0.0159	0.9995	0.9998	0.5888	0.5	550
0.9744	0.99285	0.98536	0.99602	0.96792	0.99775	0.9908	0.98	0.96732	0.99935	0.9999	0.0552	0.0139	0.4792	0.999	0.9996	0.3716	0.9987	0.9924	0.248	0.6	550
0.99964	0.99988	0.99947	0.99984	0.99964	0.99976	0.99987	0.99922	0.99997	0.99997	1	0.9982	0.0155	0.5277	1	1	0.2867	1	1	0.5034	0.1	600
0.99876	0.99953	0.99807	0.99933	0.99876	0.99936	0.99956	0.99728	0.99993	0.99977	1	0.9981	0.0154	0.6087	1	1	0.4669	1	1	0.5166	0.2	600
0.99722	0.99894	0.9956	0.99843	0.99717	0.99864	0.99899	0.99388	0.99984	0.99948	1	0.9936	0.0152	0.4792	1	1	0.4334	0.9999	1	0.509	0.3	600
0.99452	0.99804	0.99134	0.99701	0.99449	0.99727	0.99805	0.9882	0.99971	0.99903	1	0.7807	0.0149	0.5087	0.9999	0.9998	0.2267	0.9996	0.9999	0.6215	0.4	600
0.99171	0.99734	0.98105	0.99394	0.99515	0.98757	0.99842	0.98612	0.99639	0.99593	1	0.996	0.0144	0.7807	0.9998	0.999	0.2357	0.9985	0.9989	0.5564	0.5	600
0.97719	0.99384	0.97744	0.99394	0.97278	0.99944	0.99237	0.96422	0.9838	0.99977	0.9999	0.9993	0.0135	0.2012	0.999	0.9999	0.354	0.9947	0.9941	0.1329	0.6	600
0.99972	0.9999	0.99934	0.99981	0.99983	0.99952	0.99994	0.99951	0.99987	0.99987	1	0.9933	0.0155	0.8806	1	1	0.1231	1	1	0.5966	0.1	650
0.99898	0.99961	0.99767	0.99917	0.99939	0.9984	0.99975	0.9982	0.99951	0.99945	1	0.969	0.0154	0.2522	1	1	0.0391	1	1	0.5885	0.2	650
0.99771	0.99914	0.99468	0.99808	0.99862	0.99639	0.9995	0.99592	0.99893	0.99871	1	0.9996	0.0152	0.5702	1	0.9999	0.0153	0.9999	0.9999	0.5789	0.3	650
0.99548	0.99839	0.98953	0.99635	0.9973	0.99302	0.99905	0.99209	0.99795	0.99755	1	0.993	0.0149	0.8862	0.9999	0.9997	0.8098	0.9995	0.9997	0.5609	0.4	650
0.98193	0.99497	0.97212	0.99218	0.98272	0.99158	0.99502	0.96471	0.99912	0.99752	1	0.9608	0.0144	0.0267	0.9999	0.9992	0.2508	0.9992	0.9976	0.4442	0.5	650
0.98193	0.99497	0.97212	0.99218	0.98272	0.99158	0.99502	0.96471	0.99912	0.99752	0.9999	0.9201	0.0135	0.5727	0.9991	0.9984	0.3194	0.9961	0.9995	0.6115	0.6	650
0.99978	0.99992	0.99925	0.99977	0.99995	0.99928	1	0.99985	0.99945	0.99977	1	0.9453	0.0155	0.3856	1	1	0.0416	1	1	0.5926	0.1	700
0.99917	0.9997	0.99732	0.99905	0.99986	0.99751	0.99994	0.99947	0.99802	0.99913	1	0.9579	0.0154	0.3549	1	1	0.0091	1	1	0.5998	0.2	700
0.99815	0.99931	0.99393	0.9978	0.99967	0.99447	0.99987	0.99874	0.99558	0.99797	1	0.9921	0.0152	0.1455	1	0.9999	0.0182	0.9999	0.9998	0.6449	0.3	700
0.99631	0.9987	0.98808	0.99584	0.99936	0.98917	0.99975	0.99752	0.99148	0.99619	1	0.9835	0.0149	0.1471	1	0.9997	0.8952	0.9997	0.9992	0.4605	0.4	700
0.9946	0.9983	0.977	0.9926	0.99997	0.97827	0.99994	1	0.97902	0.9929	1	0.9976	0.0145	0.9715	1	0.9994	0.6191	1	0.9982	0.5814	0.5	700

0.98487	0.99584	0.96614	0.99049	0.99141	0.97827	0.99754	0.97626	0.99379	0.99367	0.9999	0.9198	0.0135	0.8077	0.9993	0.9971	0.0601	0.9956	0.9968	0.5569	0.6	700
0.99983	0.99994	0.99916	0.99975	1	0.9992	1	1	0.99919	0.99974	1	0.9956	0.0155	0.6071	1	1	0.1504	1	1	0.3186	0.1	750
0.99937	0.99977	0.99714	0.99898	0.99998	0.99719	1	1	0.9972	0.999	1	0.9978	0.0154	0.6217	1	1	0.2626	1	1	0.2548	0.2	750
0.99854	0.99946	0.99349	0.99762	0.99998	0.99366	1	1	0.99379	0.99771	1	0.9945	0.0152	0.6763	1	0.9999	0.4511	1	0.9998	0.774	0.3	750
0.99708	0.99899	0.98725	0.99553	0.99998	0.98773	0.99994	1	0.98803	0.99568	1	9952	0.015	0.7181	1	0.9998	0.4723	1	0.9994	0.6512	0.4	750
0.99578	0.9987	0.97652	0.99244	0.99811	0.98107	0.99937	0.99558	0.98517	0.99384	1	0.9611	0.0146	0.0967	0.9999	0.9992	0.003	0.9992	0.9976	0.5912	0.5	750
0.98716	0.99658	0.96038	0.98904	0.99785	0.96559	0.99937	0.99214	0.97376	0.99009	0.9999	0.9775	0.0135	0.0328	0.9998	0.09974	0.8604	0.9974	0.9927	0.4234	0.6	750
0.99986	0.99997	0.99916	0.99974	0.99992	0.99928	0.99994	0.99985	0.99945	0.99981	1	0.8857	1	0.8046	1	1	0.356	1	1	0.6249	0.1	800
0.9995	0.99983	0.99705	0.99894	0.99975	0.99751	0.99987	0.99947	0.99805	0.99916	1	0.6429	1	0.9246	1	1	0.2645	1	1	0.646	0.2	800
0.99915	0.99971	0.99354	0.99762	0.99818	0.99655	0.99931	0.99592	0.99896	0.99877	1	0.9997	1	0.0392	1	0.9999	0.4743	0.9999	0.9999	0.4408	0.3	800
0.99771	0.99923	0.98698	0.99542	0.99895	0.98933	0.99962	0.99748	0.99158	0.99626	1	0.7439	1	0.2662	1	0.9997	0.0186	0.9997	0.9992	0.6219	0.4	800
0.99678	0.99904	0.97705	0.99262	0.99364	0.98797	0.99786	0.98612	0.99649	0.99613	1	0.9657	0.9998	0.3156	0.9997	0.99	0.1877	0.9985	0.9989	0.6082	0.5	800
0.99011	0.99733	0.95915	0.98843	0.99997	0.96247	0.99994	1	0.96462	0.98896	1	0.9333	0.9997	0.6826	1	0.9981	0.5428	1	0.9949	0.701	0.6	800
0.99992	0.99998	0.99916	0.99974	0.99976	0.99952	0.99987	0.99951	0.99987	0.99987	1	0.9995	1	0.9876	1	1	0.0319	1	1	0.7662	0.1	850
0.99964	0.99989	0.99714	0.99896	0.99918	0.99848	0.99968	0.9982	0.99954	0.99948	1	0.9994	1	0.9732	1	1	0.1208	1	1	0.4244	0.2	850
0.99915	0.99971	0.99354	0.99762	0.99818	0.99655	0.99931	0.99592	0.99896	0.99877	1	0.9997	1	0.0392	1	0.9999	0.4743	0.9999	0.9999	0.4408	0.3	850
0.99826	0.99944	0.98729	0.99553	0.99645	0.99326	0.99868	0.99214	0.99802	0.99764	1	0.9908	0.9998	0.327	0.9999	0.9997	0.3937	0.9995	0.9997	0.5846	0.4	850
0.99763	0.99933	0.97859	0.99311	0.98768	0.99559	0.9959	0.97942	0.99945	0.99858	1	0.9657	0.9998	0.3156	0.9997	0.9999	0.1877	0.9995	0.9989	0.6092	0.5	850
0.99223	0.99794	0.95827	0.98818	0.99667	0.96728	0.99899	0.99238	0.97486	0.99045	1	0.9145	0.9996	0.3703	0.9997	0.9976	0.013	0.9975	0.9933	0.2733	0.6	850
0.99994	1	0.99925	0.99975	0.99954	0.99984	0.99981	0.99927	0.99997	0.99997	1	0.9998	1	0.6338	1	1	0.3369	1	1	0.4088	0.1	900
0.99975	0.99993	0.99732	0.99903	0.99843	0.99944	0.99943	0.99733	0.99993	0.99981	1	0.9999	1	0.6409	1	1	0.4788	1	1	0.4629	0.2	900
0.99939	0.99982	0.99398	0.99778	0.99647	0.99872	0.99868	0.99398	0.99984	0.99955	1	0.9972	1	0.6283	1	1	0.5328	0.9999	1	0.8703	0.3	900
0.99873	0.99961	0.98817	0.99582	0.9931	0.99751	0.99754	0.9883	0.99967	0.99916	1	0.9917	0.9999	0.5657	0.9999	0.9968	0.2527	0.9996	0.9999	0.5945	0.4	900
0.99832	0.99957	0.98092	0.99387	0.98168	0.99976	0.99395	0.98073	0.9907	0.9999	1	0.9955	0.9998	0.6763	0.9996	0.9998	0.467	0.9986	0.9998	0.585	0.5	900
0.99375	0.99843	0.95726	0.98825	0.98834	0.97819	0.99666	0.97544	0.99376	0.99387	1	0.7111	0.9994	0.4195	0.9989	0.9969	0.6466	0.9951	0.9966	0.5462	0.6	900
0.99997	1.00001	0.9993	0.99977	0.99932	1	0.99975	0.99932	0.99964	1	1	0.9998	1	0.601	1	1	0.00001	1	1	0.674	0.1	950

0.99986	0.99998	0.99763	0.99914	0.99764	0.99992	0.99912	0.99752	0.99873	1	1	0.9998	1	0.561	1	1	0.0019	1	1	0.688	0.2	950
0.99959	0.99991	0.99464	0.99801	0.99472	0.99992	0.99805	0.99442	0.9972	0.99997	1	0.9992	1	0.7037	1	1	0.0112	0.9999	0.9998	0.694	0.3	950
0.99915	0.99978	0.98949	0.99628	0.98973	0.99984	0.99628	0.98913	0.99467	0.99997	1	0.6694	0.9999	0.0644	0.9908	1	0.0684	0.9995	0.9993	0.5441	0.4	950
0.9989	0.99978	0.98377	0.9948	0.97692	0.99824	0.99237	0.98927	0.98078	0.99906	1	0.9873	0.9997	0.1879	0.9994	0.998	0.0196	0.9983	0.9974	0.6453	0.5	950
0.99554	0.9989	0.96144	0.9892	0.97835	0.99222	0.9937	0.96476	0.99906	0.99777	1	0.8181	0.9993	0.5385	0.9986	0.9984	0.4196	0.996	0.9995	0.5921	0.6	950
1	1.00002	0.99943	0.99981	0.99915	0.99992	0.99968	0.99961	0.99925	1	1	0.6001	1	0.7076	1	1	0.0078	1	1	0.6094	0.1	1000
0.99992	1.00002	0.99798	0.99926	0.99705	0.99976	0.99893	0.99864	0.9974	0.99994	1	0.78	1	0.7892	1	1	0.0212	1	1	0.6069	0.2	1000
0.99978	0.99999	0.99547	0.99831	0.99336	0.99944	0.99754	0.99694	0.99424	0.99981	1	0.9429	1	0.8765	1	1	0.0312	0.9999	0.9998	0.6115	0.3	1000
0.99945	0.9999	0.99107	0.99685	0.98706	0.99904	0.99533	0.99403	0.98894	0.99965	1	0.9504	0.9999	0.318	0.9908	0.9999	0.1233	0.9995	0.9992	0.4506	0.4	1000
0.99934	0.99994	0.98698	0.99582	0.97452	0.99182	0.99161	0.99811	0.98088	0.99726	1	0.9893	0.9998	0.7437	0.9993	0.9993	0.3644	0.9996	0.997	0.5625	0.5	1000
0.99686	0.99928	0.96583	0.99043	0.96824	0.99968	0.99061	0.96694	0.98455	0.99987	1	0.8643	0.9992	0.1403	0.9985	0.9999	0.0207	0.9953	0.9944	0.5548	0.6	1000
1.00003	1.00003	0.99952	0.99984	0.99906	0.99968	0.99968	0.99995	0.99928	0.9999	1	0.9497	1	0.4724	1	1	0.07	1	1	0.4588	0.1	1050
1	1.00006	0.99837	0.9994	0.99675	0.99888	0.9988	0.99976	0.9975	0.99961	1	0.8791	1	0.4368	1	1	0.1137	1	0.9994	0.5201	0.2	1050
0.99992	1.00004	0.99635	0.99864	0.9927	0.99759	0.99729	0.99947	0.99441	0.9991	1	0.9799	0.9992	0.4775	0.9999	0.9999	0.2228	1	0.9997	0.4465	0.3	1050
0.99972	1.00001	0.99288	0.99746	0.98575	0.99535	0.99489	0.99893	0.98917	0.99832	1	0.9968	1	0.6778	0.9998	0.9998	0.4381	0.9999	0.999	0.6	0.4	1050
0.9997	1.00009	0.99019	0.99685	0.97488	0.98356	0.9918	0.99932	0.99158	0.99448	1	0.8754	1	0.4383	0.9999	0.9988	0.589	0.9999	0.9979	0.657	0.5	1050
0.99769	0.99957	0.96878	0.99167	0.95748	0.99687	0.98789	0.98019	0.96624	0.99903	1	0.8161	0.9995	0.3369	0.9981	0.9993	0.0931	0.9944	0.9917	0.0108	0.6	1050
1.00006	1.00006	0.99965	0.99988	0.99909	0.99936	0.99968	1	0.99967	0.99981	1	0.6386	1	0.6419	1	1	0.4101	1	1	0.5857	0.1	1100
1.00006	1.00009	0.99877	0.99954	0.99683	0.99783	0.9988	0.99995	0.99893	0.99923	1	0.0378	1	0.8022	1	1	0.3205	1	1	0.5856	0.2	1100
1.00003	1.0001	0.99727	0.99898	0.99285	0.99511	0.99735	0.99981	0.99759	0.99819	1	0.8441	1	0.6155	0.9999	0.9999	0.1448	1	0.9998	0.5889	0.3	1100
0.99992	1.00011	0.99464	0.99808	0.98603	0.99062	0.99502	0.99966	0.99528	0.99664	1	0.92	1	0.4695	0.9997	0.9996	0.2165	0.9989	0.9993	0.597	0.4	1100
0.99997	1.0002	0.99314	0.9978	0.97785	0.97698	0.99288	0.99214	0.9998	0.99235	1	0.9724	1	0.6061	0.9988	0.9981	0.0011	0.9975	1	0.5931	0.5	1100
0.99865	0.99983	0.97599	0.99343	0.95474	0.98588	0.98695	0.99665	0.96689	0.99574	1	0.7624	0.9996	0.4903	0.9977	0.9978	0.5777	0.9988	0.9912	0.6635	0.6	1100
1.00006	1.00007	0.99974	0.99991	0.9992	0.99912	0.99968	0.99971	1	0.99971	1	0.9903	1	0.059	1	1	0.0644	1	1	0.5358	0.1	1150
1.00008	1.00011	0.99916	0.99968	0.99724	0.99695	0.99899	0.99893	0.99997	0.9989	1	0.9203	1	0.0121	1	1	0.0287	1	1	0.5558	0.2	1150
1.00011	1.00015	0.99811	0.99928	0.99378	0.99326	0.99767	0.99762	0.99993	0.99752	1	0.9926	1	0.0386	0.9999	0.9998	0.0064	0.9999	1	0.574	0.3	1150

1.00006	1.00019	0.99626	0.99866	0.98778	0.98693	0.99565	0.99549	0.9999	0.99532	1	0.9841	1	0.4582	0.9996	0.9994	0.0364	0.9996	1	0.5969	0.4	1150
1.00017	1.0003	0.99565	0.99861	0.98286	0.97482	0.99451	0.98199	0.99528	0.99177	1	0.4202	1	0.4407	0.9989	0.9974	0.436	0.9974	0.9999	0.5763	0.5	1150
0.99928	1.00004	0.98219	0.99508	0.95576	0.97225	0.98726	0.99888	0.98537	0.99151	1	0.7786	0.9997	0.6118	0.9969	0.9964	0.0072	0.9996	0.9937	0.5643	0.6	1150
1.00008	1.00007	0.99982	0.99995	0.99939	0.99904	0.99975	0.99932	0.9998	0.99971	1	0.9856	1	0.4571	1	1	0.0762	1	1	0.3031	0.1	1200
1.00014	1.00013	0.99947	0.99981	0.99788	0.99671	0.99918	0.99757	0.99935	0.99884	1	0.9795	1	0.4534	1	1	0.1687	1	1	0.46	0.2	1200
1.00017	1.0002	0.99881	0.99954	0.99522	0.9927	0.99817	0.99456	0.99857	0.99732	1	0.997	1	0.4896	0.9999	0.9978	0.2344	0.9998	0.9999	0.0054	0.3	1200
1.00019	1.00024	0.99763	0.99915	0.99061	0.98588	0.99666	0.98961	0.99727	0.995	1	0.9692	1	0.6887	0.9997	0.9992	0.3943	0.9991	0.9997	0.5866	0.4	1200
1.0003	1.00036	0.99763	0.99926	0.98861	0.97795	0.99634	0.97568	0.98358	0.99293	1	0.9812	1	0.3545	0.9993	0.9968	0.0302	0.9953	0.9961	0.5031	0.5	1200
0.9997	1.0002	0.98637	0.99646	0.95699	0.95782	0.98846	0.98592	0.99541	0.99203	1	0.6073	0.9998	0.4603	0.9957	0.9972	0.3373	0.9963	0.9967	0.5951	0.6	1200
1.00008	1.00008	0.99991	0.99998	0.99959	0.9992	0.99981	0.99908	0.99932	0.99974	1	0.9846	1	0.4901	1	1	0.001	1	1	0.5555	0.1	1250
1.00017	1.00015	0.99969	0.99991	0.9986	0.99719	0.99943	0.9968	0.99769	0.999	1	0.5534	1	0.4075	1	1	0.0863	0.9999	1	0.5525	0.2	1250
1.00022	1.00023	0.99934	0.99977	0.99684	0.99374	0.9988	0.99282	0.99493	0.99771	1	0.7933	0.9999	0.5313	0.9999	0.9998	0.0261	0.9996	0.9996	0.5424	0.3	1250
1.00028	1.0003	0.99868	0.99956	0.99378	0.98781	0.99779	0.98616	0.99037	0.99571	1	0.9997	1	0.6177	0.9998	0.9991	0.2785	0.9985	0.9987	0.1245	0.4	1250
1.00096	1.00044	0.99894	0.99974	0.99381	0.985	0.99798	0.97733	0.97584	0.99526	1	0.9619	1	0.2726	0.9997	0.9981	0.0003	0.9947	0.992	0.6183	0.5	1250
1.00008	1.00033	0.99182	0.99782	0.96799	0.95509	0.9913	0.96946	0.9921	0.98706	1	0.9347	0.9999	0.5426	0.9964	0.9918	0.5137	0.9921	0.9971	0.5666	0.6	1250
1.00011	1.00009	0.99996	1.00002	0.99978	0.99944	0.99987	0.99922	0.99906	0.99984	1	0.9992	1	0.3996	1	1	0.0082	1	1	0.5663	0.1	1300
1.00019	1.00018	0.99991	0.99998	0.99923	0.99816	0.99968	0.99718	0.99678	0.99932	1	0.9983	1	0.9498	1	1	0.105	0.9999	1	0.5439	0.2	1300
1.00028	1.00026	0.99974	0.99995	0.99829	0.99583	0.99931	0.99359	0.99281	0.99845	1	0.9935	0.9999	0.6835	1	0.998	0.0043	0.9996	0.9973	0.544	0.3	1300
1.00036	1.00035	0.99943	0.99986	0.99662	0.99182	0.9988	0.98743	0.98618	0.99713	1	0.9997	0.9999	0.6939	0.9999	0.9994	0.8825	0.9983	0.9974	0.6643	0.4	1300
1.0005	1.0005	0.99978	1.00005	0.99753	0.99278	0.99918	0.98616	0.97971	0.99771	1	0.9897	0.9999	0.6101	0.9999	0.9993	0.4862	0.997	0.9925	0.5787	0.5	1300
1.00033	1.00044	0.9956	0.99884	0.97914	0.9607	0.99426	0.95883	0.9734	0.98896	1	0.9946	1	0.1903	0.9977	0.9912	0.2635	0.9865	0.9892	0.3889	0.6	1300
1.00011	1.0001	1	1.00004	0.99991	0.99968	0.99994	0.99951	0.99928	0.9999	1	0.9887	1	0.4502	1	1	0.1024	1	1	0.4284	0.1	1350
1.00022	1.0002	1	1.00005	0.9997	0.99912	0.99987	0.99835	0.9975	0.99968	1	0.9334	1	0.4824	1	1	0.1684	1	1	0.4737	0.2	1350
1.0003	1.0003	1	1.00007	0.99932	0.998	0.99975	0.99621	0.99434	0.99926	1	0.9973	0.9999	0.4972	1	0.9999	0.233	0.998	0.9994	0.3253	0.3	1350
1.00041	1.0004	0.99991	1.00007	0.99866	0.99607	0.9995	0.99252	0.98885	0.99861	1	0.9933	0.9999	0.7374	1	0.9998	0.43	0.9991	0.9977	0.5974	0.4	1350
1.00055	1.00055	1.00022	1.00028	0.99954	0.99808	0.99994	0.99549	0.99174	0.99942	1	0.9464	0.9999	0.4086	1	0.9999	0.0656	0.9994	0.9979	0.6891	0.5	1350

1.00047	1.00052	0.99776	0.99952	0.98726	0.96944	0.99678	0.95563	0.9559	0.99229	1	0.9999	1	0.7069	0.9987	0.9922	0.9412	0.9806	0.9733	0.3838	0.6	1350
1.00011	1.00011	1.00004	1.00007	1	0.99992	1	0.99985	0.99971	1	1	0.9749	1	0.8577	0.3342	1	0.0175	1	1	0.5498	0.1	1400
1.00022	1.00022	1.00009	1.00012	0.99998	0.99976	1	0.99947	0.99899	0.99994	1	0.998	1	0.502	0.5001	1	0.3031	1	1	0.5733	0.2	1400
1.00033	1.00033	1.00018	0.9993	0.99992	0.99944	1	0.99879	0.99776	0.99984	1	0.9968	0.9999	0.2313	0.6502	1	0.6836	1	0.9998	0.5751	0.3	1400
1.00044	1.00044	1.00018	1.00025	0.99978	0.99896	1	0.99757	0.99554	0.99965	1	0.9885	0.9999	0.6604	0.2711	1	0.9107	0.9968	0.9994	0.4391	0.4	1400
1.00063	1.00061	1.00048	1.00048	1.00031	1.00008	1.00032	0.99981	0.99925	1.00023	1	0.97	0.9999	0.1992	0.1328	1	0.0123	1	0.9999	0.599	0.5	1400
1.00061	1.0006	0.99943	1.00002	0.99522	0.98605	0.99874	0.97325	0.96205	0.99635	1	0.9115	0.9999	0.6424	0.6632	0.9973	0.5773	0.9892	0.9748	0.6008	0.6	1400
1.00014	1.00012	1.00009	1.00011	1.00006	1	1.00006	1.00005	1	1.00006	1	0.3634	1	0.4502	1	1	0.0041	1	1	0.4785	0.1	1450
1.00025	1.00024	1.00018	1.00019	1.00014	1.00008	1.00013	1.00005	0.99993	1.0001	1	0.9888	0.9999	0.4824	1	1	0.0174	1	1	0.7902	0.2	1450
1.00039	1.00036	1.00026	1.00028	1.0002	1.00008	1.00019	1	0.99984	1.00016	1	0.9994	0.9999	0.4972	1	1	0.0123	1	1	0.4503	0.3	1450
1.0005	1.00049	1.00035	1.00039	1.00027	1.00008	1.00025	0.99995	0.99964	1.00019	1	0.9586	0.9999	0.7374	1	1	0.52	1	1	0.583	0.4	1450
1.00025	1.00024	1.00018	1.00019	1.00014	1.00008	1.00013	1.00005	0.99993	1.0001	1	0.9773	0.9999	0.4086	1	1	0.0218	1	1	0.6678	0.5	1450
1.00069	1.00067	1.00022	1.00033	0.99906	0.99639	0.99987	0.99155	0.98436	0.99906	1	0.9894	0.9999	0.7069	0.9987	0.9997	0.4862	0.998	0.9027	0.5762	0.6	1450
1.00286	1.00382	1.0032	1.00395	1.00348	1.00376	1.00403	1.00397	1.00409	1.00415	1	0.992	1	0.479	1	1	0.6349	1	1	0.5879	0.1	50
0.99912	1.00233	1.00035	1.00279	1.00129	1.00216	1.00315	1.00281	1.00337	1.00351	1	0.9946	1	0.5756	1	1	0.5778	1	1	0.5882	0.2	50
0.99263	0.99979	0.99544	1.00086	0.99757	0.99944	1.0017	1.00097	1.00217	1.00241	1	0.9986	0.073	0.5837	0.9999	0.9999	0.1062	0.9999	0.9999	0.6089	0.3	50
0.98161	0.9959	0.98732	0.99791	0.99157	0.9952	0.99943	0.99806	1.00029	1.0008	1	0.9984	0.0761	0.9414	0.9996	0.9995	0.0431	0.9996	0.9997	0.6254	0.4	50
0.96737	0.9918	0.98451	0.99743	0.99483	1.00128	1.00101	1.00417	1.00412	1.00325	0.9999	0.9974	0.0177	0.976	0.9998	0.9999	0.0513	1	1	0.3093	0.5	50
0.96377	0.99054	0.97473	0.99388	0.98256	0.98896	0.99641	0.9939	0.99766	1.00299	0.9999	0.9963	0.0184	0.9032	0.9988	0.9986	0.3984	0.9988	0.9992	0.6045	0.6	50
1.003	1.00387	1.00364	1.00411	1.00403	1.00432	1.00421	1.00441	1.00441	1.00438	1	0.9997	0.0156	0.6515	1	1	0.7606	1	1	0.5617	0.1	100
0.99962	1.00252	1.00171	1.00336	1.00309	1.004	1.00384	1.00441	1.00441	1.00425	1	0.9969	0.0158	0.5335	1	1	0.7357	1	1	0.5518	0.2	100
0.99371	1.00022	0.99846	1.00206	1.0015	1.00344	1.00321	1.00436	1.00435	1.00402	1	0.9873	0.0162	0.4783	1	1	0.6721	1	1	0.5537	0.3	100
0.98367	0.99669	0.99303	1.00011	0.99887	1.00264	1.00226	1.00431	1.00428	1.0037	1	0.9986	0.0168	0.6573	0.9999	1	0.7523	1	1	0.5834	0.4	100
0.97095	0.99306	0.9925	1.00028	1.00219	1.0044	1.00359	0.03221	0.99439	1.00441	1	0.989	0.0172	0.1439	0.9999	1	0.2361	0.9996	0.9978	0.58	0.5	100
0.92969	0.98253	0.95245	0.98801	0.9675	0.97896	0.99207	0.98741	0.99361	0.99556	0.9995	0.1162	0.0208	0.4399	0.9966	0.9962	0.0417	0.9969	0.9979	0.5088	0.6	100
1.00313	1.00393	1.00395	1.00424	1.00433	1.00448	1.00434	1.00431	1.00406	1.00441	1	0.9469	0.0156	0.5907	1	1	0.0266	1	1	0.6025	0.1	150

1.00008	1.00271	1.00281	1.00378	1.00412	1.00448	1.00428	1.00402	1.00318	1.00444	1	0.9064	0.0158	0.6236	1	1	0.2038	1	1	0.595	0.2	150	
0.99478	1.00064	1.00088	1.00302	1.00376	1.00448	1.00415	1.00344	1.00159	1.00444	1	0.5017	0.016	0.7003	1	1	0.7426	1	0.9998	0.589	0.3	150	
0.98571	0.99745	0.99763	1.00186	1.00315	9.80589	1.0039	1.00242	0.99883	1.00441	1	0.9932	0.0165	0.2735	1	1	0.0923	0.9999	0.9993	0.6134	0.4	150	
0.97422	0.9942	0.99842	1.00236	1.0045	0.99976	1.00447	0.99119	0.9866	1.00293	1	0.9977	0.0166	0.7397	1	0.9996	0.7575	0.998	0.9957	0.612	0.5	150	
0.93181	0.98408	0.96714	0.99329	0.9869	0.99872	0.99899	1.00392	1.00383	1.00258	0.9997	0.9999	0.0199	0.9295	0.9993	0.9997	0.0811	1	0.9999	0.5655	0.6	150	
1.00327	1.00397	1.00417	1.00432	1.00444	1.00432	1.0044	1.00397	1.00376	1.00438	1	0.9951	0.0156	0.5628	1	1	0.5719	1	1	0.5837	0.1	200	
1.00052	1.00288	1.00364	1.0041	1.00445	1.00392	1.0044	1.00281	1.00208	1.00425	1	0.995	0.0157	0.5791	1	1	0.7073	1	0.9999	0.5828	0.2	200	
0.99574	1.00102	1.00268	1.00373	1.00447	1.0032	1.0044	1.00068	0.99919	1.00396	1	0.9994	0.0159	0.6528	1	1	0.2212	0.9998	0.9996	0.6045	0.3	200	
0.98758	0.99816	1.00105	1.00315	1.00448	1.00192	1.00447	0.99705	0.99429	1.00354	1	0.9965	0.0162	0.9108	1	0.9999	0.00072	0.9994	0.9986	0.3044	0.4	200	
0.97735	0.99529	1.00232	1.00373	1.00244	0.99208	1.00377	0.9862	0.99085	1.00042	1	9941	0.0162	0.1368	0.9999	0.9989	0.202	0.9974	0.9976	0.0078	0.5	200	
0.94525	0.9868	0.9839	0.99805	1.0006	1.0044	1.00321	0.99801	0.98667	1.00435	0.9999	0.9916	0.0184	0.3379	0.9999	1	0.2241	0.9988	0.9932	0.1131	0.6	200	
1.00341	1.00403	1.00434	1.00438	1.00437	1.004	1.0044	1.00378	1.00389	1.00428	1	0.9947	0.0156	0.0044	1	1	0.1971	1	1	0.5617	0.1	250	
1.00096	1.00305	1.00417	1.00431	1.0042	1.00078	1.00434	1.00208	1.00256	1.0039	1	0.9828	0.0156	0.5728	1	1	0.3143	1	1	0.5682	0.2	250	
0.99667	1.00139	1.00382	1.00418	1.0039	1.00096	1.00421	0.99913	1.00029	1.00316	1	9977	0.0157	0.3183	1	0.9999	0.3174	0.9998	0.9998	0.5589	0.3	250	
0.98936	0.99883	1.00325	1.00399	1.00335	0.9976	1.00403	0.99409	0.99656	1.00203	1	0.9947	0.0159	0.1161	1	0.9996	0.0175	0.9992	0.9992	0.5208	0.4	250	
0.9804	0.99634	1.00426	1.00446	0.99762	0.98672	1.0022	0.98973	1.00065	0.99858	1	0.9995	0.0157	0.7314	0.9997	0.9987	0.3606	0.9984	0.9994	0.5997	0.5	250	
0.94921	0.98837	0.99368	1.00121	1.00453	0.99592	1.00447	0.98039	0.9733	1.002	0.9999	9225	0.0176	0.4254	1	0.9988	0.0044	0.9934	9871	0.3791	0.6	250	
0.99912	0.99966	1	1	0.9998	0.99944	0.99994	0.9994	0.99947	0.99987	0.99981	1	0.9894	0.0156	0.7359	1	1	0.0023	1	1	0.1798	0.1	300
0.99695	0.9988	1	1.00002	0.9992	0.99776	0.99975	0.99806	0.99951	0.99923	1	0.9958	0.0156	0.8379	1	1	0.0243	1	1	0.0375	0.2	300	
0.99318	0.99734	1	1	0.99815	0.99496	0.99931	0.99564	0.99886	0.99816	1	0.9995	0.0156	0.588	1	0.9999	0.0118	0.9999	0.9999	0.5048	0.3	300	
0.98672	0.99508	0.99991	1	0.9963	0.99016	0.99874	0.99162	0.99786	0.99652	1	0.9904	0.0157	0.307	0.9999	0.9996	0.2188	0.9995	0.9998	0.5665	0.4	300	
0.97889	0.99293	0.99987	1	0.98768	0.98208	0.99604	0.99356	0.99968	0.99404	1	0.9974	0.0154	0.9827	0.9995	0.999	0.4786	0.9993	0.9999	0.5827	0.5	300	
0.94753	0.98541	0.99605	0.99889	0.99611	0.97616	0.99899	0.96629	0.97602	0.9935	1	0.9955	0.0167	0.6398	0.9997	0.996	0.9467	0.9913	0.9822	0.1289	0.6	300	
0.99923	0.9997	1	1.00002	0.99959	0.99936	0.99987	0.99976	1	0.99981	1	0.9909	0.0155	0.4979	1	1	0.5063	1	1	0.6037	0.1	350	
0.99733	0.99894	1	1.00002	0.99851	0.99768	0.9995	0.99918	0.99997	0.9992	1	0.9933	0.0155	0.4922	1	1	0.0935	1	1	0.7139	0.2	350	
0.99401	0.99766	1	1.00004	0.99657	0.9948	0.99874	0.99811	0.9999	0.9981	1	0.9997	0.0155	.6774	1	0.9999	0.2415	0.9999	1	0.5986	0.3	350	

0.98829	0.99568	0.99996	1.00002	0.9932	0.98992	0.99761	0.99632	0.99984	0.99639	1	0.9971	0.0154	0.8852	0.9998	0.9997	0.0326	0.9988	1	0.4413	0.4	350
0.98147	0.99382	0.99833	0.99953	0.98326	0.98656	0.99453	0.99961	0.99111	0.99552	1	9988	0.015	0.0615	0.9995	0.9993	0.2731	0.9999	0.9978	0.2114	0.5	350
0.95767	0.98755	0.99969	0.99995	0.98795	0.96936	0.9966	0.97559	0.9938	0.99095	1	0.8006	0.0159	0.7504	0.9991	0.9961	0.0081	0.9955	0.9983	0.3676	0.6	350
0.99931	0.99974	0.99996	1	0.99944	0.99952	0.99981	1	0.99968	0.99984	1	0.9864	0.0155	0.6608	1	1	0.2287	1	1	0.7812	0.1	400
0.99766	0.99909	0.99982	0.99996	0.99793	0.99832	0.99925	0.99995	0.99886	0.99939	1	0.9847	0.0155	0.8431	1	1	0.004	1	1	0.6062	0.2	400
0.99475	0.99795	0.99956	0.99988	0.99528	0.99608	0.9983	0.9999	0.99747	0.99858	1	0.9928	0.0154	0.3297	1	0.9999	0.0305	1	0.9998	0.5906	0.3	400
0.98978	0.99623	0.99912	0.99974	0.99072	0.9924	0.99673	0.99981	0.99504	0.9973	1	0.8461	0.0153	0.8099	0.9998	0.9998	0.2224	1	0.9993	0.619	0.4	400
0.98398	0.99465	0.99561	0.99863	0.98133	0.99336	0.99384	0.99777	0.98073	0.99781	1	0.9962	0.0148	0.9288	0.9996	0.9995	0.6916	0.9996	0.9969	0.5492	0.5	400
0.96149	0.98891	0.99974	0.99998	0.97764	0.96863	0.99365	0.98896	0.99815	0.99195	1	0.0659	0.0152	0.4201	0.9984	0.9968	0.5726	0.9979	0.9997	0.579	0.6	400
0.99942	0.99978	0.99987	0.99996	0.99934	0.99976	0.99981	0.99995	0.99929	0.99994	1	0.1785	0.0155	0.5816	1	1	0.2528	1	1	0.5706	0.1	450
0.99799	0.99921	0.99952	0.99984	0.99766	0.9992	0.99918	0.99976	0.9975	0.99971	1	0.9378	0.0155	0.3496	1	1	0.0804	1	0.9999	0.5471	0.2	450
0.99546	0.99824	0.99882	0.9996	0.99469	0.99808	0.99805	0.99937	0.99439	0.99929	1	0.7185	0.0159	0.3896	1	1	0.2307	1	0.9997	0.529	0.3	450
0.99115	0.99674	0.99763	0.99919	0.98959	0.99624	0.99629	0.99879	0.9891	0.99868	1	0.9999	0.0151	0.5367	0.9999	0.9999	0.1541	0.9999	0.999	0.5722	0.4	450
0.98623	0.99542	0.9921	0.99749	0.98217	0.9988	0.99409	0.98891	0.98096	0.99958	1	0.9981	0.0146	8.3E-05	0.9997	0.9999	0.3788	0.9983	0.9974	0.3367	0.5	450
0.96424	0.99011	0.99675	0.99919	0.96828	0.97544	0.99119	0.99927	0.98326	0.99285	1	0.9394	0.0146	0.3904	0.9982	0.9976	0.0127	0.9998	0.9926	0.1698	0.6	450
1.0039	1.00421	1.00417	1.00434	1.00378	1.0044	1.00421	1.00402	1.00367	1.00441	1	0.9718	0.0155	0.3886	1	1	0.0717	1	1	0.5615	0.1	500
1.00267	1.00373	1.00347	1.0041	1.00215	1.00424	1.00359	1.003	1.00185	1.00435	1	0.9472	0.0154	0.4178	1	1	0.0262	1	1	0.4764	0.2	500
1.00052	1.00289	1.00224	1.00364	0.99929	1.00408	1.00252	1.00126	0.99867	1.00428	1	0.9861	0.0153	0.3107	1	1	0.0251	0.9999	0.9998	0.5256	0.3	500
0.99678	1.00161	1.00009	1.00292	0.99439	1.00376	1.00082	0.99821	0.99341	1.00415	1	0.9998	0.015	0.0391	0.9999	1	0.1798	0.9995	0.9992	0.5403	0.4	500
0.99263	1.00051	0.99263	1.00063	0.98978	1.00416	0.99956	0.98489	0.99526	1.00425	1	0.9953	0.0145	98276	0.9997	1	0.4334	0.9983	0.9981	0.5441	0.5	500
0.97559	0.99607	0.99649	1.00223	0.97165	0.99296	0.99478	1.00048	0.97132	1.00097	1	9696	0.0142	0.3671	0.9988	0.9986	0.2006	0.9988	0.9913	0.4573	0.6	500
1.00399	1.00425	1.00404	1.00429	1.0039	1.0044	1.00421	1.00373	1.00406	1.00441	1	0.9905	0.0155	0.1997	1	1	0.453	1	1	0.5093	0.1	550
1.00294	1.00384	1.00298	1.00392	1.00257	1.0044	1.00371	1.00194	1.00318	1.00438	1	0.9967	0.0154	0.9192	1	1	0.8736	1	1	0.5431	0.2	550
1.00111	1.00312	1.00114	1.00323	1.00024	1.00432	1.00283	0.99874	1.00165	1.00435	1	0.9938	0.0152	0.0201	1	1	0.8408	1	0.9998	0.5247	0.3	550
0.99794	1.00204	0.99794	1.00214	0.99624	1.00424	1.00151	0.99341	0.99916	1.00431	1	0.9857	0.0149	0.6901	0.9999	1	0.8316	0.9999	0.9994	0.5023	0.4	550
0.99453	1.00116	0.98895	0.9994	0.99466	1.00776	1.0012	0.98387	1.00389	1.0028	1	0.9884	0.0144	0.4432	0.9997	0.9995	0.0159	0.9995	0.9998	0.5888	0.5	550

9791.39	0.99722	0.99	1.0004	0.97273	1.00224	0.99516	0.9847	0.97203	1.00374	0.9999	0.0552	0.0139	0.4792	0.999	0.9996	0.3716	0.9987	0.9924	0.248	0.6	550
1.00407	1.00428	1.0039	1.00425	1.00407	1.00424	1.00428	1.00368	1.00438	1.00435	1	0.9982	0.0155	0.5277	1	1	0.2867	1	1	0.5034	0.1	600
1.01907	1.01269	1.04571	1.01652	1.08243	1.1141	1.02365	1.23528	1.04137	1.16699	1	0.9981	0.0154	0.6087	1	1	0.4669	1	1	0.5166	0.2	600
1.00165	1.00334	1.00009	1.00283	1.00163	1.00312	1.0034	0.9984	1.00425	1.0037	1	0.9936	0.0152	0.4792	1	1	0.4334	0.9999	1	0.509	0.3	600
0.99898	1.00243	0.99588	1.00141	0.99897	1.00184	1.00245	0.99274	1.00412	1.00345	1	0.7807	0.0149	0.5087	0.9999	0.9998	0.2267	0.9996	0.9999	0.6215	0.4	600
0.99623	1.00173	0.9857	0.99831	0.99962	0.99224	1.00283	0.99065	1.00084	1.00032	1	0.996	0.0144	0.7807	0.9998	0.999	0.2357	0.9985	0.9989	0.5564	0.5	600
0.98191	0.99821	0.98219	0.99831	0.97756	1.00392	0.99673	0.9691	0.98839	1.00419	0.9999	0.9993	0.0135	0.2012	0.999	0.9999	0.354	0.9947	0.9941	0.1329	0.6	600
1.00412	1.0043	1.00377	1.0042	1.00425	1.004	1.00434	1.00392	1.00428	1.00428	1	0.9933	0.0155	0.8806	1	1	0.1231	1	1	0.5966	0.1	650
1.00341	1.00402	1.00211	1.00359	1.00382	1.00288	1.00415	1.00262	1.00396	1.00383	1	0.969	0.0154	0.2522	1	1	0.0391	1	1	0.5885	0.2	650
1.00214	1.00353	0.99917	1.00248	1.00306	1.00096	1.0039	1.00039	1.00337	1.00309	1	0.9996	0.0152	0.5702	1	0.9999	0.0153	0.9999	0.9999	0.5789	0.3	650
0.99992	1.00278	0.99408	1.00074	1.00176	0.9976	1.00346	0.99661	1.0024	1.00193	1	0.993	0.0149	0.8862	0.9999	0.9997	0.8098	0.9995	0.9997	0.5609	0.4	650
0.98656	0.99934	0.97693	0.99654	0.98735	0.99616	0.99937	0.96949	1.00354	1.0019	1	0.9608	0.0144	0.0267	0.9999	0.9992	0.2508	0.9992	0.9976	0.4442	0.5	650
0.98656	0.99934	0.97693	0.99654	0.98735	0.99616	0.99937	0.96949	1.00354	1.0019	0.9999	0.9201	0.0135	0.5727	0.9991	0.9984	0.3194	0.9961	0.9995	0.6115	0.6	650
1.0044	1.0045	1.00404	1.00446	1.00481	1.00456	1.00478	1.00533	1.00545	1.00486	1	0.9453	0.0155	0.3856	1	1	0.0416	1	1	0.5926	0.1	700
1.0039	1.00432	1.00246	1.00387	1.00473	1.00312	1.00478	1.00504	1.00428	1.00435	1	0.9579	0.0154	0.3549	1	1	0.0091	1	1	0.5998	0.2	700
1.00256	1.00371	0.99846	1.0022	1.00409	0.99896	1.00428	1.00315	1.00006	1.00238	1	0.9921	0.0152	0.1455	1	0.9999	0.0182	0.9999	0.9998	0.6449	0.3	700
1.00077	1.0031	0.99267	1.00023	1.00378	0.99384	1.00415	1.00194	0.99601	1.00058	1	0.9835	0.0149	0.1471	1	0.9997	0.8952	0.9997	0.9992	0.4605	0.4	700
0.99907	1.0027	0.98171	0.99698	1.00439	0.98296	1.00434	1.00441	0.98371	0.99726	1	0.9976	0.0145	0.9715	1	0.9994	0.6191	1	0.9982	0.5814	0.5	700
0.98947	1.00021	0.971	0.99483	0.99593	0.98296	1.00195	0.98092	0.99831	0.99804	0.9999	0.9198	0.0135	0.8077	0.9993	0.9971	0.0601	0.9956	0.9968	0.5569	0.6	700
1.00423	1.00435	1.0036	1.00415	1.00442	1.00368	1.0044	1.00441	1.00363	1.00415	1	0.9956	0.0155	0.6071	1	1	0.1504	1	1	0.3186	0.1	750
1.00377	1.00417	1.00158	1.00337	1.00442	1.00168	1.0044	1.00441	1.00165	1.00341	1	0.9978	0.0154	0.6217	1	1	0.2626	1	1	0.2548	0.2	750
1.00294	1.00386	0.99803	1.00202	1.0044	0.99824	1.0044	1.00441	0.99828	1.00213	1	0.9945	0.0152	0.6763	1	0.9999	0.4511	1	0.9998	0.774	0.3	750
1.00151	1.00338	0.99184	0.99991	1.0044	0.9924	1.00434	1.00441	0.9926	1.00006	1	9952	0.015	0.7181	1	0.9998	0.4723	1	0.9994	0.6512	0.4	750
1.00025	1.00309	0.98122	0.9968	0.99973	0.98576	1.00371	1.00005	0.98975	0.99823	1	0.9611	0.0146	0.0967	0.9999	0.9992	0.003	0.9992	0.9976	0.5912	0.5	750
0.99178	1.00097	0.96539	0.99339	1.0023	0.97048	1.00377	0.99666	0.97852	0.99446	0.9999	0.9775	0.0135	0.0328	0.9998	0.09974	0.8604	0.9974	0.9927	0.4234	0.6	750
1.00429	1.00437	1.0036	1.00413	1.00434	1.00376	1.00434	1.00426	1.00386	1.00419	1	0.8857	1	0.8046	1	1	0.356	1	1	0.6249	0.1	800

1.00393	1.00424	1.00154	1.00336	1.00418	1.00208	1.00428	1.00387	1.0025	1.00354	1	0.6429	1	0.9246	1	1	0.2645	1	1	0.646	0.2	800
1.00357	1.00411	0.99803	1.00202	1.00262	1.00104	1.00371	1.00039	1.00341	1.00316	1	0.9997	1	0.0392	1	0.9999	0.4743	0.9999	0.9999	0.4408	0.3	800
1.00294	1.00396	0.99526	1.00105	1.00406	0.99736	1.00447	1.00363	0.99964	1.00213	1	0.7439	1	0.2662	1	0.9997	0.0186	0.9997	0.9992	0.6219	0.4	800
1.00124	1.00343	0.98175	0.99698	0.99814	0.99264	1.00226	0.9907	1.00094	1.00052	1	0.9657	0.9998	0.3156	0.9997	0.99	0.1877	0.9985	0.9989	0.6082	0.5	800
3.41258	3.72815	3.54018	3.74405	3.61846	3.67395	3.74467	3.18951	2.48584	3.70331	1	0.9333	0.9997	0.6826	1	0.9981	0.5428	1	0.9949	0.701	0.6	800
1.00432	1.00438	1.0036	1.00415	1.00418	1.004	1.00428	1.00392	1.00428	1.00428	1	0.9995	1	0.9876	1	1	0.0319	1	1	0.7662	0.1	850
1.00404	1.00429	1.00158	1.00337	1.00362	1.00296	1.00409	1.00262	1.00396	1.00386	1	0.9994	1	0.9732	1	1	0.1208	1	1	0.4244	0.2	850
1.00357	1.00411	0.99803	1.00202	1.00262	1.00104	1.00371	1.00039	1.00341	1.00316	1	0.9997	1	0.0392	1	0.9999	0.4743	0.9999	0.9999	0.4408	0.3	850
1.00269	1.00384	0.99188	0.99991	1.00091	0.99784	1.00308	0.99661	1.00243	1.00206	1	0.9908	0.9998	0.327	0.9999	0.9997	0.3937	0.9995	0.9997	0.5846	0.4	850
1.00206	1.00373	0.98329	0.99749	0.99227	1.00008	1.00031	0.98407	1.00386	1.00296	1	0.9657	0.9998	0.3156	0.9997	0.9999	0.1877	0.9995	0.9989	0.6092	0.5	850
0.99676	1.00233	0.96324	0.99251	1.00114	0.97216	1.0034	0.9969	0.97953	0.99478	1	0.9145	0.9996	0.3703	0.9997	0.9976	0.013	0.9975	0.9933	0.2733	0.6	850
1.00434	1.0044	1.00368	1.00415	1.00396	1.00432	1.00421	1.00368	1.00438	1.00435	1	0.9998	1	0.6338	1	1	0.3369	1	1	0.4088	0.1	900
1.00415	1.00435	1.0018	1.00343	1.00287	1.00392	1.00384	1.00174	1.00435	1.00422	1	0.9999	1	0.6409	1	1	0.4788	1	1	0.4629	0.2	900
1.00379	1.00422	0.99846	1.00218	1.00092	1.0032	1.00308	0.99845	1.00425	1.00396	1	0.9972	1	0.6283	1	1	0.5328	0.9999	1	0.8703	0.3	900
1.00316	1.00402	0.99276	1.00021	0.99762	1.002	1.00189	0.99288	1.00409	1.00354	1	0.9917	0.9999	0.5657	0.9999	0.9968	0.2527	0.9996	0.9999	0.5945	0.4	900
1.00275	1.00397	0.98561	0.99824	0.98635	1.00424	0.9983	0.98537	0.99523	1.00431	1	0.9955	0.9998	0.6763	0.9996	0.9998	0.467	0.9986	0.9998	0.585	0.5	900
0.99824	1.00282	0.96223	0.99258	0.99292	0.98288	1.00107	0.98014	0.99822	0.99823	1	0.7111	0.9994	0.4195	0.9989	0.9969	0.6466	0.9951	0.9966	0.5462	0.6	900
1.00437	1.00441	1.00373	1.00418	1.00375	1.0044	1.00415	1.00373	1.00406	1.00441	1	0.9998	1	0.601	1	1	0.00001	1	1	0.674	0.1	950
1.00426	1.00438	1.00206	1.00353	1.0021	1.0044	1.00352	1.00199	1.00318	1.00441	1	0.9998	1	0.561	1	1	0.0019	1	1	0.688	0.2	950
1.00401	1.00431	0.99912	1.00243	0.9992	1.0044	1.00245	0.99889	1.00165	1.00438	1	0.9992	1	0.7037	1	1	0.0112	0.9999	0.9998	0.694	0.3	950
1.00355	1.00417	0.99403	1.00067	0.99428	1.00432	1.00069	0.99366	0.99912	1.00435	1	0.6694	0.9999	0.0644	0.9908	1	0.0684	0.9995	0.9993	0.5441	0.4	950
1.00333	1.00418	0.98842	0.99917	0.98163	1.00272	0.99679	0.9938	0.9854	1.0038	1	0.9873	0.9997	0.1879	0.9994	0.998	0.0196	0.9983	0.9974	0.6453	0.5	950
1	1.0033	0.96635	0.99355	0.98304	0.9968	0.99805	0.96959	1.0035	1.00216	1	0.8181	0.9993	0.5385	0.9986	0.9984	0.4196	0.996	0.9995	0.5921	0.6	950
1.0044	1.00442	1.00386	1.0042	1.00357	1.0044	1.00409	1.00407	1.00367	1.00438	1	0.6001	1	0.7076	1	1	0.0078	1	1	0.6094	0.1	1000
1.00434	1.00442	1.00246	1.00366	1.0015	1.00424	1.00333	1.0031	1.00185	1.00431	1	0.78	1	0.7892	1	1	0.0212	1	1	0.6069	0.2	1000
1.00418	1.00439	0.99996	1.00271	0.99785	1.00392	1.00189	1.0014	0.9987	1.00422	1	0.9429	1	0.8765	1	1	0.0312	0.9999	0.9998	0.6115	0.3	1000

1.00388	1.0043	0.99561	1.00123	0.99165	1.00352	0.99975	0.9985	0.99348	1.00402	1	0.9504	0.9999	0.318	0.9908	0.9999	0.1233	0.9995	0.9992	0.4506	0.4	1000
1.00377	1.00435	0.99158	1.00021	0.97927	0.9964	0.99604	1.00252	0.98553	1.00164	1	0.9893	0.9998	0.7437	0.9993	0.9993	0.3644	0.9996	0.997	0.5625	0.5	1000
1.00129	1.00367	0.9707	0.98655	0.97304	1.00416	0.99497	0.97172	0.98916	1.00425	1	0.8643	0.9992	0.1403	0.9985	0.9999	0.0207	0.9953	0.9944	0.5548	0.6	1000
1.00443	1.00444	1.00395	1.00424	1.00349	1.00416	1.00409	1.00436	1.0037	1.00431	1	0.9497	1	0.4724	1	1	0.07	1	1	0.4588	0.1	1050
1.0044	1.00446	1.00281	1.0038	1.00121	1.00336	1.00321	1.00421	1.00195	1.00402	1	0.8791	1	0.4368	1	1	0.1137	1	0.9994	0.5201	0.2	1050
1.00432	1.00444	1.00083	1.00304	0.99721	1.00208	1.0017	1.00387	0.9989	1.00351	1	0.9799	0.9992	0.4775	0.9999	0.9999	0.2228	1	0.9997	0.4465	0.3	1050
1.00412	1.00441	0.99737	1.00186	0.99036	0.99984	0.99931	1.00339	0.99371	1.00274	1	0.9968	1	0.6778	0.9998	0.9998	0.4381	0.9999	0.999	0.6	0.4	1050
1.00412	1.00449	0.99474	1.00123	0.97963	0.98824	0.99616	1.00378	0.99611	0.99887	1	0.8754	1	0.4383	0.9999	0.9988	0.589	0.9999	0.9979	0.657	0.5	1050
1.00214	1.00397	0.97364	0.99601	0.96237	1.00136	0.99226	0.98479	0.971	1.00345	1	0.8161	0.9995	0.3369	0.9981	0.9993	0.0931	0.9944	0.9917	0.0108	0.6	1050
1.00445	1.00446	1.00408	1.00427	1.00351	1.00384	1.00409	1.00441	1.00412	1.00422	1	0.6386	1	0.6419	1	1	0.4101	1	1	0.5857	0.1	1100
1.00465	1.00465	1.00368	1.00427	1.00223	1.00328	1.00384	1.00538	1.00522	1.00431	1	0.0378	1	0.8022	1	1	0.3205	1	1	0.5856	0.2	1100
1.00443	1.00451	1.00171	1.00337	0.99737	0.99968	1.00176	1.00407	1.00201	1.00261	1	0.8441	1	0.6155	0.9999	0.9999	0.1448	1	0.9998	0.5889	0.3	1100
1.00432	1.00451	0.99912	1.00248	0.99063	0.9952	0.99943	1.00407	0.99974	1.00103	1	0.92	1	0.4695	0.9997	0.9996	0.2165	0.9989	0.9993	0.597	0.4	1100
1.00437	1.0046	0.99763	1.00218	0.98256	0.98176	0.99723	0.99661	1.00425	0.99672	1	0.9724	1	0.6061	0.9988	0.9981	0.0011	0.9975	1	0.5931	0.5	1100
1.00308	1.00424	0.98074	0.9978	0.95971	0.99048	0.99126	1.00107	0.97164	1.0001	1	0.7624	0.9996	0.4903	0.9977	0.9978	0.5777	0.9988	0.9912	0.6635	0.6	1100
1.00445	1.00447	1.00417	1.00431	1.00364	1.0036	1.00409	1.00412	1.00441	1.00412	1	0.9903	1	0.059	1	1	0.0644	1	1	0.5358	0.1	1150
1.00451	1.00451	1.0036	1.00408	1.00169	1.00144	1.0034	1.00339	1.00438	1.00332	1	0.9203	1	0.0121	1	1	0.0287	1	1	0.5558	0.2	1150
1.00451	1.00455	1.00254	1.00367	0.99828	0.99776	1.00208	1.00208	1.00435	1.0019	1	0.9926	1	0.0386	0.9999	0.9998	0.0064	0.9999	1	0.574	0.3	1150
1.00448	1.00459	1.0007	1.00306	0.99235	0.9916	1.00006	0.99995	1.00431	0.99971	1	0.9841	1	0.4582	0.9996	0.9994	0.0364	0.9996	1	0.5969	0.4	1150
1.00456	1.0047	1.00013	1.00301	0.98751	0.9796	0.99887	0.98663	0.99977	0.99614	1	0.4202	1	0.4407	0.9989	0.9974	0.436	0.9974	0.9999	0.5763	0.5	1150
1.00371	1.00444	0.98693	0.99947	0.49071	0.97712	0.99163	1.00329	0.98998	0.99588	1	0.7786	0.9997	0.6118	0.9969	0.9964	0.0072	0.9996	0.9937	0.5643	0.6	1150
1.00448	1.00448	1.00426	1.00434	1.00381	1.00352	1.00415	1.00373	1.00422	1.00409	1	0.9856	1	0.4571	1	1	0.0762	1	1	0.3031	0.1	1200
1.00454	1.00453	1.0039	1.0042	1.00234	1.00128	1.00359	1.00203	1.00376	1.00325	1	0.9795	1	0.4534	1	1	0.1687	1	1	0.46	0.2	1200
1.00456	1.0046	1.00325	1.00395	0.9997	0.99728	1.00258	0.99908	1.00298	1.00174	1	0.997	1	0.4896	0.9999	0.9978	0.2344	0.9998	0.9999	0.0054	0.3	1200
1.00459	1.00464	1.00206	1.00355	0.99514	0.99048	1.00107	0.99414	1.00172	0.99939	1	0.9692	1	0.6887	0.9997	0.9992	0.3943	0.9991	0.9997	0.5866	0.4	1200
1.00473	1.00477	1.00206	1.00366	0.9932	0.98272	1.00075	0.98039	0.98819	0.9973	1	0.9812	1	0.3545	0.9993	0.9968	0.0302	0.9953	0.9961	0.5031	0.5	1200

1.0041	1.0046	0.99096	1.00083	0.96193	0.96271	0.99283	0.99046	0.99961	0.99655	1	0.6073	0.9998	0.4603	0.9957	0.9972	0.3373	0.9963	0.9967	0.5951	0.6	1200
1.00448	1.00448	1.00434	1.00438	1.00401	1.00368	1.00421	1.00354	1.00376	1.00415	1	0.9846	1	0.4901	1	1	0.001	1	1	0.5555	0.1	1250
1.00456	1.00455	1.00412	1.00431	1.00304	1.00176	1.00384	1.00126	1.00214	1.00341	1	0.5534	1	0.4075	1	1	0.0863	0.9999	1	0.5525	0.2	1250
1.00481	1.0048	1.00417	1.00443	1.00234	1.00024	1.00377	0.99961	1.00149	1.00306	1	0.7933	0.9999	0.5313	0.9999	0.9998	0.0261	0.9996	0.9996	0.5424	0.3	1250
1.00467	1.00471	1.00311	1.00395	0.99829	0.99248	1.00214	0.11899	0.99491	1.0001	1	0.9997	1	0.6177	0.9998	0.9991	0.2785	0.9985	0.9987	0.1245	0.4	1250
1.00481	1.00484	1.00338	1.00413	0.99831	0.98968	1.00239	0.98203	0.9805	0.99965	1	0.9619	1	0.2726	0.9997	0.9981	0.0003	0.9947	0.992	0.6183	0.5	1250
1.00448	1.00473	0.99636	1.0022	0.97284	0.96007	0.99566	0.97419	0.99659	0.99137	1	0.9347	0.9999	0.5426	0.9964	0.9918	0.5137	0.9921	0.9971	0.5666	0.6	1250
1.00451	1.00449	1.00439	1.00441	1.0042	1.00392	1.00428	1.00363	1.0035	1.00422	1	0.9992	1	0.3996	1	1	0.0082	1	1	0.5663	0.1	1300
1.00478	1.00474	1.00456	1.00461	1.00412	1.00344	1.00447	1.00281	1.00273	1.00431	1	0.9983	1	0.9498	1	1	0.105	0.9999	1	0.5439	0.2	1300
1.00412	1.00466	1.00417	1.00434	1.00273	1.0004	1.00371	0.99811	0.99731	1.00287	1	0.9935	0.9999	0.6835	1	0.998	0.0043	0.9996	0.9973	0.544	0.3	1300
1.00475	1.00475	1.00386	1.00408	1.0011	0.9964	1.00315	0.99201	0.99075	1.00151	1	0.9997	0.9999	0.6939	0.9999	0.9994	0.8825	0.9983	0.9974	0.6643	0.4	1300
1.00489	1.0049	1.00421	1.00446	1.00199	0.99736	1.00359	0.9908	0.98439	1.00209	1	0.9897	0.9999	0.6101	0.9999	0.9993	0.4862	0.997	0.9925	0.5787	0.5	1300
1.00473	1.00484	1.00009	1.00322	0.98391	0.96575	0.99868	0.96377	0.97813	0.99333	1	0.9946	1	0.1903	0.9977	0.9912	0.2635	0.9865	0.9892	0.3889	0.6	1300
1.00451	1.0045	1.00443	1.00443	1.00434	1.00416	1.00434	1.00397	1.0037	1.00431	1	0.9887	1	0.4502	1	1	0.1024	1	1	0.4284	0.1	1350
1.00462	1.0046	1.00443	1.00446	1.00412	1.0036	1.00428	1.00276	1.00195	1.00409	1	0.9334	1	0.4824	1	1	0.1684	1	1	0.4737	0.2	1350
1.0047	1.0047	1.00443	1.00446	1.00376	1.00248	1.00415	1.00068	0.99883	1.00367	1	0.9973	0.9999	0.4972	1	0.9999	0.233	0.998	0.9994	0.3253	0.3	1350
1.00574	0.34507	1.00597	1.00487	1.00544	1.00424	1.00453	1.00276	1.00146	1.00412	1	0.9933	0.9999	0.7374	1	0.9998	0.43	0.9991	0.9977	0.5974	0.4	1350
1.00497	1.00496	1.00465	1.00469	1.00396	1.00256	1.00434	1	0.99627	1.0038	1	0.9464	0.9999	0.4086	1	0.9999	0.0656	0.9994	0.9979	0.6891	0.5	1350
1.00489	1.00493	1.00224	1.00392	0.99185	0.97432	1.00113	0.96058	0.96074	0.99665	1	0.9999	1	0.7069	0.9987	0.9922	0.9412	0.9806	0.9733	0.3838	0.6	1350
1.00454	1.00451	1.00447	1.00446	1.00442	1.0044	1.0044	1.00426	1.00412	1.00438	1	0.9749	1	0.8577	0.3342	1	0.0175	1	1	0.5498	0.1	1400
1.00465	1.00462	1.00452	1.00453	1.0044	1.00424	1.0044	1.00387	1.00344	1.00435	1	0.998	1	0.502	0.5001	1	0.3031	1	1	0.5733	0.2	1400
1.00475	1.00473	1.00456	1.00459	1.00434	1.00392	1.0044	1.0032	1.00221	1.00422	1	0.9968	0.9999	0.2313	0.6502	1	0.6836	1	0.9998	0.5751	0.3	1400
1.00486	1.00485	1.00461	1.00464	1.00422	1.00344	1.0044	1.00203	1.00003	1.00406	1	0.9885	0.9999	0.6604	0.2711	1	0.9107	0.9968	0.9994	0.4391	0.4	1400
1.00503	1.00502	1.00487	1.00489	1.00473	1.00456	1.00472	1.00421	1.0037	1.00464	1	0.97	0.9999	0.1992	0.1328	1	0.0123	1	0.9999	0.599	0.5	1400
1.005	1.00501	1.00386	1.00441	0.99972	0.99072	1.00315	0.97806	0.96694	1.00074	1	0.9115	0.9999	0.6424	0.6632	0.9973	0.5773	0.9892	0.9748	0.6008	0.6	1400
1.00454	1.00452	1.00452	1.0045	1.00448	1.00448	1.00447	1.00446	1.00441	1.00448	1	0.3634	1	0.4502	1	1	0.0041	1	1	0.4785	0.1	1450

1.00465	1.00465	1.00461	1.00459	1.00456	1.00456	1.00453	1.00446	1.00435	1.00451	1	0.9888	0.9999	0.4824	1	1	0.0174	1	1	0.7902	0.2	1450
1.00478	1.00477	1.00469	1.00469	1.00462	1.00456	1.00459	1.00446	1.00425	1.00454	1	0.9994	0.9999	0.4972	1	1	0.0123	1	1	0.4503	0.3	1450
1.00489	1.0049	1.00478	1.00478	1.00469	1.00456	1.00465	1.00436	1.00406	1.0046	1	0.9586	0.9999	0.7374	1	1	0.52	1	1	0.583	0.4	1450
1.00465	1.00465	1.00461	1.00459	1.00456	1.00456	1.00453	1.00446	1.00435	1.00451	1	0.9773	0.9999	0.4086	1	1	0.0218	1	1	0.6678	0.5	1450
1.00508	1.00507	1.00465	1.00475	1.00351	1.00088	1.00428	0.99608	0.98903	1.00345	1	0.9894	0.9999	0.7069	0.9987	0.9997	0.4862	0.998	0.9027	0.5762	0.6	1450
0.99845	0.99942	0.99881	0.99956	0.99907	0.9993	0.99963	0.99953	0.99968	0.99975	1	0.992	1	0.479	1	1	0.6349	1	1	0.5879	0.1	50
0.99474	0.99794	0.99595	0.9984	0.99689	0.99775	0.99878	0.9984	0.99899	0.99912	1	0.9946	1	0.5756	1	1	0.5778	1	1	0.5882	0.2	50
0.98828	0.99541	0.99105	0.99647	0.99318	0.99503	0.99725	0.99657	0.99779	0.99803	1	0.9986	0.073	0.5837	0.9999	0.9999	0.1062	0.9999	0.9999	0.6089	0.3	50
0.97731	0.99154	0.98296	0.99353	0.98721	0.99075	0.99505	0.99365	0.99593	0.9964	1	0.9984	0.0761	0.9414	0.9996	0.9995	0.0431	0.9996	0.9997	0.6254	0.4	50
0.96311	0.98747	0.98019	0.99307	0.99046	0.99681	0.99658	0.99976	0.99975	0.99887	0.9999	0.9974	0.0177	0.976	0.9998	0.9999	0.0513	1	1	0.3093	0.5	50
0.95956	0.9862	0.97043	0.98953	0.97823	0.98454	0.99206	0.98951	0.99329	0.99425	0.9999	0.9963	0.0184	0.9032	0.9988	0.9986	0.3984	0.9988	0.9992	0.6045	0.6	50
0.99859	0.99948	0.99923	0.99971	0.9996	0.99984	0.99982	1	1	0.99997	1	0.9997	0.0156	0.6515	1	1	0.7606	1	1	0.5617	0.1	100
0.99522	0.99813	0.99732	0.99894	0.99868	0.99953	0.99945	1	1	0.99984	1	0.9969	0.0158	0.5335	1	1	0.7357	1	1	0.5518	0.2	100
0.98935	0.99583	0.99408	0.99766	0.99709	0.99907	0.99884	0.99995	0.99997	0.99962	1	0.9873	0.0162	0.4783	1	1	0.6721	1	1	0.5537	0.3	100
0.97936	0.99232	0.98867	0.99573	0.99449	0.99813	0.99786	0.99986	0.99987	0.99931	1	0.9986	0.0168	0.6573	0.9999	1	0.7523	1	1	0.5834	0.4	100
0.96668	0.98871	0.98816	0.99589	0.99778	1	0.99921	0.99643	0.99004	1	1	0.989	0.0172	0.1439	0.9999	1	0.2361	0.9996	0.9978	0.58	0.5	100
0.9256	0.97822	0.94827	0.98368	0.96325	0.97467	0.98772	0.98302	0.98925	0.99121	0.9995	0.1162	0.0208	0.4399	0.9966	0.9962	0.0417	0.9969	0.9979	0.5088	0.6	100
0.99872	0.99953	0.99953	0.99983	0.99992	1	0.99994	0.99991	0.99968	1.00003	1	0.9469	0.0156	0.5907	1	1	0.0266	1	1	0.6025	0.1	150
0.9957	0.99831	0.99842	0.99939	0.99971	1	0.99988	0.99958	0.99877	1.00003	1	0.9064	0.0158	0.6236	1	1	0.2038	1	1	0.595	0.2	150
0.99039	0.99625	0.99651	0.99863	0.99935	1	0.99976	0.99901	0.9972	1.00003	1	0.5017	0.016	0.7003	1	1	0.7426	1	0.9998	0.589	0.3	150
0.98137	0.99308	0.99327	0.99747	0.99875	1	0.99951	0.99802	0.99449	1.00003	1	0.9932	0.0165	0.2735	1	1	0.0923	0.9999	0.9993	0.6134	0.4	150
0.96994	0.98985	0.99403	0.99797	1.00008	0.99534	1.00006	0.98678	0.98229	0.99853	1	0.9977	0.0166	0.7397	1	0.9996	0.7575	0.998	0.9957	0.612	0.5	150
0.92771	0.97976	0.96289	0.98892	0.98256	0.99425	0.99456	0.99953	0.99943	0.99819	0.9997	0.9999	0.0199	0.9295	0.9993	0.9997	0.0811	1	0.9999	0.5655	0.6	150
0.99885	0.99957	0.99979	0.99991	1.00002	0.99984	1	0.99953	0.99937	0.99997	1	0.9951	0.0156	0.5628	1	1	0.5719	1	1	0.5837	0.1	200
0.99613	0.99849	0.99923	0.99969	1.00003	0.99946	1	0.99835	0.9977	0.99984	1	0.995	0.0157	0.5791	1	1	0.7073	1	0.9999	0.5828	0.2	200
0.99138	0.99663	0.99825	0.99932	1.00005	0.99876	1	0.99628	0.9948	0.99956	1	0.9994	0.0159	0.6528	1	1	0.2212	0.9998	0.9996	0.6045	0.3	200

0.97304	0.99378	0.99663	0.99875	1.00006	0.99744	1	0.99266	0.98992	0.99916	1	0.9965	0.0162	0.9108	1	0.9999	0.00072	0.9994	0.9986	0.3044	0.4	200
0.97304	0.99093	0.99795	0.99932	0.99804	0.98764	0.99939	0.98184	0.98651	0.99603	1	9941	0.0162	0.1368	0.9999	0.9989	0.202	0.9974	0.9976	0.0078	0.5	200
0.94111	0.98248	0.97959	0.99367	0.99619	0.99992	0.99878	0.99365	0.98235	0.99997	0.9999	0.9916	0.0184	0.3379	0.9999	1	0.2241	0.9988	0.9932	0.1131	0.6	200
0.91327	0.99963	0.99991	0.99998	0.99995	0.99961	1	0.99934	0.9995	0.99991	1	0.9947	0.0156	0.0044	1	1	0.1971	1	1	0.5617	0.1	250
0.99656	0.99865	0.99974	0.9999	0.99979	0.99845	0.99994	0.99765	0.99817	0.9995	1	0.9828	0.0156	0.5728	1	1	0.3143	1	1	0.5682	0.2	250
0.99228	0.997	0.9994	0.99978	0.99948	0.9965	0.99982	0.99468	0.9959	0.99878	1	9977	0.0157	0.3183	1	0.9999	0.3174	0.9998	0.9998	0.5589	0.3	250
0.98502	0.99445	0.99885	0.99959	0.99779	0.99316	0.99963	0.9897	0.99219	0.99762	1	0.9947	0.0159	0.1161	1	0.9996	0.0175	0.9992	0.9992	0.5208	0.4	250
0.97611	0.99198	0.99983	0.99997	0.99324	0.98228	0.99786	0.98537	0.99628	0.99421	1	0.9995	0.0157	0.7314	0.9997	0.9987	0.3606	0.9984	0.9994	0.5997	0.5	250
0.94503	0.98405	0.98935	0.99682	1.00011	0.99145	1.00006	0.97606	0.96902	0.99762	0.9999	9225	0.0176	0.4254	1	0.9988	0.0044	0.9934	9871	0.3791	0.6	250
0.99909	0.99967	1	1	0.99979	0.99938	0.99994	0.99944	0.99987	0.99981	1	0.9894	0.0156	0.7359	1	1	0.0023	1	1	0.1798	0.1	300
0.99696	0.9988	1	1.00002	0.99919	0.99775	0.99969	0.99807	0.9995	0.99922	1	0.9958	0.0156	0.8379	1	1	0.0243	1	1	0.0375	0.2	300
0.99319	0.99734	1	1	0.99814	0.99495	0.99933	0.99563	0.9989	0.99819	1	0.9995	0.0156	0.588	1	0.9999	0.0118	0.9999	0.9999	0.5048	0.3	300
0.98671	0.9951	0.99991	1	0.99629	0.99013	0.99872	0.99163	0.99786	0.99653	1	0.9904	0.0157	0.307	0.9999	0.9996	0.2188	0.9995	0.9998	0.5665	0.4	300
0.97888	0.99293	0.99987	1.00002	0.98767	0.98205	0.99603	0.99356	0.99968	0.99406	1	0.9974	0.0154	0.9827	0.9995	0.999	0.4786	0.9993	0.9999	0.5827	0.5	300
0.94752	0.98542	0.99604	0.99889	0.9961	0.97606	0.99896	0.96627	0.97602	0.99353	1	0.9955	0.0167	0.6398	0.9997	0.996	0.9467	0.9913	0.9822	0.1289	0.6	300
0.9992	0.99971	1	1.00002	0.99959	0.9993	0.99988	0.99976	1	0.99981	1	0.9909	0.0155	0.4979	1	1	0.5063	1	1	0.6037	0.1	350
0.9973	0.99895	1	1.00002	0.99849	0.99767	0.99945	0.99915	0.99997	0.99919	1	0.9933	0.0155	0.4922	1	1	0.0935	1	1	0.7139	0.2	350
0.99399	0.99766	1	1.00003	0.99819	0.99479	0.99878	0.99807	0.99991	0.99809	1	0.9997	0.0155	.6774	1	0.9999	0.2415	0.9999	1	0.5986	0.3	350
0.98828	0.99568	0.99996	1.00002	0.9932	0.98982	0.99762	0.99633	0.99984	0.9964	1	0.9971	0.0154	0.8852	0.9998	0.9997	0.0326	0.9988	1	0.4413	0.4	350
0.98147	0.99382	0.99834	0.99952	0.98326	0.98656	0.99456	0.99958	0.99111	0.99553	1	9988	0.015	0.0615	0.9995	0.9993	0.2731	0.9999	0.9978	0.2114	0.5	350
0.95766	0.98756	0.9997	0.99995	0.98794	0.96938	0.99658	0.97559	0.99382	0.99096	1	0.8006	0.0159	0.7504	0.9991	0.9961	0.0081	0.9955	0.9983	0.3676	0.6	350
0.99931	0.99974	0.99996	1	0.99942	0.99953	0.99982	1	0.99968	0.99984	1	0.9864	0.0155	0.6608	1	1	0.2287	1	1	0.7812	0.1	400
0.99765	0.99909	0.99983	0.99997	0.99793	0.99821	0.99927	0.99995	0.9989	0.99941	1	0.9847	0.0155	0.8431	1	1	0.004	1	1	0.6062	0.2	400
0.99477	0.99796	0.99957	0.99988	0.99528	0.99604	0.99829	0.99986	0.99748	0.99856	1	0.9928	0.0154	0.3297	1	0.9999	0.0305	1	0.9998	0.5906	0.3	400
0.98975	0.99623	0.99911	0.99973	0.99071	0.99238	0.9967	0.99976	0.99505	0.99731	1	0.8461	0.0153	0.8099	0.9998	0.9998	0.2224	1	0.9993	0.619	0.4	400
0.98396	0.99467	0.99561	0.99863	0.98132	0.99332	0.99389	0.99774	0.98075	0.99781	1	0.9962	0.0148	0.9288	0.9996	0.9995	0.6916	0.9996	0.9969	0.5492	0.5	400

0.96148	0.98892	0.99974	0.99998	0.97762	0.96853	0.99371	0.98895	0.99814	0.99196	1	0.0659	0.0152	0.4201	0.9984	0.9968	0.5726	0.9979	0.9997	0.579	0.6	400
0.99941	0.99979	0.99987	0.99997	0.99935	0.99977	0.99976	0.99991	0.99931	0.99994	1	0.1785	0.0155	0.5816	1	1	0.2528	1	1	0.5706	0.1	450
0.99797	0.99921	0.99949	0.99985	0.99766	0.99915	0.99914	0.99972	0.99751	0.99972	1	0.9378	0.0155	0.3496	1	1	0.0804	1	0.9999	0.5471	0.2	450
0.99546	0.99825	0.99881	0.99959	0.99469	0.99806	0.99804	0.99934	0.99439	0.99931	1	0.7185	0.0159	0.3896	1	1	0.2307	1	0.9997	0.529	0.3	450
0.99114	0.99674	0.99761	0.9992	0.98959	0.99627	0.99627	0.99873	0.98913	0.99869	1	0.9999	0.0151	0.5367	0.9999	0.9999	0.1541	0.9999	0.999	0.5722	0.4	450
0.9862	0.99543	0.99212	0.99749	0.98215	0.99876	0.99413	0.9889	0.98097	0.99959	1	0.9981	0.0146	8.3E-05	0.9997	0.9999	0.3788	0.9983	0.9974	0.3367	0.5	450
0.96425	0.99012	0.99676	0.99918	0.96826	0.97544	0.9912	0.99925	0.98327	0.99287	1	0.9394	0.0146	0.3904	0.9982	0.9976	0.0127	0.9998	0.9926	0.1698	0.6	450
0.99949	0.99982	0.99974	0.99993	0.99936	0.99992	0.99976	0.99958	0.99928	1	1	0.9718	0.0155	0.3886	1	1	0.0717	1	1	0.5615	0.1	500
0.99826	0.99933	0.99906	0.99969	0.99775	0.99984	0.99921	0.99859	0.99745	0.99994	1	0.9472	0.0154	0.4178	1	1	0.0262	1	1	0.4764	0.2	500
0.9961	0.9985	0.99783	0.99923	0.9949	0.99961	0.99811	0.9968	0.9943	0.99987	1	0.9861	0.0153	0.3107	1	1	0.0251	0.9999	0.9998	0.5256	0.3	500
0.99239	0.99721	0.9957	0.99851	0.99001	0.9993	0.99646	0.99379	0.98907	0.99975	1	0.9998	0.015	0.0391	0.9999	1	0.1798	0.9995	0.9992	0.5403	0.4	500
0.98825	0.99613	0.98828	0.99623	0.98543	0.99969	0.99517	0.98053	0.99089	0.99984	1	0.9953	0.0145	98276	0.9997	1	0.4334	0.9983	0.9981	0.5441	0.5	500
0.9713	0.99171	0.99212	0.99783	0.96738	0.98858	0.99041	0.9961	0.96707	0.99659	1	9696	0.0142	0.3671	0.9988	0.9986	0.2006	0.9988	0.9913	0.4573	0.6	500
0.99957	0.99985	0.99962	0.99988	0.99948	1	0.99982	0.99929	0.99965	1	1	0.9905	0.0155	0.1997	1	1	0.453	1	1	0.5093	0.1	550
0.99853	0.99943	0.99859	0.9995	0.99817	0.99992	0.99933	99.7507	0.9988	1	1	0.9967	0.0154	0.9192	1	1	0.8736	1	1	0.5431	0.2	550
0.99672	0.99873	0.99676	0.99882	0.99584	0.99992	0.99847	0.99436	0.99729	0.99997	1	0.9938	0.0152	0.0201	1	1	0.8408	1	0.9998	0.5247	0.3	550
0.99354	0.99765	0.99357	0.99775	0.99187	0.99984	0.99707	0.98904	0.99477	0.99991	1	0.9857	0.0149	0.6901	0.9999	1	0.8316	0.9999	0.9994	0.5023	0.4	550
0.99015	0.99677	0.98462	0.99501	0.99027	0.99534	0.99682	0.97954	0.9995	0.9984	1	0.9884	0.0144	0.4432	0.9997	0.9995	0.0159	0.9995	0.9998	0.5888	0.5	550
0.97483	0.99284	0.98564	0.99601	0.96845	0.99782	0.99077	0.98034	0.96776	0.99934	0.9999	0.0552	0.0139	0.4792	0.999	0.9996	0.3716	0.9987	0.9924	0.248	0.6	550
0.99965	0.99987	0.99949	0.99985	0.99965	0.99984	0.99988	0.99925	1	0.99994	1	0.9982	0.0155	0.5277	1	1	0.2867	1	1	0.5034	0.1	600
1.0146	1.00825	1.04112	1.01205	1.07768	1.10919	1.01912	1.22983	1.03681	1.16188	1	0.9981	0.0154	0.6087	1	1	0.4669	1	1	0.5166	0.2	600
0.99725	0.99894	0.9957	0.99843	0.99723	0.99868	1.00996	0.99398	0.99984	0.9995	1	0.9936	0.0152	0.4792	1	1	0.4334	0.9999	1	0.509	0.3	600
0.99458	0.99803	0.99152	0.99701	0.99458	0.99736	0.99804	0.98838	0.99972	0.99903	1	0.7807	0.0149	0.5087	0.9999	0.9998	0.2267	0.9996	0.9999	0.6215	0.4	600
0.99186	0.99734	0.98138	0.99394	0.99522	0.9878	0.99841	0.98631	0.99647	0.99593	1	0.996	0.0144	0.7807	0.9998	0.999	0.2357	0.9985	0.9989	0.5564	0.5	600
0.9776	0.99383	0.97789	0.99394	0.97326	0.99946	0.99236	0.96481	0.98405	0.99978	0.9999	0.9993	0.0135	0.2012	0.999	0.9999	0.354	0.9947	0.9941	0.1329	0.6	600
0.99971	0.9999	0.99936	0.9998	0.99983	0.99953	0.99994	0.99948	0.99987	0.99987	1	0.9933	0.0155	0.8806	1	1	0.1231	1	1	0.5966	0.1	650

0.99899	0.99963	0.9977	0.99918	0.99941	0.99845	0.99976	0.99821	0.99956	0.99944	1	0.969	0.0154	0.2522	1	1	0.0391	1	1	0.5885	0.2	650
0.99773	0.99913	0.99476	0.99807	0.99865	0.9965	0.99951	0.99595	0.99899	0.99872	1	0.9996	0.0152	0.5702	1	0.9999	0.0153	0.9999	0.9999	0.5789	0.3	650
0.99554	0.99839	0.98973	0.99635	0.99735	0.99316	0.99902	0.99219	0.99801	0.99756	1	0.993	0.0149	0.8862	0.9999	0.9997	0.8098	0.9995	0.9997	0.5609	0.4	650
0.98225	0.99496	0.9726	0.99216	0.98301	0.99176	0.99499	0.96524	0.99915	0.99753	1	0.9608	0.0144	0.0267	0.9999	0.9992	0.2508	0.9992	0.9976	0.4442	0.5	650
0.98225	0.99496	0.9726	0.99216	0.98301	0.99176	0.99499	0.96524	0.99915	0.99753	0.9999	0.9201	0.0135	0.5727	0.9991	0.9984	0.3194	0.9961	0.9995	0.6115	0.6	650
1	1.00011	0.99966	1.00005	1.0004	1.00016	1.00037	1.00089	1.00104	1.00047	1	0.9453	0.0155	0.3856	1	1	0.0416	1	1	0.5926	0.1	700
0.99949	0.99993	0.99804	0.99947	1.00032	0.99868	1.00037	1.00061	0.99987	0.99994	1	0.9579	0.0154	0.3549	1	1	0.0091	1	1	0.5998	0.2	700
0.99816	0.99932	0.99408	0.9978	0.99968	0.99456	0.99988	0.99873	0.99568	0.998	1	0.9921	0.0152	0.1455	1	0.9999	0.0182	0.9999	0.9998	0.6449	0.3	700
0.99637	0.99871	0.98833	0.99583	0.99936	0.98943	0.99976	0.99755	0.99165	0.99622	1	0.9835	0.0149	0.1471	1	0.9997	0.8952	0.9997	0.9992	0.4605	0.4	700
0.99469	0.9983	0.97742	0.99259	0.99998	0.97863	0.99994	1	0.97939	0.9929	1	0.9976	0.0145	0.9715	1	0.9994	0.6191	1	0.9982	0.5814	0.5	700
0.98513	0.99583	0.96672	0.99047	0.99155	0.97863	0.99756	0.97657	0.99392	0.99365	0.9999	0.9198	0.0135	0.8077	0.9993	0.9971	0.0601	0.9956	0.9968	0.5569	0.6	700
0.99981	0.99995	0.99919	0.99974	1	0.99922	1	1	0.99924	0.99975	1	0.9956	0.0155	0.6071	1	1	0.1504	1	1	0.3186	0.1	750
0.99936	0.99978	0.99719	0.99898	1	0.99728	1	1	0.99729	0.99903	1	0.9978	0.0154	0.6217	1	1	0.2626	1	1	0.2548	0.2	750
0.99853	0.99947	0.99365	0.99763	1	0.99378	0.99994	1	0.99389	0.99772	1	0.9945	0.0152	0.6763	1	0.9999	0.4511	1	0.9998	0.774	0.3	750
0.99709	0.99898	0.98747	0.99553	0.99998	0.98795	0.99994	1	0.98825	0.99568	1	9952	0.015	0.7181	1	0.9998	0.4723	1	0.9994	0.6512	0.4	750
0.99584	0.9987	0.97695	0.99244	0.99816	0.98143	0.99933	0.99563	0.98541	0.99384	1	0.9611	0.0146	0.0967	0.9999	0.9992	0.003	0.9992	0.9976	0.5912	0.5	750
0.98743	0.99658	0.96114	0.98904	0.99788	0.9662	0.99939	0.99224	0.97422	0.99009	0.9999	0.9775	0.0135	0.0328	0.9998	0.09974	0.8604	0.9974	0.9927	0.4234	0.6	750
0.99987	0.99997	0.99919	0.99973	0.99994	0.9993	0.99994	0.99986	0.68434	0.99978	1	0.8857	1	0.8046	1	1	0.356	1	1	0.6249	0.1	800
0.99952	0.99984	0.99715	0.99896	0.99977	0.99759	0.99988	0.99944	0.99811	0.99916	1	0.6429	1	0.9246	1	1	0.2645	1	1	0.646	0.2	800
0.99915	0.99972	0.99365	0.99763	0.99822	0.99658	0.99933	0.996	0.99899	0.99878	1	0.9997	1	0.0392	1	0.9999	0.4743	0.9999	0.9999	0.4408	0.3	800
0.99853	0.99956	0.99092	0.99665	0.99965	0.99301	1.00006	0.9992	0.99527	0.99772	1	0.7439	1	0.2662	1	0.9997	0.0186	0.9997	0.9992	0.6219	0.4	800
0.99682	0.99904	0.97746	0.99261	0.99374	0.98819	0.99786	0.98631	0.99657	0.99612	1	0.9657	0.9998	0.3156	0.9997	0.99	0.1877	0.9985	0.9989	0.6082	0.5	800
3.39758	3.71183	3.52463	3.7277	3.6025	3.65768	3.72823	3.17546	2.47495	3.68706	1	0.9333	0.9997	0.6826	1	0.9981	0.5428	1	0.9949	0.701	0.6	800
0.99989	0.99998	0.99919	0.99973	0.99977	0.99953	0.99988	0.99948	0.99987	0.99987	1	0.9995	1	0.9876	1	1	0.0319	1	1	0.7662	0.1	850
0.99963	0.99989	0.99719	0.99898	0.99921	0.99852	0.99969	0.99821	0.99956	0.99947	1	0.9994	1	0.9732	1	1	0.1208	1	1	0.4244	0.2	850
0.99915	0.99972	0.99365	0.99763	0.99822	0.99658	0.99933	0.996	0.99899	0.99878	1	0.9997	1	0.0392	1	0.9999	0.4743	0.9999	0.9999	0.4408	0.3	850

0.99829	0.99943	0.98752	0.99553	0.99651	0.99339	0.99872	0.99224	0.99805	0.99765	1	0.9908	0.9998	0.327	0.9999	0.9997	0.3937	0.9995	0.9997	0.5846	0.4	850
0.99765	0.99933	0.97899	0.9931	0.98791	0.99565	0.99591	0.97973	0.99946	0.99859	1	0.9657	0.9998	0.3156	0.9997	0.9999	0.1877	0.9995	0.9989	0.6092	0.5	850
0.99236	0.99794	0.95901	0.98815	1.00282	0.96783	0.99896	0.99247	0.97526	0.99043	1	0.9145	1	0.3703	0.9997	0.9976	0.013	0.9975	0.9933	0.2733	0.6	850
0.99995	1	0.99928	0.99974	0.99956	0.99984	0.99982	0.99925	1	0.99997	1	0.9998	1	0.6338	1	1	0.3369	1	1	0.4088	0.1	900
0.99976	0.99994	0.9974	0.99903	0.99846	0.99946	0.99939	0.99737	999.029	0.99981	1	0.9999	1	0.6409	1	1	0.4788	1	1	0.4629	0.2	900
0.99939	0.99982	0.99408	0.99778	0.99653	0.99876	0.99866	0.99403	0.99984	0.99956	1	0.9972	1	0.6283	1	1	0.5328	0.9999	1	0.8703	0.3	900
0.99875	0.99962	0.98841	0.99583	0.99323	0.99759	0.99749	0.98848	0.99972	0.99916	1	0.9917	0.9999	0.5657	0.9999	0.9968	0.2527	0.9996	0.9999	0.5945	0.4	900
0.99834	0.99957	0.98125	0.99387	0.98201	0.99984	0.99395	0.981	0.99089	0.99991	1	0.9955	0.9998	0.6763	0.9996	0.9998	0.467	0.9986	0.9998	0.585	0.5	900
0.99386	0.99843	0.95799	0.98822	0.98855	0.97855	0.99664	0.97582	0.99386	0.99384	1	0.7111	0.9994	0.4195	0.9989	0.9969	0.6466	0.9951	0.9966	0.5462	0.6	900
0.99997	1.00001	0.99936	0.99978	0.99935	1	0.99976	0.99929	0.99965	1	1	0.9998	1	0.601	1	1	0.00001	1	1	0.674	0.1	950
0.99984	0.99998	0.9977	0.99913	0.9977	1	0.99914	0.99755	0.99877	1	1	0.9998	1	0.561	1	1	0.0019	1	1	0.688	0.2	950
0.9996	0.9999	0.99476	0.99802	0.99481	0.99992	0.99804	0.9945	0.99726	0.99997	1	0.9992	1	0.7037	1	1	0.0112	0.9999	0.9998	0.694	0.3	950
0.99915	0.99978	0.98969	0.99628	0.98991	0.99992	0.99633	0.98928	0.99477	0.99994	1	0.6694	0.9999	0.0644	0.9908	1	0.0684	0.9995	0.9993	0.5441	0.4	950
0.99891	0.99978	0.98406	0.99479	0.97732	0.99829	0.99236	0.98942	0.98109	0.99941	1	0.9873	0.9997	0.1879	0.9994	0.998	0.0196	0.9983	0.9974	0.6453	0.5	950
0.99562	0.9989	0.96212	0.98919	0.97874	0.99238	0.99365	0.96529	0.99909	0.99778	1	0.8181	0.9993	0.5385	0.9986	0.9984	0.4196	0.996	0.9995	0.5921	0.6	950
1	1.00002	0.99945	0.9998	0.99916	0.99992	0.99969	0.99962	0.99928	1	1	0.6001	1	0.7076	1	1	0.0078	1	1	0.6094	0.1	1000
0.99992	1.00002	0.99804	0.99927	0.99711	0.99977	0.9989	0.99864	0.99748	0.99994	1	0.78	1	0.7892	1	1	0.0212	1	1	0.6069	0.2	1000
0.99976	0.99998	0.99557	0.99831	0.99347	0.99953	0.99749	0.99699	0.99436	0.99974	1	0.9429	1	0.8765	1	1	0.0312	0.9999	0.9998	0.6115	0.3	1000
0.99944	0.9999	0.99127	0.99684	0.98729	0.99907	0.99536	0.99407	0.98913	0.99962	1	0.9504	0.9999	0.318	0.9908	0.9999	0.1233	0.9995	0.9992	0.4506	0.4	1000
0.99936	0.99995	0.98722	0.99582	0.97496	0.992	0.99163	0.99812	0.98119	0.99725	1	0.9893	0.9998	0.7437	0.9993	0.9993	0.3644	0.9996	0.997	0.5625	0.5	1000
0.9969	0.99928	0.96643	0.99042	0.96878	0.99969	0.99059	0.96745	0.98481	0.99984	1	0.8643	0.9992	0.1403	0.9985	0.9999	0.0207	0.9953	0.9944	0.5548	0.6	1000
1	1.00004	0.99953	0.99983	0.99909	0.99969	0.99969	0.99995	0.99931	0.99991	1	0.9497	1	0.4724	1	1	0.07	1	1	0.4588	0.1	1050
0.99997	1.00005	0.99842	0.9994	0.99682	0.99891	0.99878	0.99976	0.99757	0.99962	1	0.8791	1	0.4368	1	1	0.1137	1	0.9994	0.5201	0.2	1050
0.99989	1.00005	0.99646	0.99863	0.99282	0.99767	0.99725	0.99944	0.99452	0.99912	1	0.9799	0.9992	0.4775	0.9999	0.9999	0.2228	1	0.9997	0.4465	0.3	1050
0.99971	1.00001	0.99301	0.99746	0.986	0.99541	0.99493	0.99892	0.98935	0.99834	1	0.9968	1	0.6778	0.9998	0.9998	0.4381	0.9999	0.999	0.6	0.4	1050
0.99971	1.00009	0.99037	0.99684	0.97533	0.98391	0.99181	0.99934	0.99174	0.9945	1	0.8754	1	0.4383	0.9999	0.9988	0.589	0.9999	0.9979	0.657	0.5	1050

0.99773	0.99957	0.96937	0.99165	0.95816	0.99689	0.9879	0.98048	0.96675	0.99903	1	0.8161	0.9995	0.3369	0.9981	0.9993	0.0931	0.9944	0.9917	0.0108	0.6	1050
1.00003	1.00005	0.99966	0.99988	0.9991	0.99938	0.99969	0.99995	0.99972	0.99981	1	0.6386	1	0.6419	1	1	0.4101	1	1	0.5857	0.1	1100
1.00021	1.00026	0.99928	0.99986	0.99752	0.99883	0.99939	1.00094	1.00082	0.99991	1	0.0378	1	0.8022	1	1	0.3205	1	1	0.5856	0.2	1100
1	1.00011	0.99732	0.99898	0.99298	0.99526	0.99731	0.99981	0.99764	0.99822	1	0.8441	1	0.6155	0.9999	0.9999	0.1448	1	0.9998	0.5889	0.3	1100
0.99989	1.00011	0.99472	0.99809	0.98627	0.99083	0.99505	0.99962	0.99537	0.99665	1	0.92	1	0.4695	0.9997	0.9996	0.2165	0.9989	0.9993	0.597	0.4	1100
0.99997	1.0002	0.99327	0.9978	0.97823	0.97739	0.99285	0.99224	0.99984	0.99234	1	0.9724	1	0.6061	0.9988	0.9981	0.0011	0.9975	1	0.5931	0.5	1100
0.99867	0.99984	0.97644	0.99341	0.95549	0.98609	0.98692	0.99666	0.96742	0.99572	1	0.7624	0.9996	0.4903	0.9977	0.9978	0.5777	0.9988	0.9912	0.6635	0.6	1100
1.00005	1.00006	0.99974	0.99991	0.99922	0.99915	0.99969	0.99972	1	0.99972	1	0.9903	1	0.059	1	1	0.0644	1	1	0.5358	0.1	1150
1.00008	1.00011	0.99919	0.99968	0.99726	0.99705	0.99896	0.99897	1	0.99894	1	0.9203	1	0.0121	1	1	0.0287	1	1	0.5558	0.2	1150
1.00008	1.00015	0.99813	0.99928	0.99388	0.99339	0.99768	0.99765	0.99997	0.99753	1	0.9926	1	0.0386	0.9999	0.9998	0.0064	0.9999	1	0.574	0.3	1150
1.00005	1.00018	0.99634	0.99865	0.98799	0.98718	0.99566	0.99553	0.99991	0.99534	1	0.9841	1	0.4582	0.9996	0.9994	0.0364	0.9996	1	0.5969	0.4	1150
1.00016	1.00029	0.99574	0.9986	0.98316	0.97529	0.9945	0.98227	0.9954	0.99177	1	0.4202	1	0.4407	0.9989	0.9974	0.436	0.9974	0.9999	0.5763	0.5	1150
0.99931	1.00004	0.98257	0.99508	0.95665	0.9728	0.98729	0.99887	0.98563	0.99149	1	0.7786	0.9997	0.6118	0.9969	0.9964	0.0072	0.9996	0.9937	0.5643	0.6	1150
1.00005	1.00007	0.99987	0.99995	0.99941	0.99907	0.99976	0.99929	0.99981	0.99972	1	0.9856	1	0.4571	1	1	0.0762	1	1	0.3031	0.1	1200
1.00011	1.00014	0.99949	0.9998	0.99793	0.99681	0.99921	0.9976	0.99937	0.99884	1	0.9795	1	0.4534	1	1	0.1687	1	1	0.46	0.2	1200
1.00016	1.00019	0.99881	0.99954	0.99531	0.99285	0.99823	0.99464	0.99861	0.99734	1	0.997	1	0.4896	0.9999	0.9978	0.2344	0.9998	0.9999	0.0054	0.3	1200
1.00016	1.00025	0.9977	0.99915	0.99076	0.98617	0.99664	0.98979	0.99732	0.995	1	0.9692	1	0.6887	0.9997	0.9992	0.3943	0.9991	0.9997	0.5866	0.4	1200
1.00029	1.00036	0.99766	0.99925	0.98883	0.9784	0.99633	0.97606	0.98387	0.99293	1	0.9812	1	0.3545	0.9993	0.9968	0.0302	0.9953	0.9961	0.5031	0.5	1200
0.99971	1.00019	0.98662	0.99645	0.95771	0.9585	0.98845	0.98608	0.99524	0.99221	1	0.6073	0.9998	0.4603	0.9957	0.9972	0.3373	0.9963	0.9967	0.5951	0.6	1200
1.00008	1.00009	0.99991	0.99997	0.9996	0.99922	0.99982	0.99911	0.99937	0.99975	1	0.9846	1	0.4901	1	1	0.001	1	1	0.5555	0.1	1250
1.00013	1.00016	0.99974	0.9999	0.99863	0.99728	0.99945	0.99685	0.99776	0.999	1	0.5534	1	0.4075	1	1	0.0863	0.9999	1	0.5525	0.2	1250
1.0004	1.0004	0.99974	1.00003	0.99793	0.9958	0.99933	0.9952	0.9971	0.99866	1	0.7933	0.9999	0.5313	0.9999	0.9998	0.0261	0.9996	0.9996	0.5424	0.3	1250
1.00027	1.0003	0.99872	0.99956	0.9939	0.98803	0.99774	0.98636	0.99055	0.99572	1	0.9997	1	0.6177	0.9998	0.9991	0.2785	0.9985	0.9987	0.1245	0.4	1250
1.0004	1.00044	0.99898	0.99973	0.99393	0.98531	0.99798	0.97766	0.97621	0.99528	1	0.9619	1	0.2726	0.9997	0.9981	0.0003	0.9947	0.992	0.6183	0.5	1250
1.00008	1.00033	0.99199	0.9978	0.96855	0.95586	0.99126	0.9699	0.99222	0.98705	1	0.9347	0.9999	0.5426	0.9964	0.9918	0.5137	0.9921	0.9971	0.5666	0.6	1250
1.00008	1.0001	1	1	0.99979	0.99946	0.99988	0.9992	0.99909	0.99981	1	0.9992	1	0.3996	1	1	0.0082	1	1	0.5663	0.1	1300

1.00035	1.00034	1.00017	1.0002	0.9997	0.99899	1.00006	0.9984	0.99833	0.99994	1	0.9983	1	0.9498	1	1	0.105	0.9999	1	0.5439	0.2	1300
1.00024	1.00027	0.99974	0.99993	0.99833	0.99596	0.99933	0.9937	0.99294	0.99847	1	0.9935	0.9999	0.6835	1	0.998	0.0043	0.9996	0.9973	0.544	0.3	1300
1.00032	1.00035	0.99949	0.99985	0.9967	0.992	0.99878	0.98763	0.98642	0.99712	1	0.9997	0.9999	0.6939	0.9999	0.9994	0.8825	0.9983	0.9974	0.6643	0.4	1300
1.00048	1.00049	0.99979	1.00005	0.99758	0.99293	0.99921	0.98641	0.98008	0.99772	1	0.9897	0.9999	0.6101	0.9999	0.9993	0.4862	0.997	0.9925	0.5787	0.5	1300
1.00032	1.00044	0.9957	0.99882	0.97959	0.96153	0.99426	0.95955	0.97385	0.98896	1	0.9946	1	0.1903	0.9977	0.9912	0.2635	0.9865	0.9892	0.3889	0.6	1300
1.00011	1.00011	1.00004	1.00003	0.99992	0.99977	0.99994	0.99953	0.99931	0.99991	1	0.9887	1	0.4502	1	1	0.1024	1	1	0.4284	0.1	1350
1.00019	1.0002	1.00004	1.00005	0.99971	0.99915	0.99988	0.99835	0.99754	0.99969	1	0.9334	1	0.4824	1	1	0.1684	1	1	0.4737	0.2	1350
1.00029	1.0003	1	1.00007	0.99935	0.99806	0.99976	0.99628	0.99445	0.99925	1	0.9973	0.9999	0.4972	1	0.9999	0.233	0.998	0.9994	0.3253	0.3	1350
1.00131	1.00071	1.00153	1.00046	1.00102	0.99984	1.00012	0.99835	0.99707	0.99972	1	0.9933	0.9999	0.7374	1	0.9998	0.43	0.9991	0.9977	0.5974	0.4	1350
1.00053	1.00056	1.00021	1.00027	0.99956	0.99813	0.99994	0.99558	0.9919	0.99941	1	0.9464	0.9999	0.4086	1	0.9999	0.0656	0.9994	0.9979	0.6891	0.5	1350
1.00045	1.00052	0.99783	0.99952	0.98749	0.97	0.99676	0.95635	0.95655	0.99227	1	0.9999	1	0.7069	0.9987	0.9922	0.9412	0.9806	0.9733	0.3838	0.6	1350
1.00011	1.00012	1.00009	1.00007	1.00002	0.99992	1	0.99986	0.99972	1	1	0.9749	1	0.8577	0.3342	1	0.0175	1	1	0.5498	0.1	1400
1.00021	1.00022	1.00013	1.00012	0.99998	0.99977	1	0.99948	0.99902	0.99994	1	0.998	1	0.502	0.5001	1	0.3031	1	1	0.5733	0.2	1400
1.00032	1.00033	1.00017	1.00017	0.99992	0.99946	1	0.99878	0.99779	0.99984	1	0.9968	0.9999	0.2313	0.6502	1	0.6836	1	0.9998	0.5751	0.3	1400
1.00043	1.00044	1.00021	1.00022	0.9998	0.99899	1	0.9976	0.99565	0.99966	1	0.9885	0.9999	0.6604	0.2711	1	0.9107	0.9968	0.9994	0.4391	0.4	1400
1.00061	1.00061	1.00047	1.00048	1.00032	1.00008	1.00031	0.99976	0.99931	1.00022	1	0.97	0.9999	0.1992	0.1328	1	0.0123	1	0.9999	0.599	0.5	1400
1.00059	1.0006	0.99949	1.00002	0.99533	0.98632	0.99872	0.97375	0.96269	0.99634	1	0.9115	0.9999	0.6424	0.6632	0.9973	0.5773	0.9892	0.9748	0.6008	0.6	1400
1.00011	1.00013	1.00009	1.0001	1.00008	1	1.00006	1	1	1.00006	1	0.3634	1	0.4502	1	1	0.0041	1	1	0.4785	0.1	1450
1.00024	1.00025	1.00021	1.00019	1.00014	1.00008	1.00012	1.00005	0.99997	1.00009	1	0.9888	0.9999	0.4824	1	1	0.0174	1	1	0.7902	0.2	1450
1.00037	1.00036	1.0003	1.00029	1.00021	1.00008	1.00018	1	0.99984	1.00016	1	0.9994	0.9999	0.4972	1	1	0.0123	1	1	0.4503	0.3	1450
1.00048	1.00049	1.00038	1.00038	1.00027	1.00016	1.00024	0.99991	0.99965	1.00019	1	0.9586	0.9999	0.7374	1	1	0.52	1	1	0.583	0.4	1450
1.00024	1.00025	1.00021	1.00019	1.00014	1.00008	1.00012	1.00005	0.99997	1.00009	1	0.9773	0.9999	0.4086	1	1	0.0218	1	1	0.6678	0.5	1450
1.00067	1.00067	1.00021	1.00032	0.99909	0.99643	0.99988	0.99167	0.98469	0.99906	1	0.9894	0.9999	0.7069	0.9987	0.9997	0.4862	0.998	0.9027	0.5762	0.6	1450
0.99846	0.99942	0.99879	0.99955	0.99909	0.99935	0.99968	0.99956	0.9997	0.99974	1	0.992	1	0.479	1	1	0.6349	1	1	0.5879	0.1	50
0.99476	0.99794	0.99593	0.9984	0.9969	0.99772	0.99878	0.99842	0.99897	0.99911	1	0.9946	1	0.5756	1	1	0.5778	1	1	0.5882	0.2	50
0.98828	0.9954	0.99105	0.99645	0.99319	0.99502	0.99731	0.99659	0.99778	0.99803	1	0.9986	0.073	0.5837	0.9999	0.9999	0.1062	0.9999	0.9999	0.6089	0.3	50

0.97732	0.99153	0.98295	0.99353	0.98721	0.99078	0.99506	0.99368	0.99593	0.99642	1	0.9984	0.0761	0.9414	0.9996	0.9995	0.0431	0.9996	0.9997	0.6254	0.4	50
0.96314	0.98746	0.98018	0.99306	0.99046	0.99682	0.9966	0.99975	0.99974	0.99885	0.9999	0.9974	0.0177	0.976	0.9998	0.9999	0.0513	1	1	0.3093	0.5	50
0.95955	0.98619	0.97043	0.98951	0.97825	0.98458	0.99204	0.98953	0.99328	0.99425	0.9999	0.9963	0.0184	0.9032	0.9988	0.9986	0.3984	0.9988	0.9992	0.6045	0.6	50
0.9986	0.99947	0.99919	0.9997	0.99962	0.99984	0.99987	1	1.00003	0.99997	1	0.9997	0.0156	0.6515	1	1	0.7606	1	1	0.5617	0.1	100
0.99523	0.99813	0.99732	0.99894	0.99869	0.99959	0.99949	1	1	0.99984	1	0.9969	0.0158	0.5335	1	1	0.7357	1	1	0.5518	0.2	100
0.98938	0.99583	0.99409	0.99767	0.99711	0.99902	0.99885	0.99995	0.99997	0.99964	1	0.9873	0.0162	0.4783	1	1	0.6721	1	1	0.5537	0.3	100
0.97937	0.99231	0.98868	0.99572	0.99449	0.9982	0.99788	0.9999	0.9999	0.99931	1	0.9986	0.0168	0.6573	0.9999	1	0.7523	1	1	0.5834	0.4	100
0.9667	0.9887	0.98814	0.99588	0.99779	1	0.99923	0.99644	0.99004	0.99865	1	0.989	0.0172	0.1439	0.9999	1	0.2361	0.9996	0.9978	0.58	0.5	100
0.92563	0.97822	0.94828	0.98367	0.96325	0.97462	0.98775	0.98306	0.98925	0.9912	0.9995	0.1162	0.0208	0.4399	0.9966	0.9962	0.0417	0.9969	0.9979	0.5088	0.6	100
0.99874	0.99953	0.99955	0.99982	0.99992	1	1	0.9999	0.99967	1.00003	1	0.9469	0.0156	0.5907	1	1	0.0266	1	1	0.6025	0.1	150
0.99571	0.99831	0.99843	0.99937	0.99971	1	0.99987	0.9996	0.99878	1.00003	1	0.9064	0.0158	0.6236	1	1	0.2038	1	1	0.595	0.2	150
0.99041	0.99624	0.99651	0.99862	0.99936	1	0.99974	0.99901	0.99722	1.00003	1	0.5017	0.016	0.7003	1	1	0.7426	1	0.9998	0.589	0.3	150
0.98139	0.99308	0.99329	0.99747	0.99875	1	0.99955	0.99802	0.99447	1.00003	1	0.9932	0.0165	0.2735	1	1	0.0923	0.9999	0.9993	0.6134	0.4	150
0.96995	0.98985	0.99405	0.99796	1.00008	0.99535	1.00006	0.98681	0.9823	0.99852	1	0.9977	0.0166	0.7397	1	0.9996	0.7575	0.998	0.9957	0.612	0.5	150
0.92759	0.97975	0.96282	0.9889	0.98255	0.99429	0.99461	0.99951	0.99944	0.99816	0.9997	0.9999	0.0199	0.9295	0.9993	0.9997	0.0811	1	0.9999	0.5655	0.6	150
0.99888	0.99957	0.99978	0.99991	1.00003	0.99984	1	0.99956	0.99937	0.99997	1	0.9951	0.0156	0.5628	1	1	0.5719	1	1	0.5837	0.1	200
0.99616	0.99849	0.99924	0.9997	1.00005	0.99943	1	0.99837	0.99772	0.99984	1	0.995	0.0157	0.5791	1	1	0.7073	1	0.9999	0.5828	0.2	200
0.99139	0.99662	0.99826	0.99932	1.00006	0.99869	1.00006	0.9963	0.99481	0.99957	1	0.9994	0.0159	0.6528	1	1	0.2212	0.9998	0.9996	0.6045	0.3	200
0.98327	0.99378	0.99664	0.99875	1.00008	0.99747	1.00006	0.99269	0.98994	0.99915	1	0.9965	0.0162	0.9108	1	0.9999	0.00072	0.9994	0.9986	0.3044	0.4	200
0.97306	0.99092	0.99794	0.9993	0.99805	0.98768	0.99942	0.98182	0.98653	0.99603	1	9941	0.0162	0.1368	0.9999	0.9989	0.202	0.9974	0.9976	0.0078	0.5	200
0.94113	0.98248	0.9796	0.99367	0.99621	0.99992	0.99878	0.99363	0.98236	0.99997	0.9999	0.9916	0.0184	0.3379	0.9999	1	0.2241	0.9988	0.9932	0.1131	0.6	200
0.99899	0.99962	0.99991	0.99996	0.99995	0.99959	1	0.99936	0.9995	0.9999	1	0.9947	0.0156	0.0044	1	1	0.1971	1	1	0.5617	0.1	250
0.99658	0.99864	0.99973	0.99989	0.99979	0.99845	0.99994	0.99768	0.99818	0.99947	1	0.9828	0.0156	0.5728	1	1	0.3143	1	1	0.5682	0.2	250
0.99232	0.99699	0.99942	0.99977	0.99949	0.99657	0.99987	0.99472	0.99593	0.99875	1	9977	0.0157	0.3183	1	0.9999	0.3174	0.9998	0.9998	0.5589	0.3	250
0.98503	0.99445	0.99884	0.99959	0.99895	0.99315	0.99968	0.98973	0.99219	0.99764	1	0.9947	0.0159	0.1161	1	0.9996	0.0175	0.9992	0.9992	0.5208	0.4	250
0.97612	0.99197	0.99982	0.99996	0.99324	0.98229	0.99788	0.98538	0.99629	0.99422	1	0.9995	0.0157	0.7314	0.9997	0.9987	0.3606	0.9984	0.9994	0.5997	0.5	250

0.94492	0.98402	0.98931	0.99681	1.00011	0.99143	1.00006	0.976	0.96896	0.9976	0.9999	9225	0.0176	0.4254	1	0.9988	0.0044	0.9934	9871	0.3791	0.6	250
0.9991	0.99966	1	1	0.99979	0.99935	0.99994	0.99946	0.99987	0.9998	1	0.9894	0.0156	0.7359	1	1	0.0023	1	1	0.1798	0.1	300
0.99697	0.9988	1	1	0.9992	0.9978	0.99974	0.99807	0.9995	0.99921	1	0.9958	0.0156	0.8379	1	1	0.0243	1	1	0.0375	0.2	300
0.99319	0.99734	0.99996	1	0.99815	0.99494	0.99936	0.99565	0.99891	0.99816	1	0.9995	0.0156	0.588	1	0.9999	0.0118	0.9999	0.9999	0.5048	0.3	300
0.98674	0.99509	0.99991	0.99998	0.99629	0.99013	0.99872	0.9916	0.99788	0.99652	1	0.9904	0.0157	0.307	0.9999	0.9996	0.2188	0.9995	0.9998	0.5665	0.4	300
0.97889	0.99292	0.99987	1	0.98768	0.98205	0.99602	0.99358	0.9997	0.99406	1	0.9974	0.0154	0.9827	0.9995	0.999	0.4786	0.9993	0.9999	0.5827	0.5	300
0.94752	0.98541	0.99602	0.99889	0.99612	0.97609	0.99897	0.96626	0.97604	0.9935	1	0.9955	0.0167	0.6398	0.9997	0.996	0.9467	0.9913	0.9822	0.1289	0.6	300
0.99922	0.99971	1	1	0.99958	0.99935	0.99987	0.99975	1	0.9998	1	0.9909	0.0155	0.4979	1	1	0.5063	1	1	0.6037	0.1	350
0.99734	0.99895	1	1.00002	0.9985	0.99772	0.99949	0.99916	0.99997	0.99918	1	0.9933	0.0155	0.4922	1	1	0.0935	1	1	0.7139	0.2	350
0.994	0.99766	1	1.00002	0.99656	0.99478	0.99878	0.99812	0.99993	0.9981	1	0.9997	0.0155	.6774	1	0.9999	0.2415	0.9999	1	0.5986	0.3	350
0.98831	0.99568	0.99996	1.00002	0.99321	0.98988	0.99763	0.99634	0.99983	0.99639	1	0.9971	0.0154	0.8852	0.9998	0.9997	0.0326	0.9988	1	0.4413	0.4	350
0.9815	0.99382	0.99834	0.99952	0.98327	0.98654	0.99455	0.9996	0.99113	0.99553	1	9988	0.015	0.0615	0.9995	0.9993	0.2731	0.9999	0.9978	0.2114	0.5	350
0.95753	0.98754	0.99969	0.99993	0.98792	0.96924	0.9966	0.9755	0.99381	0.99097	1	0.8006	0.0159	0.7504	0.9991	0.9961	0.0081	0.9955	0.9983	0.3676	0.6	350
0.99933	0.99974	0.99996	1	0.99942	0.99951	0.99981	1	0.9997	0.99987	1	0.9864	0.0155	0.6608	1	1	0.2287	1	1	0.7812	0.1	400
0.99767	0.99908	0.99982	0.99996	0.9965	0.99829	0.99929	0.99995	0.99891	0.99938	1	0.9847	0.0155	0.8431	1	1	0.004	1	1	0.6062	0.2	400
0.99476	0.99796	0.9996	0.99987	0.99528	0.99608	0.99827	0.9999	0.99749	0.99856	1	0.9928	0.0154	0.3297	1	0.9999	0.0305	1	0.9998	0.5906	0.3	400
0.98977	0.99623	0.99911	0.99973	0.99073	0.99241	0.99673	0.99975	0.99507	0.99731	1	0.8461	0.0153	0.8099	0.9998	0.9998	0.2224	1	0.9993	0.619	0.4	400
0.98399	0.99466	0.99562	0.99864	0.98133	0.99331	0.99391	0.99778	0.98074	0.9978	1	0.9962	0.0148	0.9288	0.9996	0.9995	0.6916	0.9996	0.9969	0.5492	0.5	400
0.9614	0.9889	0.99973	0.99998	0.97756	0.9685	0.99371	0.98894	0.99815	0.99195	1	0.0659	0.0152	0.4201	0.9984	0.9968	0.5726	0.9979	0.9997	0.579	0.6	400
0.99941	0.99978	0.99987	0.99996	0.99934	0.99976	0.99981	0.99995	0.99931	0.99993	1	0.1785	0.0155	0.5816	1	1	0.2528	1	1	0.5706	0.1	450
0.99798	0.99921	0.99951	0.99984	0.99767	0.9991	0.99917	0.9997	0.99752	0.9997	1	0.9378	0.0155	0.3496	1	1	0.0804	1	0.9999	0.5471	0.2	450
0.99549	0.99824	0.99879	0.99959	0.99469	0.99804	0.99808	0.99936	0.99441	0.99931	1	0.7185	0.0159	0.3896	1	1	0.2307	1	0.9997	0.529	0.3	450
0.99114	0.99674	0.99763	0.99919	0.98959	0.99625	0.99634	0.99877	0.98911	0.99865	1	0.9999	0.0151	0.5367	0.9999	0.9999	0.1541	0.9999	0.999	0.5722	0.4	450
0.98621	0.99542	0.99213	0.99749	0.98216	0.99878	0.99416	0.98894	0.98097	0.99957	1	0.9981	0.0146	8.3E-05	0.9997	0.9999	0.3788	0.9983	0.9974	0.3367	0.5	450
0.96426	0.99012	0.99673	0.99918	0.96827	0.97544	0.99121	0.99926	0.98326	0.99284	1	0.9394	0.0146	0.3904	0.9982	0.9976	0.0127	0.9998	0.9926	0.1698	0.6	450
0.9995	0.99981	0.99973	0.99993	0.99938	0.99992	0.99981	0.9996	0.99927	1	1	0.9718	0.0155	0.3886	1	1	0.0717	1	1	0.5615	0.1	500

0.99829	0.99933	0.99906	0.99968	0.99776	0.99984	0.99923	0.99862	0.99745	0.99993	1	0.9472	0.0154	0.4178	1	1	0.0262	1	1	0.4764	0.2	500
0.99613	0.9985	0.99781	0.99923	0.9949	0.99967	0.99814	0.99684	0.99431	0.99987	1	0.9861	0.0153	0.3107	1	1	0.0251	0.9999	0.9998	0.5256	0.3	500
0.9924	0.99721	0.99566	0.99851	0.99003	0.99927	0.99647	0.99383	0.98908	0.99974	1	0.9998	0.015	0.0391	0.9999	1	0.1798	0.9995	0.9992	0.5403	0.4	500
0.98828	0.99612	0.98828	0.99624	0.98544	0.99967	0.99525	0.98054	0.9909	0.99984	1	0.9953	0.0145	98276	0.9997	1	0.4334	0.9983	0.9981	0.5441	0.5	500
0.97132	0.99171	0.99213	0.99781	0.96739	0.98858	0.99044	0.9961	0.96708	0.99658	1	9696	0.0142	0.3671	0.9988	0.9986	0.2006	0.9988	0.9913	0.4573	0.6	500
0.99958	0.99984	0.9996	0.99987	0.99949	1	0.99987	0.99931	0.99967	1	1	0.9905	0.0155	0.1997	1	1	0.453	1	1	0.5093	0.1	550
0.99854	0.99943	0.99857	0.9995	0.99818	0.99992	0.99936	0.99748	0.99881	0.99997	1	0.9967	0.0154	0.9192	1	1	0.8736	1	1	0.5431	0.2	550
0.99672	0.99873	0.99673	0.99882	0.99584	0.99992	0.99846	0.99437	0.99729	0.99997	1	0.9938	0.0152	0.0201	1	1	0.8408	1	0.9998	0.5247	0.3	550
0.99355	0.99764	0.99356	0.99774	0.99186	0.99984	0.99711	0.98903	0.99477	0.9999	1	0.9857	0.0149	0.6901	0.9999	1	0.8316	0.9999	0.9994	0.5023	0.4	550
0.99019	0.99677	0.98461	0.995	0.99028	0.99527	0.99679	0.97955	0.9995	0.99839	1	0.9884	0.0144	0.4432	0.9997	0.9995	0.0159	0.9995	0.9998	0.5888	0.5	550
0.97483	0.99284	0.98564	0.996	0.96845	0.9978	0.99076	0.98039	0.96777	0.99934	0.9999	0.0552	0.0139	0.4792	0.999	0.9996	0.3716	0.9987	0.9924	0.248	0.6	550
0.99966	0.99987	0.99946	0.99984	0.99966	0.99984	0.99987	0.99926	1	0.99993	1	0.9982	0.0155	0.5277	1	1	0.2867	1	1	0.5034	0.1	600
0.99879	0.99953	0.99812	0.99934	0.99879	0.99943	0.99955	0.99733	0.99993	0.99977	1	0.9981	0.0154	0.6087	1	1	0.4669	1	1	0.5166	0.2	600
0.99725	0.99895	0.99571	0.99842	0.99723	0.99861	0.99897	0.99397	0.99987	0.99947	1	0.9936	0.0152	0.4792	1	1	0.4334	0.9999	1	0.509	0.3	600
0.99462	0.99804	0.9915	0.99701	0.99458	0.99739	0.99808	0.98839	0.99974	0.99905	1	0.7807	0.0149	0.5087	0.9999	0.9998	0.2267	0.9996	0.9999	0.6215	0.4	600
0.99187	0.99734	0.98139	0.99392	0.99524	0.98784	0.99846	0.98632	0.99649	0.99593	1	0.996	0.0144	0.7807	0.9998	0.999	0.2357	0.9985	0.9989	0.5564	0.5	600
0.97757	0.99382	0.97785	0.99392	0.97321	0.99943	0.99237	0.96478	0.98405	0.99977	0.9999	0.9993	0.0135	0.2012	0.999	0.9999	0.354	0.9947	0.9941	0.1329	0.6	600
0.99972	0.9999	0.99937	0.99978	0.99984	0.99951	0.99994	0.99951	0.9999	0.99987	1	0.9933	0.0155	0.8806	1	1	0.1231	1	1	0.5966	0.1	650
0.99902	0.99962	0.99772	0.99918	0.99941	0.99845	0.99981	0.99822	0.99957	0.99944	1	0.969	0.0154	0.2522	1	1	0.0391	1	1	0.5885	0.2	650
0.99776	0.99914	0.99477	0.99806	0.99866	0.99649	0.99949	0.996	0.99897	0.99869	1	0.9996	0.0152	0.5702	1	0.9999	0.0153	0.9999	0.9999	0.5789	0.3	650
0.99554	0.99838	0.98971	0.99634	0.99736	0.99323	0.99904	0.99225	0.99801	0.99754	1	0.993	0.0149	0.8862	0.9999	0.9997	0.8098	0.9995	0.9997	0.5609	0.4	650
0.98226	0.99495	0.97262	0.99217	0.98301	0.99176	0.99506	0.96523	0.99917	0.9975	1	0.9608	0.0144	0.0267	0.9999	0.9992	0.2508	0.9992	0.9976	0.4442	0.5	650
0.98226	0.99495	0.97262	0.99217	0.98301	0.99176	0.99506	0.96523	0.99917	0.9975	0.9999	0.9201	0.0135	0.5727	0.9991	0.9984	0.3194	0.9961	0.9995	0.6115	0.6	650
0.99978	0.99992	0.99928	0.99977	0.99997	0.99927	1	0.99985	0.99947	0.99977	1	0.9453	0.0155	0.3856	1	1	0.0416	1	1	0.5926	0.1	700
0.99919	0.9997	0.99741	0.99905	0.99987	0.99755	0.99994	0.99946	0.99808	0.99915	1	0.9579	0.0154	0.3549	1	1	0.0091	1	1	0.5998	0.2	700
0.99818	0.9993	0.99405	0.9978	0.99968	0.99453	0.99987	0.99872	0.9957	0.998	1	0.9921	0.0152	0.1455	1	0.9999	0.0182	0.9999	0.9998	0.6449	0.3	700

0.99638	0.9987	0.98832	0.99584	0.99938	0.98939	0.99974	0.99753	0.99166	0.99619	1	0.9835	0.0149	0.1471	1	0.9997	0.8952	0.9997	0.9992	0.4605	0.4	700
0.9947	0.99829	0.97741	0.9926	0.99998	0.97862	1	1	0.97942	0.99291	1	0.9976	0.0145	0.9715	1	0.9994	0.6191	1	0.9982	0.5814	0.5	700
0.98514	0.99583	0.96671	0.99046	0.99156	0.97862	0.99756	0.97659	0.99394	0.99366	0.9999	0.9198	0.0135	0.8077	0.9993	0.9971	0.0601	0.9956	0.9968	0.5569	0.6	700
0.99983	0.99994	0.99919	0.99973	1	0.99918	1	1	0.99924	0.99977	1	0.9956	0.0155	0.6071	1	1	0.1504	1	1	0.3186	0.1	750
0.99938	0.99976	0.99718	0.99898	1	0.99723	1	1	0.99729	0.99901	1	0.9978	0.0154	0.6217	1	1	0.2626	1	1	0.2548	0.2	750
0.99854	0.99946	0.99365	0.99763	1	0.9938	1	1	0.99391	0.9977	1	0.9945	0.0152	0.6763	1	0.9999	0.4511	1	0.9998	0.774	0.3	750
0.99711	0.99898	0.98747	0.99552	1	0.988	1	1	0.98825	0.9957	1	9952	0.015	0.7181	1	0.9998	0.4723	1	0.9994	0.6512	0.4	750
0.99585	0.99869	0.97691	0.99242	0.99816	0.9814	0.99936	0.99565	0.98544	0.99386	1	0.9611	0.0146	0.0967	0.9999	0.9992	0.003	0.9992	0.9976	0.5912	0.5	750
0.98739	0.99657	0.96108	0.98901	0.99789	0.96614	0.99942	0.99225	0.97419	0.99008	0.9999	0.9775	0.0135	0.0328	0.9998	0.09974	0.8604	0.9974	0.9927	0.4234	0.6	750
0.99989	0.99996	0.99919	0.99973	0.99994	0.99935	1	0.99985	0.99947	0.9998	1	0.8857	1	0.8046	1	1	0.356	1	1	0.6249	0.1	800
0.99952	0.99983	0.99714	0.99894	0.99978	0.99763	0.99994	0.99946	0.99811	0.99915	1	0.6429	1	0.9246	1	1	0.2645	1	1	0.646	0.2	800
0.99916	0.99971	0.99365	0.99762	0.99823	0.99665	0.99929	0.996	0.99901	0.99875	1	0.9997	1	0.0392	1	0.9999	0.4743	0.9999	0.9999	0.4408	0.3	800
0.99776	0.99923	0.9872	0.99541	0.99898	0.98956	0.99962	0.99753	0.99173	0.99626	1	0.7439	1	0.2662	1	0.9997	0.0186	0.9997	0.9992	0.6219	0.4	800
0.99683	0.99904	0.97745	0.9926	0.99375	0.98825	0.99788	0.98632	0.99656	0.99612	1	0.9657	0.9998	0.3156	0.9997	0.99	0.1877	0.9985	0.9989	0.6082	0.5	800
0.9903	0.99732	0.95987	0.9884	0.99998	0.96304	0.99994	1	0.96519	0.98893	1	0.9333	0.9997	0.6826	1	0.9981	0.5428	1	0.9949	0.701	0.6	800
0.99992	0.99998	0.99919	0.99973	0.99978	0.99959	0.99994	0.99951	0.9999	0.99987	1	0.9995	1	0.9876	1	1	0.0319	1	1	0.7662	0.1	850
0.99966	0.99989	0.99718	0.99896	0.99922	0.99853	0.99968	0.99822	0.99957	0.99947	1	0.9994	1	0.9732	1	1	0.1208	1	1	0.4244	0.2	850
0.99916	0.99971	0.99365	0.99762	0.99823	0.99665	0.99929	0.996	0.99901	0.99875	1	0.9997	1	0.0392	1	0.9999	0.4743	0.9999	0.9999	0.4408	0.3	850
0.99829	0.99943	0.98752	0.99552	0.99652	0.99339	0.99872	0.99225	0.99808	0.99767	1	0.9908	0.9998	0.327	0.9999	0.9997	0.3937	0.9995	0.9997	0.5846	0.4	850
0.99767	0.99933	0.97897	0.9931	0.98792	0.99568	0.99596	0.97975	0.99947	0.99859	1	0.9657	0.9998	0.3156	0.9997	0.9999	0.1877	0.9995	0.9989	0.6092	0.5	850
0.99238	0.99794	0.95499	0.98815	0.99676	0.96785	0.99897	0.99249	0.97525	0.99041	1	0.9145	0.9996	0.3703	0.9997	0.9976	0.013	0.9975	0.9933	0.2733	0.6	850
0.99994	0.99999	0.99924	0.99975	0.99957	0.99984	0.99987	0.99926	1	0.99997	1	0.9998	1	0.6338	1	1	0.3369	1	1	0.4088	0.1	900
0.99975	0.99993	0.99741	0.99903	0.99847	0.99943	0.99942	0.99733	0.99993	0.9998	1	0.9999	1	0.6409	1	1	0.4788	1	1	0.4629	0.2	900
0.99941	0.99982	0.99409	0.99778	0.99653	0.99878	0.99872	0.99407	0.99987	0.99954	1	0.9972	1	0.6283	1	1	0.5328	0.9999	1	0.8703	0.3	900
0.99877	0.99962	0.98837	0.99582	0.99324	0.99755	0.99756	0.98849	0.9997	0.99915	1	0.9917	0.9999	0.5657	0.9999	0.9968	0.2527	0.9996	0.9999	0.5945	0.4	900
0.99837	0.99957	0.98125	0.99385	0.98202	0.99984	0.99397	0.98103	0.9909	0.9999	1	0.9955	0.9998	0.6763	0.9996	0.9998	0.467	0.9986	0.9998	0.585	0.5	900

0.99386	0.99842	0.95799	0.98822	0.98856	0.97854	0.99666	0.97585	0.99388	0.99383	1	0.7111	0.9994	0.4195	0.9989	0.9969	0.6466	0.9951	0.9966	0.5462	0.6	900
0.99997	1.00001	0.99933	0.99977	0.99934	1	0.99981	0.99931	0.99967	1	1	0.9998	1	0.601	1	1	0.00001	1	1	0.674	0.1	950
0.99986	0.99998	0.99767	0.99912	0.9977	1	0.99917	0.99758	0.99881	1	1	0.9998	1	0.561	1	1	0.0019	1	1	0.688	0.2	950
0.99961	0.9999	0.99477	0.99801	0.99482	0.99992	0.99808	0.99452	0.99729	0.99997	1	0.9992	1	0.7037	1	1	0.0112	0.9999	0.9998	0.694	0.3	950
0.99916	0.99978	0.98967	0.99627	0.98991	0.99992	0.99634	0.98928	0.99477	0.99993	1	0.6694	0.9999	0.0644	0.9908	1	0.0684	0.9995	0.9993	0.5441	0.4	950
0.99893	0.99978	0.98407	0.99478	0.97732	0.99829	0.99243	0.98943	0.98111	0.99938	1	0.9873	0.9997	0.1879	0.9994	0.998	0.0196	0.9983	0.9974	0.6453	0.5	950
0.99563	0.9989	0.96211	0.98917	0.97874	0.99241	0.99365	0.96533	0.99911	0.99777	1	0.8181	0.9993	0.5385	0.9986	0.9984	0.4196	0.996	0.9995	0.5921	0.6	950
1	1.00002	0.99942	0.9998	0.99917	0.99992	0.99974	0.99965	0.99931	0.99997	1	0.6001	1	0.7076	1	1	0.0078	1	1	0.6094	0.1	1000
0.99994	1.00001	0.99803	0.99925	0.99711	0.99976	0.99891	0.99867	0.99749	0.9999	1	0.78	1	0.7892	1	1	0.0212	1	1	0.6069	0.2	1000
0.99978	0.99998	0.99557	0.99831	0.99348	0.99951	0.99756	0.99699	0.99434	0.9998	1	0.9429	1	0.8765	1	1	0.0312	0.9999	0.9998	0.6115	0.3	1000
0.99947	0.9999	0.99123	0.99685	0.98729	0.99902	0.99538	0.99412	0.98915	0.99964	1	0.9504	0.9999	0.318	0.9908	0.9999	0.1233	0.9995	0.9992	0.4506	0.4	1000
0.99938	0.99994	0.9872	0.99581	0.97497	0.992	0.99166	0.99812	1.31209	0.99724	1	0.9893	0.9998	0.7437	0.9993	0.9993	0.3644	0.9996	0.997	0.5625	0.5	1000
0.99692	0.99927	0.96645	0.99041	0.96878	0.99967	0.99063	0.96745	0.98485	0.99984	1	0.8643	0.9992	0.1403	0.9985	0.9999	0.0207	0.9953	0.9944	0.5548	0.6	1000
1.00003	1.00003	0.99955	0.99984	0.99909	0.99967	0.99968	0.99995	0.99931	0.9999	1	0.9497	1	0.4724	1	1	0.07	1	1	0.4588	0.1	1050
1	1.00004	0.99843	0.99939	0.99682	0.99894	0.99885	0.99975	0.99758	0.99961	1	0.8791	1	0.4368	1	1	0.1137	1	0.9994	0.5201	0.2	1050
0.99992	1.00004	0.99642	0.99864	0.99282	0.99763	0.99731	0.99946	0.99451	0.99911	1	0.9799	0.9992	0.4775	0.9999	0.9999	0.2228	1	0.9997	0.4465	0.3	1050
0.99972	1.00001	0.99298	0.99745	0.98601	0.99543	0.99493	0.99896	0.98938	0.99833	1	0.9968	1	0.6778	0.9998	0.9998	0.4381	0.9999	0.999	0.6	0.4	1050
0.99972	1.00008	0.99038	0.99685	0.97534	0.98384	0.99185	0.99936	0.99173	0.99448	1	0.8754	1	0.4383	0.9999	0.9988	0.589	0.9999	0.9979	0.657	0.5	1050
0.99776	0.99956	0.96935	0.99165	0.95816	0.9969	0.98794	0.98049	0.96675	0.99905	1	0.8161	0.9995	0.3369	0.9981	0.9993	0.0931	0.9944	0.9917	0.0108	0.6	1050
1.00006	1.00004	0.99964	0.99987	0.9991	0.99935	0.99968	1	0.9997	0.9998	1	0.6386	1	0.6419	1	1	0.4101	1	1	0.5857	0.1	1100
1.00006	1.00008	0.99879	0.99953	0.9969	0.99788	0.99885	0.9999	0.99897	0.99921	1	0.0378	1	0.8022	1	1	0.3205	1	1	0.5856	0.2	1100
1.00003	1.0001	0.99732	0.99896	0.99298	0.99527	0.99737	0.9998	0.99765	0.99819	1	0.8441	1	0.6155	0.9999	0.9999	0.1448	1	0.9998	0.5889	0.3	1100
0.99992	1.0001	0.99472	0.99808	0.98629	0.99078	0.99506	0.99965	0.9954	0.99665	1	0.92	1	0.4695	0.9997	0.9996	0.2165	0.9989	0.9993	0.597	0.4	1100
0.99997	1.00019	0.99329	0.99778	0.97825	0.9774	0.99288	0.99225	0.99983	0.99235	1	0.9724	1	0.6061	0.9988	0.9981	0.0011	0.9975	1	0.5931	0.5	1100
0.99868	0.99983	0.97642	0.9934	0.9555	0.98613	0.98691	0.99669	0.96741	0.99573	1	0.7624	0.9996	0.4903	0.9977	0.9978	0.5777	0.9988	0.9912	0.6635	0.6	1100
1.00006	1.00006	0.99978	0.99991	0.99923	0.9991	0.99974	0.9997	1	0.99974	1	0.9903	1	0.059	1	1	0.0644	1	1	0.5358	0.1	1150

1.00008	1.0001	0.99919	0.99968	0.9973	0.99706	0.99897	0.99896	1	0.99892	1	0.9203	1	0.0121	1	1	0.0287	1	1	0.5558	0.2	1150
1.00011	1.00015	0.99812	0.99927	0.99389	0.99339	0.99769	0.99768	0.99997	0.9975	1	0.9926	1	0.0386	0.9999	0.9998	0.0064	0.9999	1	0.574	0.3	1150
1.00008	1.00018	0.99633	0.99866	1.00398	0.98719	0.9957	0.99555	0.99993	0.99534	1	0.9841	1	0.4582	0.9996	0.9994	0.0364	0.9996	1	0.5969	0.4	1150
1.00017	1.00029	0.99575	0.9986	0.98317	0.97528	0.99448	0.98227	0.9954	0.99176	1	0.4202	1	0.4407	0.9989	0.9974	0.436	0.9974	0.9999	0.5763	0.5	1150
0.99933	1.00003	0.98255	0.99507	0.95653	0.97275	0.9873	0.99891	0.98561	0.99149	1	0.7786	0.9997	0.6118	0.9969	0.9964	0.0072	0.9996	0.9937	0.5643	0.6	1150
1.00008	1.00007	0.99987	0.99993	0.99941	0.9991	0.99981	0.99931	0.99983	0.9997	1	0.9856	1	0.4571	1	1	0.0762	1	1	0.3031	0.1	1200
1.00014	1.00013	0.99946	0.99978	0.99792	0.99682	0.99923	0.99763	0.99937	0.99885	1	0.9795	1	0.4534	1	1	0.1687	1	1	0.46	0.2	1200
1.00017	1.00019	0.99884	0.99953	0.99532	0.9929	0.9982	0.99467	0.99861	0.99734	1	0.997	1	0.4896	0.9999	0.9978	0.2344	0.9998	0.9999	0.0054	0.3	1200
1.0002	1.00024	0.99767	0.99914	0.99078	0.98613	0.99666	0.98978	0.99735	0.99498	1	0.9692	1	0.6887	0.9997	0.9992	0.3943	0.9991	0.9997	0.5866	0.4	1200
1.00031	1.00036	0.99767	0.99925	0.98883	0.97838	0.99634	0.97609	0.98385	0.99294	1	0.9812	1	0.3545	0.9993	0.9968	0.0302	0.9953	0.9961	0.5031	0.5	1200
0.99972	1.00019	0.98658	0.99643	0.95772	0.95847	0.98852	0.98612	0.99524	0.99218	1	0.6073	0.9998	0.4603	0.9957	0.9972	0.3373	0.9963	0.9967	0.5951	0.6	1200
1.00008	1.00008	0.99991	0.99996	0.9996	0.99918	0.99987	0.99911	0.99937	0.99974	1	0.9846	1	0.4901	1	1	0.001	1	1	0.5555	0.1	1250
1.00017	1.00016	0.99973	0.99989	0.99863	0.99731	0.99949	0.99684	0.99775	0.99901	1	0.5534	1	0.4075	1	1	0.0863	0.9999	1	0.5525	0.2	1250
1.00022	1.00022	0.99937	0.99975	0.99692	0.99388	0.99878	0.99294	0.99504	0.9977	1	0.7933	0.9999	0.5313	0.9999	0.9998	0.0261	0.9996	0.9996	0.5424	0.3	1250
1.00028	1.00029	0.99875	0.99953	0.99391	0.98809	0.99782	0.98642	0.99057	0.99573	1	0.9997	1	0.6177	0.9998	0.9991	0.2785	0.9985	0.9987	0.1245	0.4	1250
1.00042	1.00043	0.99897	0.99971	0.99393	0.98531	0.99801	0.97767	0.97624	0.99527	1	0.9619	1	0.2726	0.9997	0.9981	0.0003	0.9947	0.992	0.6183	0.5	1250
1.00008	1.00033	0.99199	0.9978	0.96856	0.95585	0.99127	0.96987	0.99222	0.98703	1	0.9347	0.9999	0.5426	0.9964	0.9918	0.5137	0.9921	0.9971	0.5666	0.6	1250
1.00011	1.00009	1	1	0.99979	0.99951	0.99994	0.99921	0.99911	0.9998	1	0.9992	1	0.3996	1	1	0.0082	1	1	0.5663	0.1	1300
1.0002	1.00018	0.99991	0.99998	0.99926	0.9982	0.99968	0.99723	0.99686	0.99931	1	0.9983	1	0.9498	1	1	0.105	0.9999	1	0.5439	0.2	1300
1.00028	1.00026	0.99973	0.99993	0.99832	0.99592	0.99936	0.99368	0.99295	0.99846	1	0.9935	0.9999	0.6835	1	0.998	0.0043	0.9996	0.9973	0.544	0.3	1300
1.00034	1.00035	0.99946	0.99984	0.99669	0.992	0.99878	0.98765	0.9864	0.99714	1	0.9997	0.9999	0.6939	0.9999	0.9994	0.8825	0.9983	0.9974	0.6643	0.4	1300
1.0005	1.00049	0.99978	1.00004	0.99759	0.99298	0.99923	0.98642	0.98008	0.9977	1	0.9897	0.9999	0.6101	0.9999	0.9993	0.4862	0.997	0.9925	0.5787	0.5	1300
1.00034	1.00043	0.99571	0.99882	0.97953	0.9614	0.99429	0.95945	0.97379	0.98893	1	0.9946	1	0.1903	0.9977	0.9912	0.2635	0.9865	0.9892	0.3889	0.6	1300
1.00011	1.0001	1.00004	1.00002	0.99992	0.99976	1	0.99956	0.99931	0.9999	1	0.9887	1	0.4502	1	1	0.1024	1	1	0.4284	0.1	1350
1.0002	1.0002	1.00004	1.00005	0.99973	0.9991	0.99987	0.99837	0.99755	0.99967	1	0.9334	1	0.4824	1	1	0.1684	1	1	0.4737	0.2	1350
1.00031	1.00029	1	1.00005	0.99934	0.99804	0.99974	0.9963	0.99444	0.99924	1	0.9973	0.9999	0.4972	1	0.9999	0.233	0.998	0.9994	0.3253	0.3	1350

1.00039	1.00039	0.99991	1.00005	0.99871	0.99616	0.99955	0.99264	0.98908	0.99862	1	0.9933	0.9999	0.7374	1	0.9998	0.43	0.9991	0.9977	0.5974	0.4	1350
1.00056	1.00055	1.00022	1.00027	0.99957	0.99812	0.99994	0.9956	0.99189	0.99941	1	0.9464	0.9999	0.4086	1	0.9999	0.0656	0.9994	0.9979	0.6891	0.5	1350
1.00048	1.00052	0.99785	0.99952	0.9875	0.96997	0.99679	0.95634	0.95655	0.99225	1	0.9999	1	0.7069	0.9987	0.9922	0.9412	0.9806	0.9733	0.3838	0.6	1350
1.00011	1.00011	1.00004	1.00005	1.00002	0.99992	1	0.99985	0.99974	1	1	0.9749	1	0.8577	0.3342	1	0.0175	1	1	0.5498	0.1	1400
1.00022	1.00021	1.00013	1.00011	1	0.99976	1	0.99946	0.99904	0.99993	1	0.998	1	0.502	0.5001	1	0.3031	1	1	0.5733	0.2	1400
1.00034	1.00033	1.00018	1.00016	0.99994	0.99951	1	0.99881	0.99782	0.99984	1	0.9968	0.9999	0.2313	0.6502	1	0.6836	1	0.9998	0.5751	0.3	1400
1.00045	1.00044	1.00022	1.00022	0.99981	0.99894	1	0.99763	0.99563	0.99964	1	0.9885	0.9999	0.6604	0.2711	1	0.9107	0.9968	0.9994	0.4391	0.4	1400
1.00062	1.00061	1.00049	1.00047	1.00034	1.00008	1.00032	0.9998	0.99931	1.00023	1	0.97	0.9999	0.1992	0.1328	1	0.0123	1	0.9999	0.599	0.5	1400
1.00059	1.00059	0.99946	1	0.99533	0.98637	0.99878	0.97372	0.96271	0.99635	1	0.9115	0.9999	0.6424	0.6632	0.9973	0.5773	0.9892	0.9748	0.6008	0.6	1400
1.00014	1.00012	1.00009	1.00009	1.00008	1	1.00006	1.00005	1	1.00007	1	0.3634	1	0.4502	1	1	0.0041	1	1	0.4785	0.1	1450
1.00025	1.00025	1.00018	1.00018	1.00014	1.00008	1.00013	1.00005	0.99997	1.0001	1	0.9888	0.9999	0.4824	1	1	0.0174	1	1	0.7902	0.2	1450
1.00036	1.00036	1.00027	1.00027	1.00021	1.00008	1.00019	1	0.99987	1.00013	1	0.9994	0.9999	0.4972	1	1	0.0123	1	1	0.4503	0.3	1450
1.0005	1.00048	1.0004	1.00038	1.00027	1.00008	1.00026	0.99995	0.99967	1.0002	1	0.9586	0.9999	0.7374	1	1	0.52	1	1	0.583	0.4	1450
1.00025	1.00025	1.00018	1.00018	1.00014	1.00008	1.00013	1.00005	0.99997	1.0001	1	0.9773	0.9999	0.4086	1	1	0.0218	1	1	0.6678	0.5	1450
1.00067	1.00066	1.00022	1.00032	0.9991	0.99641	0.99987	0.9917	0.98471	0.99905	1	0.9894	0.9999	0.7069	0.9987	0.9997	0.4862	0.998	0.9027	0.5762	0.6	1450